doi.org/10.26434/chemrxiv.8299715.v1

Diversity Focused Semisyntheses of Tetronate Polyether Ionophores

Shaoquan Lin, Han Liu, Esben B. Svenningsen, Christine Pedersen, Peter Nørby, Thomas Tørring, Thomas Poulsen

Submitted date: 20/06/2019 • Posted date: 21/06/2019

Citation information: Lin, Shaoquan; Liu, Han; Svenningsen, Esben B.; Pedersen, Christine; Nørby, Peter; Tørring, Thomas; et al. (2019): Diversity Focused Semisyntheses of Tetronate Polyether Ionophores. ChemRxiv. Preprint.

The polyether ionophores are complex natural products capable of transporting cations across biological membranes. Many family members possess highly potent antimicrobial activity and a few selected compounds have ability to target particularly aggressive cancer cells. Despite these interesting perspectives, a detailed understanding of the cellular mode-of-action of polyether ionophores is generally lacking. In principle, broad mapping of structure-activity relationships across several biological activities could provide mechanistic insights as well as identification of lead structures but access to structural diversity within the overall class is synthetically very challenging. In this manuscript, we demonstrate that novel polyether ionophores can be constructed by recycling components of highly abundant polyethers. We provide the first examples of synthetically incorporating halogen-functionalized tetronic acids as cation-binding groups into polyether ionophores and we identify analogs with strong anti-bacterial activity and minimal effects on mammalian cells.

File list (3)

Diversity focused semisyntheses of tetronate polyether ionophores

Shaoquan Lin[1,‡], Han Liu[1,‡], Esben B. Svenningsen[1], Christine N. Pedersen[1], Peter Nørby[1], Thomas Tørring[2], Thomas B. Poulsen[1,*]

[1] Department of Chemistry, Aarhus University, Langelandsgade 140, DK-8000, Aarhus C, Denmark.

[2] Department of Engineering – Microbial Biosynthesis, Aarhus University, Gustav Wieds Vej 10, DK-8000, Aarhus C, Denmark

*e-mail: thpou@chem.au.dk

‡ These authors contributed equally

Abstract

The polyether ionophores are complex natural products capable of transporting cations across biological membranes. Many family members possess highly potent antimicrobial activity and a few selected compounds have ability to target particularly aggressive cancer cells. Despite these interesting perspectives, a detailed understanding of the cellular mode-of-action of polyether ionophores is generally lacking. In principle, broad mapping of structure-activity relationships across several biological activities could provide mechanistic insights as well as identification of lead structures but access to structural diversity within the overall class is synthetically very challenging. In this manuscript, we demonstrate that novel polyether ionophores can be constructed by recycling components of highly abundant polyethers. We provide the first examples of synthetically incorporating halogen-functionalized tetronic acids as cation-binding groups into polyether ionophores and we identify analogs with strong anti-bacterial activity and minimal effects on mammalian cells.

Introduction

The polyether ionophore natural products have been a constant fix-point for organic chemistry since the 1960s.[1] The daunting complexity of compounds such as monensin, salinomycin, and X-206 challenged the abilities of chemists to identify their precise molecular structures[2,3] and has served as inspiration for the development of novel synthetic methods[4,5,6,7,8] and retrosynthetic analysis.[9] Elegant syntheses of members of this superfamily (>100 molecules) of natural products have been reported, the majority during the 1980–1990s.[10,11,12] Since then, the raison d'être of natural product synthesis has changed substantially: Ideality in synthesis-design has become a fulcrum for methodological innovation[13,14] which has also inspired remarkably efficient routes to members of the polyether ionophores.[12,15,16,17]

Through strategic integration[18] of complex molecule synthesis with studies of biological mechanisms, the field of synthesis can catalyze new discoveries within the life sciences. Diversity oriented synthesis,[19] biology oriented synthesis,[20] analogue oriented synthesis,[21] diverted total synthesis,[22] complexity-to-diversity-strategies,[23] and pharmacophore-directed retrosynthesis[24] are all different strategic flavors directed towards generating innovative complex structures with potential pharmacological utility.[25,26]

The polyether ionophores have thus far escaped attention from efforts that seek to harness their complex structures as fundamental entities of diversity.[2,27] There may be several reasons for this, but the most important is likely that these compounds are typically considered biologically uninteresting as the perturbation of ion gradients is thought to result in pleiotropic effects on cellular systems. At least in eukaryotic cells, this highly simplistic view of the activity of polyether ionophores is almost certainly deceptive: we do not really know in which of the many endomembranes ionophores operate and which ions they transport. In fact, recent discoveries concerning the biological activity of salinomycin (Sal),[28] a canonical potassium-ionophore and surprising selective inhibitor of stem-like cancer cells,[29] suggest that the compound does not even act as an ionophore, but instead sequesters iron in lysosomes which can trigger a type of regulated oxidative cell death known as ferroptosis/oxytosis[30] or directly bind protein targets as was recently shown with nucleolin.[31]

The main feature of polyether ionophores is their antibiotic activity and they are extensively applied in the agricultural industry to control parasitic infections in poultry and as growth promoters in ruminating animals.[32,33] The latter effect presumably is due to remodeling of the rumen microbiota by the ionophores. Importantly, studies show that polyether ionophores do not display cross-resistance with other major antibiotics and are therefore active in drug-resistant bacterial strains[34] although their activity is currently restricted to gram-positive strains. The lack of gram-negative activity is not mechanistically understood. As antibiotic

78 resistance continues to spread, agents such as the colistins, that were previously shelved due
79 to safety issues, have now been reintroduced to the clinic. We suggest that it is due diligence to
80 seriously consider the antibiotic potential that may lie in the polyether ionophores[34] and that
81 the field of synthesis should consider how we can deliver truly novel molecules within this
82 class.
83 Here, we outline an approach that can be used to prepare numerous novel polyether
84 ionophores and which takes advantage of two key aspects of this class of compounds: 1) the
85 availability of selected members – the feedstock polyether ionophores e.g. lasalocid,
86 salinomycin, monensin – on a massive scale and 2) the overall structure of polyethers being
87 essentially a series of connected "modules" (Figure 1a). We suggest that by disassembling these
88 modules and then re-combining them with material made through total synthesis, we will be
89 able to access – in a concise manner – an interesting new structural domain related to the
90 natural polyether ionophores (Figure 1a). Some of the resulting compounds will maintain
91 ionophore-activity, but in others, due to subtle structural alterations, this activity will be
92 erased. As the molecular complexity will remain high such "ionophore-dead polyethers" may
93 carry novel biological activities which – with the advent of new methods for small molecule
94 bioactivity-profiling – it is becoming increasingly possible to explore. Importantly, this
95 synthetic approach harnesses the tremendous knowledge generated during prior synthesis
96 efforts for the construction of building blocks and for effecting fragment coupling.[10,11,12]

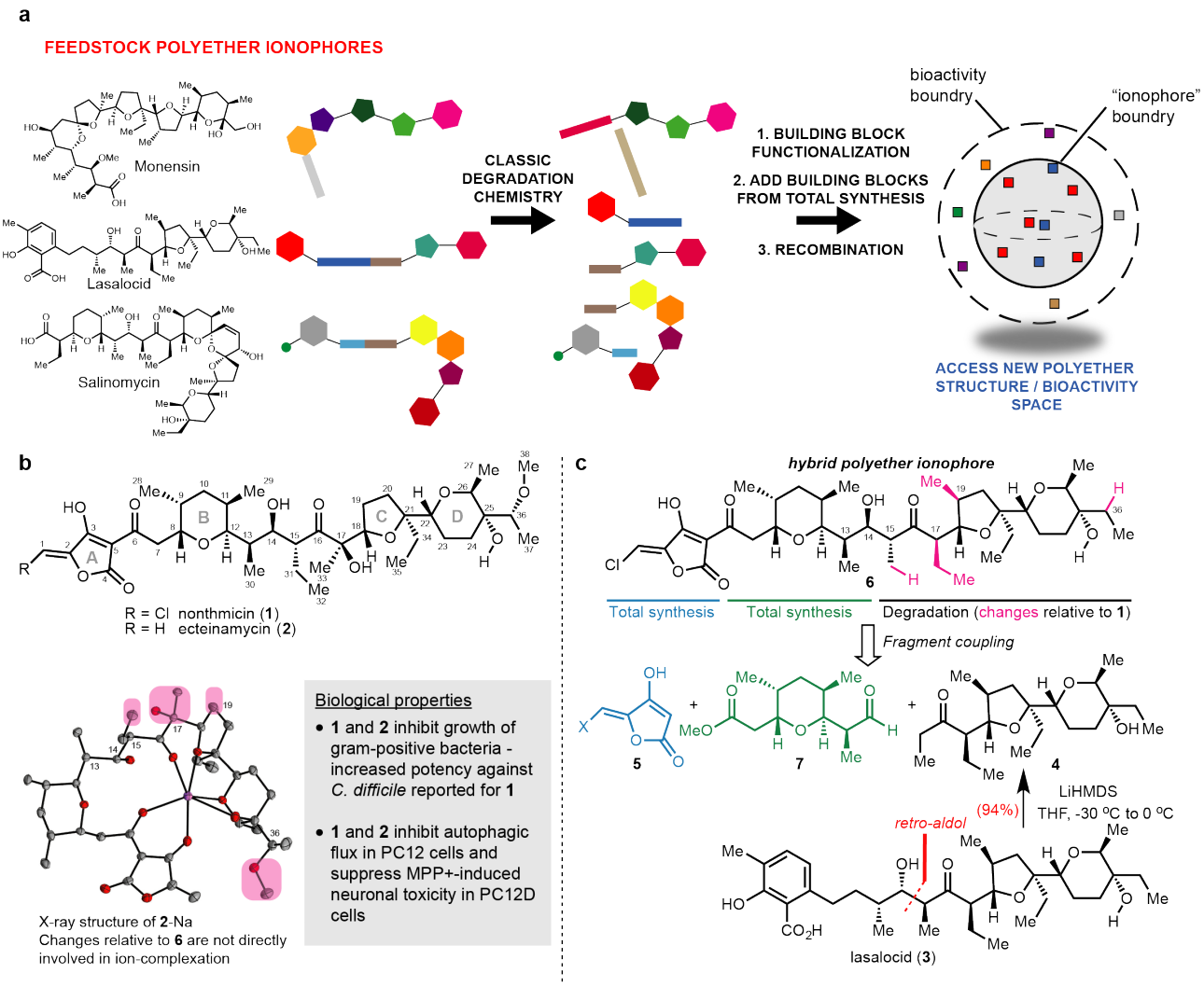

Figure 1 | Accessing structural diversity within the polyether ionophores. (a) Flowchart depicting the overall concept of reconstructing new polyether scaffolds by recycling elements from abundant feedstock polyether ionophores. The resulting "hybrid" molecules (non-red squares) are plotted in a hypothetical structure and bioactivity space to illustrate the relation of these compounds to the natural polyethers (red squares). The compounds that possess strong ionophore activity constitute a sub-space of a larger bioactivity-space that can be explored using hybrid polyethers. (b) Chemical structures and biological properties of polyether ionophores nonthmicin and ecteinamycin. The X-ray structure[35] depicts ecteinamycin bound to a single sodium-ion and chemical groups on the hydrophopic periphery that have been altered in the target hybrid polyether **6** have been circled in pink. No crystal structure of nonthmicin is available. (c) Chemical structure of the hybrid polyether **6** and

indication of the required fragments and the origin of these fragments. The main fragment, ketone **4**, can be obtained in a single synthetic step from lasalocid.

Results

Degradation of abundant polyether ionophores as the foundation of diversity synthesis of complex polyethers

To provide a proof-of-concept example, we placed our focus on a novel polyether ionophore, nonthmicin (**1**) (Figure 1b), recently reported to possess several types of interesting biological activities including antibiotic and neuroprotective activity.[35] Nonthmicin is of particular interest also for structural reasons as this natural product features an unprecedented chloromethylidene tetronic acid building block, that comprise the cation-binding group of the molecule. Another compound, ecteinamycin (**2**), which differs from **1** only by the absence of the chlorine-atom was reported almost simultaneously by the Bugni lab to be a potent anti-clostridial antibiotic (Figure 1b).[36] As we carefully inspected the structure of **1** and **2**, we noticed that the eastern portion (the C-D rings) displayed significant similarity to lasalocid (**3**) which is available on multi-kg scale. Based on knowledge generated during the classic structure-elucidation studies and then total synthesis of **3**,[37,38] we postulated that we could first liberate ketone **4** through a retro-aldol reaction and then develop a short and convergent route to advanced analogs of **1** (Figure 1c). Furthermore, inspection of the published X-ray crystal structure of **2**-Na[35] indicated that none of the resulting structural changes (pink in Figure 1b-c) would directly perturb coordination of the metal ion, at least from the solid-state structure. If successful, this approach would first of all test the fundamental question if swapping modules from different polyether ionophores would even be compatible with sustained antibiotic activity of the resulting hybrid molecules, with **6** as the initial target structure.

We started our studies by optimizing the retro-aldol reaction of **3** and found that exposure to LiHMDS at low temperature could result in the formation of ketone **4** in excellent yield (94%). This reaction has been carried out on >10 gram scale which underscores the high availability of an advanced building block such as **4**. We next focused our attention on the preparation of the two remaining building blocks, tetrahydropyran-derivative **7** and the challenging halomethylidene tetronic acid moiety **5** found in both **6** and **1**.

Construction of tetrahydropyran building block

The preparation of the targeted tetrahydropyran-derivative was started from (-)-2,4-dimethylglutaric acid (+)-α-methylbenzylamine salt (**9**)[39,40] (Figure 2). This salt was readily processed to the diol, which underwent mono-TBS protection followed by TEMPO/$PhI(OAc)_2$ oxidation[41] to afford aldehyde **11**. We initially proposed that the target building block could be constructed via an intramolecular oxa-Michael reaction[42] following initial cross-aldol coupling and Horner-Emmons reaction. However, only a trace of the cyclization product was observed and this route was eventually abandoned. Inspired by the Guindon's Narasin fragment synthesis,[43] we envisioned that the Mukaiyama aldol addition of a silylketene acetal to an oxocarbenium intermediate could also deliver the desired tetrahydropyran-derivative. Towards this end, aldehyde **11** first underwent a $CrCl_2$-catalyzed Nozaki-Hiyama-Kishi crotylation reaction[44] followed by the cleavage of the silyl ether with HOAc/THF/H_2O and TEMPO/$PhI(OAc)_2$-promoted lactone formation[45]. This afforded an inseparable diastereomeric mixture (1.8:1, 65% isolated yield) of lactone **12** which was reduced by DIBAL-H to deliver the lactol that was trapped *in situ* with Ac_2O to afford the corresponding acetate. At this stage, the major diastereomer **13** – ultimately found to be the desired configuration at C12 and C13 – could be isolated in 52% yield. Using $BF_3 \cdot OEt_2$ as the Lewis acid, **13** was then exposed to ((1-methoxyvinyl)oxy)trimethylsilane at low temperature which provided methyl ester **14** as a

single diastereomer (confirmed by X-ray) in excellent yield. Finally, ozonolysis of **14** followed by reductive work-up with triphenylphosphine generated aldehyde **7** (Figure 2).

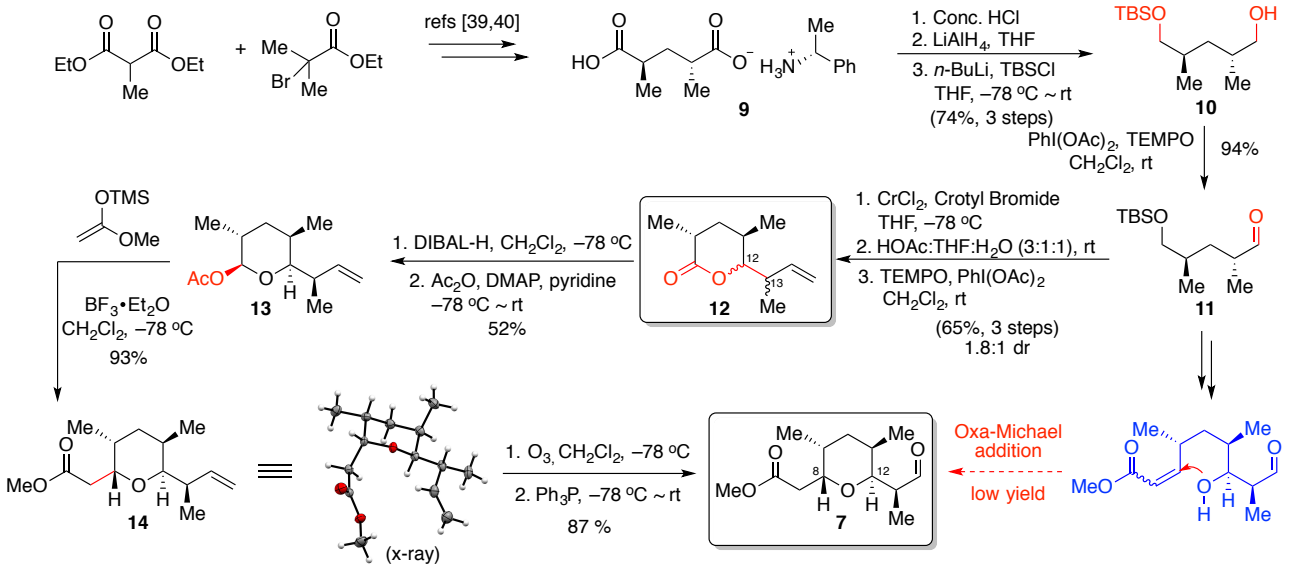

Figure 2 | Stereoselective synthesis of tetrahydropyran (THP) building block **7**. Two C-C coupling reactions are used to construct the stereocenters at C12 and C8, the latter being a highly selective addition of a silyl ketene acetal to the oxacarbenium-ion derived from **13** to generate the desired *trans*-C8,C12 relative configuration. In turn, the sequence was initiated from optically pure salt **9**, which is accessible via a known procedure. An alternative route to closure of the THP-ring via an oxa-Michael cyclization failed. THF = tetrahydrofuran, TBSCl = *tert*-butyldimethylsilyl chloride, TEMPO = (2,2,6,6-tetramethylpiperidin-1-yl)oxyl, DMAP = *N,N*-dimethylpyridine-4-amine, DIBAL-H = diisobutylaluminium hydride.

Synthesis of the halomethylidene tetronic acid building block

As the most intriguing structural subunit of nonthmicin and **6**, the 3-acyl-5-chloromethylidene tetronic acid became the next focus. With the overall aim to facilitate structural diversity within the polyether ionophores, the ideal approach to this building block should also allow access to other variants such as the methylidene and bromomethylidene species (Figure 3a). Although

the construction of this small and densely functionalized unit has not previously been realized, published syntheses of natural products containing the nonhalogenated version provide precious lessons (Figure 3b).[40-43] We opted not to pursue strategies based on organolithium reagent addition[42] due to the demand of fully protected coupling partners and the uncertain stability of the chlorovinyl moiety to organolithium chemistry. Likewise, approaches based on the Eschenmoser methenylation[43] were not considered due to unavailability of the chlorinated version of the reagent. Mindful of the presumed lability of the halomethylidene species and the multiple functional groups present in the coupling partner, we selected a DCC-mediated late-stage coupling as the most appealing strategy[41] and we therefore decided to target the tetronate building blocks bearing an easily-removable protecting group (TMSE). After a series of unsuccessful attempts (direct NMe_2/Cl exchange, construction of organotin or organoselenium intermediates, see Supporting Information Figure S1 for more details), we realized the synthesis of the halomethylidene tetronate via a formal C-H halogenation approach (Figure 3c). The *O*-TMSE protected tetronate **19** was prepared via intramolecular Wittig cyclization[41] from trityl protected α-hydroxyl TMSE ester **17** and the Bestmann reagent, and the methylidene group was installed via MsCl-mediated elimination. The formal C-H halogenation was then facilitated by dichlorination ($KMnO_4$-TMSCl)[44]/dibromination (Br_2)[45] of methylidene tetronate and subsequent elimination (DBU) to furnish the target halomethylidene tetronates **8a** and **8b** with desired (*Z*)-configuration.

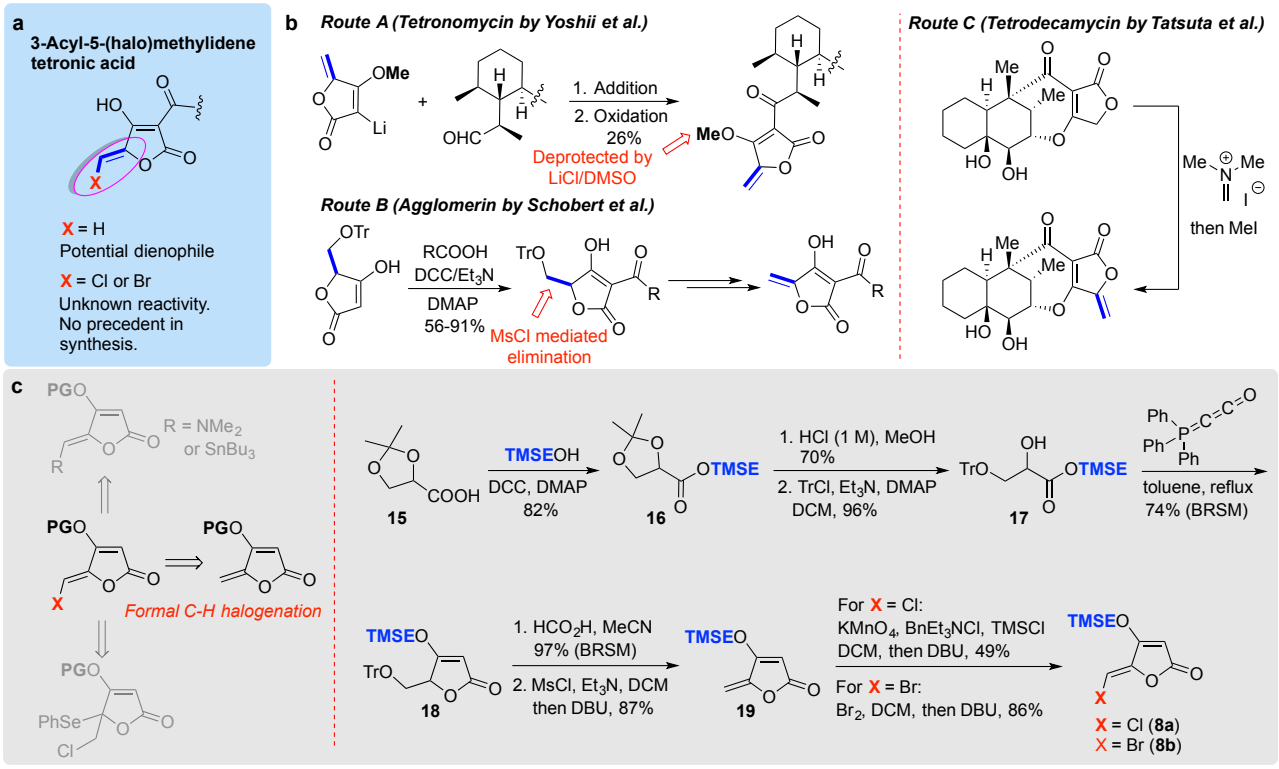

Figure 3 | Development of a synthesis of TMSE-protected 5-(halo)methylidene tetronic acid. (a) Chemical structure of the targeted 3-acyltetronic acid-derivatives found in nonthmicin/ecteinamycin and **6**. No previous syntheses of the halogenated variants have been reported. (b) Examples of known methods used to prepare non-halogenated variants. (c) From several synthesis strategies attempted (see also Figure S1, supporting information) a formal C-H halogenation of protected 5-methylidene tetronic acid was developed. Construction of the required TMSE-protected 5-methylidene precursor **19** for these reactions was carried out in 6 steps from the commercial racemic acetonide-protected glycerate **15**. This sequence allowed for preparation of both the chlorine and bromine-variants (**8a** and **8b**).

Aldol Fragment coupling

With access to the required building blocks, we initiated the fragment coupling sequence. Analysis of the composition of the stereotriad at C13-C15 in **6** suggests that the desired configuration could be achieved via the effectuation of an *anti*-aldol reaction with Felkin-control of the secondary alcohol at C14. This type of stereocontrol is usually reinforcing[46]

212 although in the present case, due to the stereogenic center at C17, double stereodifferentiation
213 in the aldol reaction is required.[47] We first attempted formation of the (*E*)-boron enolate from
214 **4** or the C25-OTES protected derivative **21** using (cHex)$_2$BCl-NEt$_3$ but useful conversion to the
215 enolate could not be achieved. In fact, the only known aldol reactions using **4** were carried out
216 in the classic syntheses of lasalocid **3**4 and utilized *in situ* formation of the zinc-enolate from **4**
217 which generates preferentially the configuration found in **3** – also *anti*-aldol-Felkin – and which
218 differs from the configuration needed to make **6** at all of the three stereocenters. Although this
219 aldol coupling utilized a different aldehyde compared to **7**, we evaluated the possibilities for
220 favoring the desired aldol product as being low. Consequently, we decided to instead rely on
221 the Lewis acid catalyzed Mukaiyama aldol reaction which is known to maintain Felkin-
222 selectivity. [48] Importantly, double stereodifferentiation in Mukaiyama aldol reactions is
223 established from classic studies by Evans[49] thus providing a theoretical framework for the
224 analysis of the key fragment coupling reaction. Despite the lack of very closely related reactions
225 in the literature, we expected that formation of the desired *anti*-aldol isomer (14*R*,15*R*; *anti*
226 15,17-Me↔Et) would still be challenging due to the intrinsic preference for *syn*-aldol products
227 in the Mukaiyama-aldol reaction and the combined diastereofacial bias from the stereocenters
228 already present in aldehyde **7** and ketone **4**. Formation of the *anti*-aldol products would
229 demand use of the (*Z*)-silylenolate, whereas the corresponding (*E*)-enolate could be expected
230 to reinforce the formation of a *syn*-aldol product (14*R*,15*S*; *syn* 15,17-Me↔Et). Our first
231 attempts at enolizing ketone **4** afforded some surprising results: While the (*Z*)-TES-enolate **20a**
232 could be readily formed with excess TESOTf and 2,6-lutidine with concomitant protection of
233 the tertiary alcohol at C25, formation of the corresponding (*E*)-enolate could not be accessed
234 cleanly (Figure 4a). After extensive experimentation, we found that substitution of 2,6-lutidine
235 with less hindered pyridine and inverting the sequence of reagent addition (pyridine added to
236 a pre-equilibrated solution of C25-OTES protected ketone **21** and TESOTf) could afford a nearly

1:1 mixture of the (*Z*)/(*E*)-TES-enolates (**20a**/**20b**) which could be partially separated by flash chromatography. Gratifyingly, upon exposure of the enolates to aldehyde **7** at low temperature in the presence of BF_3•OEt_2, aldol coupling proceeded in excellent yield (Figure 4b). Although we could detect formation of all four putative aldol diastereomers by TLC (P1-P4 based on silical gel mobility), the reaction using an enriched (ratio 1:2.3 *Z/E*) (*E*)-TES-enolate was highly selective for the P3-isomer (P2: 7%, P3: 81%) whereas the pure (*Z*)-TES-enolate afforded a mixture of P2 and P3 (P2: 56%, P3: 30%). Subsequent stereochemical assignment of the respective compounds by X-ray crystallography revealed P3 to be the (*14R*,*15S*)-configured product (**23**) in accord with the above analysis and P2 to be the desired isomer (14*R*,15*R*) (**22**).

End game coupling and purification

Both aldol products (**22** and **23**) underwent a two-step deprotection sequence, involving first Olah's reagent to remove the C25-OTES group and then trimethyltin hydroxide to cleave the methyl ester (Figure 4c).[50] The latter conditions were found to be critical to avoid retro-aldol cleavage.

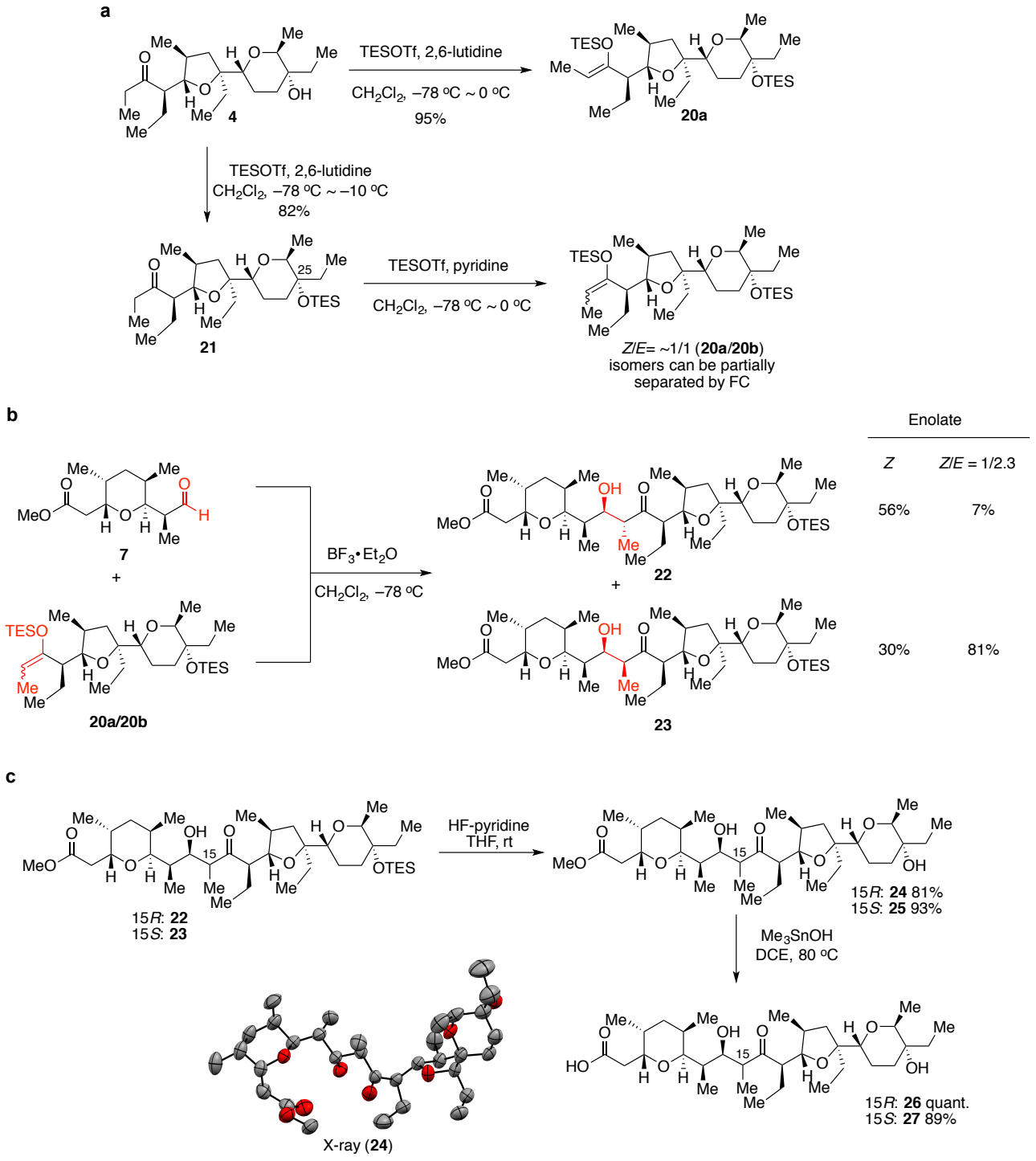

Figure 4 | Fragment-coupling via boron trifluoride-mediated Mukaiyama-aldol reaction. (a) The (*Z*)-TES-enolate **20a** could be readily obtained, but special procedures had to be developed to access mixtures of (*E*)- and (*Z*)-TES-enolates. Purification could be used to further enrich the (*E*)-TES-enolate **20b**. (b) Aldol reaction affords two major products (**22** and **23**) depending on the configuration of the silyl-enolate derived from ketone **4**. Compound **22** was confirmed by

X-ray analysis of derivative **24** to be the initially targeted aldol-product (c) Both aldol products **22** and **23** could be processed towards the final fragment coupling in two high-yielding steps. TESOTf = triethylsilyltrifluoromethanesulfonate, DCE = 1,2-dichloroethane.

With the desired acid fragments (**26** and **27**) and *O*-TMSE protected tetronates (**19** and **8a-b**) in hand, we started to investigate the final fragment coupling reaction. After TBAF-mediated deprotection of the *O*-TMSE group on **8a** and simple extraction, the crude tetronic acid was submitted to DCC coupling with carboxylic acid **26** (Figure 5a). Fortunately, the desired product **6** was smoothly formed in 24 hours with full conversion of **26**, and 59% yield (as the sodium salt, **6**-Na) was obtained by preparative HPLC using MeCN-10 mM NH_4HCO_3 as eluent.[35] It is worth to note that the sodium salt (formed by subsequent $NaHCO_3$ treatment and extraction) show much better solubility in organic solvents than the acid form, which indicates the formation of a lipophilic complex, a featured property of polyether ionophores. Encouraged by this result, the bromine-analog **29** and hydrogen-analog **30**, as well as the chlorine-analog **31** bearing 15-(*S*) configuration, were synthesized following the same procedure in 42-58% yields (Figure 5a). We managed to prepare crystals that were suitable for X-ray diffraction from both **6**, **29,** and **31** and the resulting structures revealed the formation of a cage-like structure by the "naturally-configured" 15-(*R*) analogs **6** and **29** while a dimeric complex was formed by the corresponding 15-(*S*)-configured compound **31**. This clearly indicates the critical role played by evolutionary conformational design[51] on the cation-binding properties of the polyether ionophores. Anticipating that small structural changes would potentially have a large impact on the biological activities, we finally generated an additional derivative of **32** (Figure 5a) by performing an *anti*-selective Evans-Saksena[52] reduction of the carbonyl group in **26** followed by coupling with the tetronic acid derived from **8a** (Figure S2).

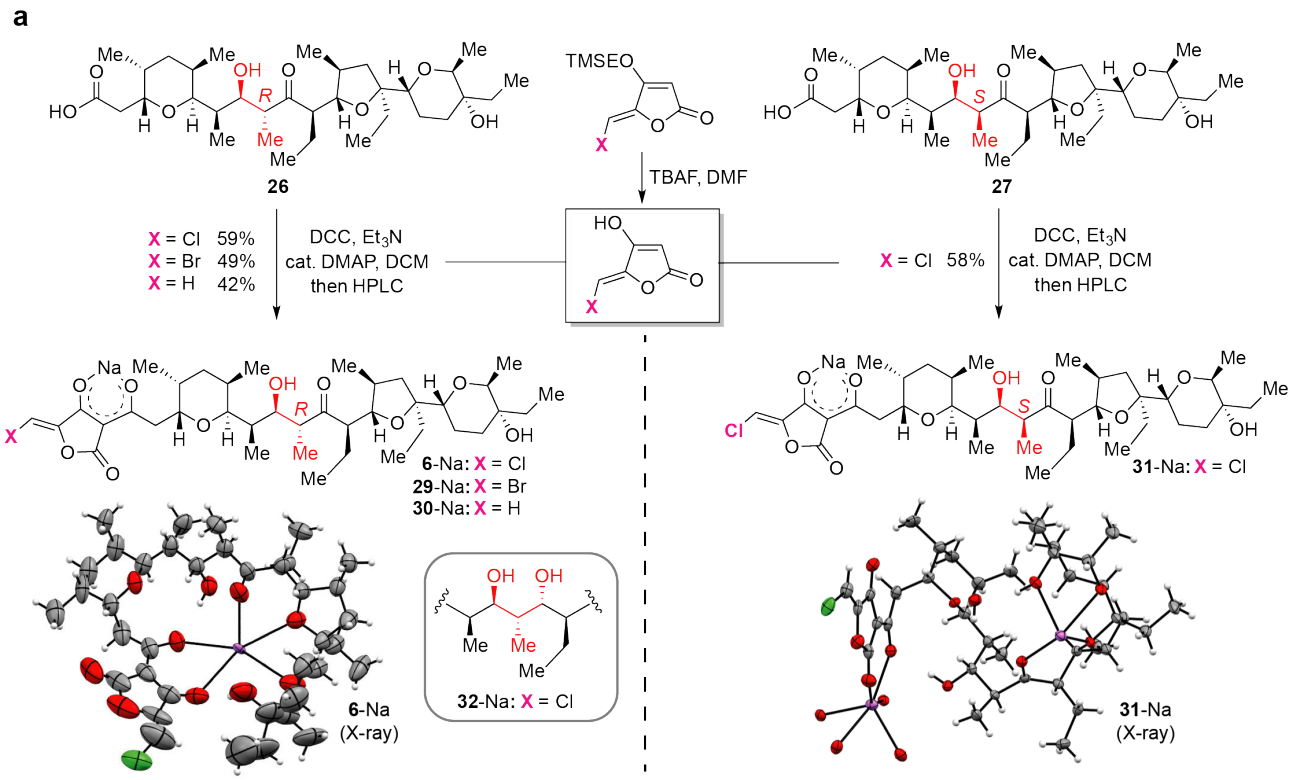

b

strain	MIC (μg/mL)							
	Lasalocid	**6**	**29**	**30**	**31**	**32**	salinomycin	vanco
S. aureus	2	8	4	32	>32	8	2	1
S. aureus MRSA USA 300 je2	2	8	8	32	>32	8-16	4	1
S. aureus ATCC 29213	4-8	8	8	32	>32	8-16	2	0.5
P. auroginosa	>32	>32	>32	nd	>32	nd	nd	>32
E. coli	>32	>32	>32	nd	>32	nd	nd	>32

cell line	IC_{50} (μM)							
	Lasalocid	**6**	**29**	**30**	**31**	**32**	salinomycin	vanco
U2OS	10±0.8	7.5±0.3	6.8±0.6	22±0.8	36±2	5.9±1.1	5.8±0.8	nd
MCF-7	6.3±2.2	16±2	13±1	26±2	42±7	6.8±0.6	4.5±1.5	nd

Figure 5. Final coupling sequence and biological activities of the hybrid tetronate polyethers. (a) Mild conditions were developed for effecting the coupling of unprotected (halo)-methylidene tetronates to acids **26** or **27**. The structures of **6**, **29** (see supporting information) and **31**, all as the sodium salts, were solved by X-ray diffraction. (b) Anti-bacterial activity and effects on mammalian cell viability were evaluated for all compounds using canonical polyether ionophores (salinomycin and lasalocid) and vancomycin as the controls. For full inhibition curves see supporting information Fig. S3 and Fig. S4. MIC-values is mean (*N=3*) and mammalian cell viability is mean ± sd (*N=3*). nd = not determined.

Antibacterial and anti-proliferative activity of hybrid tetronate polyethers

In order to probe the biological properties of the hybrid polyethers, we first performed an evaluation of their anti-bacterial activity against a small panel of *S. aureus* strains (gram-positive) and two different gram-negative strains (*P. auroginosa* and *E. Coli*). To our delight, these experiments showed that compounds **6** and **29** did indeed maintain antibacterial activity with a potency comparable to lasalocid and salinomycin against both wild-type and drug-resistant *S. aureus* (Figure 5b and Fig. S3). Comparing the activity of **6**, **29**, and **30**, it is clear that the halogen augments the contribution of the tetronic acid as the methylene-analog **30** was significantly less active. Compound **31**, being epimeric to **6** at C15, was completely devoid of activity (MIC >32 μg/mL), while **32** was equally active to **6**. None of the compounds were active against gram-negative strains. Next, we evaluated inhibitory activity against human cancer cell lines (U2OS and MCF7, Figure 5b) which afforded micromolar IC_{50}'s of all the compounds. We noted however distinctively more shallow inhibition curves for the natural products, especially salinomycin (Figure S4), indicating that these compounds perturb mammalian cells over a larger span of concentrations.

Bioactivity analysis using morphological profiling

Modulation of cell viability is a coarse measure of the biological activity of a small molecule. To provide a more nuanced analysis of the activities of the polyethers in mammalian cells, we subjected all compounds to morphological profiling[53,54] in U2OS osteosarcoma cells. This image-based method can generate bioactivity profiles of small molecules in an unbiased manner that can be used statistically to reveal mechanistic similarities. Given the limited detailed knowledge about the activity of polyether ionophores in mammalian cells, this approach could potentially illuminate how structural changes impact the overall cellular perturbation.

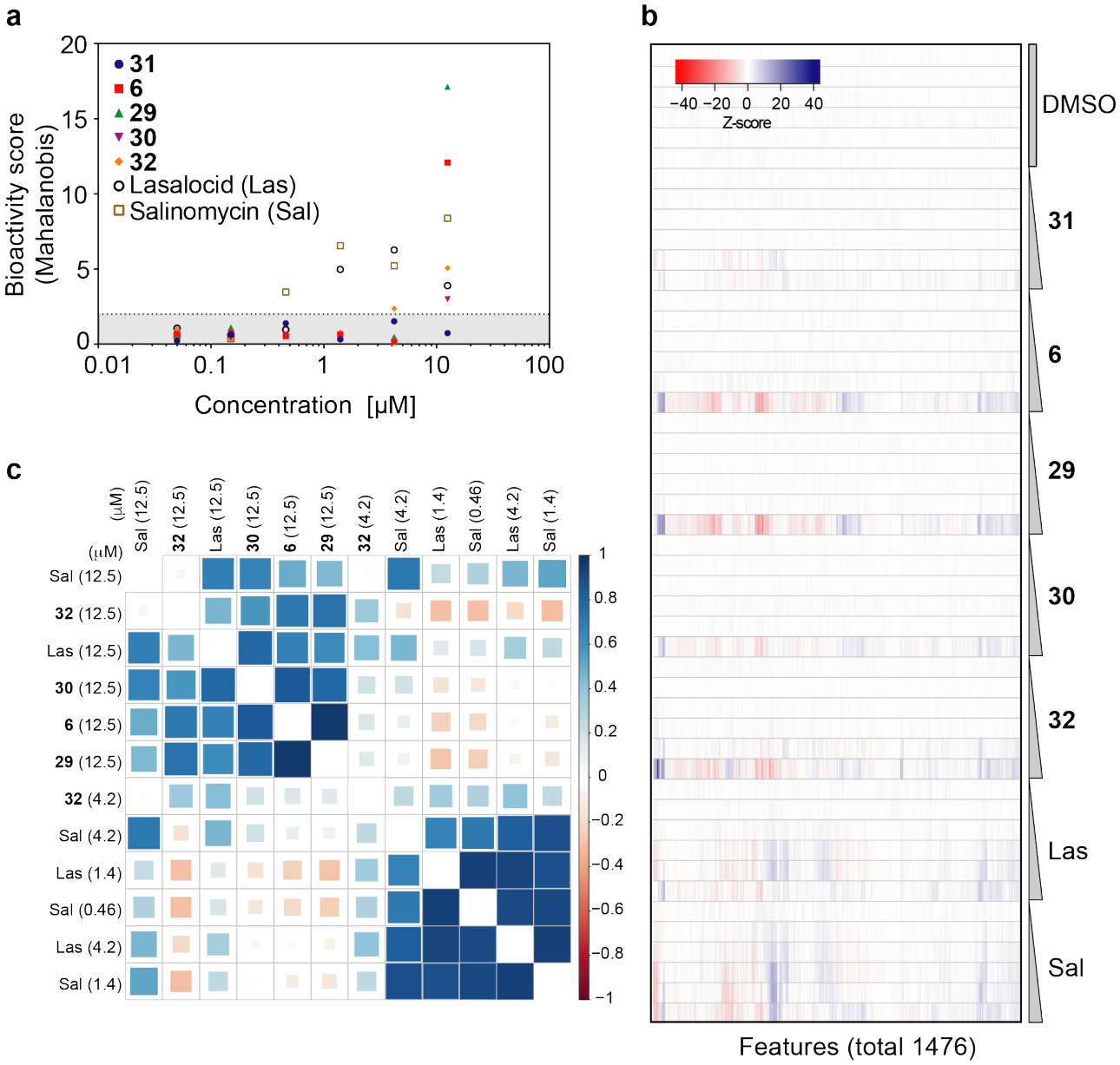

Figure 6. Morphological profiling. (a) Bioactivity scores as measured by the Mahalanobis distance to DMSO control. The grey area (Mahalanobis distance < 2) indicates inactivity. Sal and Las show activity at a lower concentration than the hybrid ionophores. (b) Heatmap of full morphological profiles. The color corresponds to the Z-score calculated from averaged profiles. **6**, **29**, **30** and **32** shows similar profiles at the highest concentration (12.5 µM). Note that the shown DMSO treatments are kept separate from the other DMSO controls used in the normalization step. (c) Pearson correlation matrix of active compounds ordered by hierarchical clustering. Two clusters with distinct bioactivities are formed, one containing lower

concentrations of Las and Sal and one containing high concentrations of both hybrid ionophores and Las and Sal. The color and size of the squares indicates the Pearson correlation coefficient.

All compounds were tested at six different concentrations (0.05-12.5 μM) and we used salinomycin and lasalocid as controls. First, we calculated the Mahalanobis distance for all compound treatments to DMSO controls as an overall measure for above-background activity in the assay (Figure 6a and Figure S5-7). Using a rather strict threshold (see Supporting Information for details and Fig. S6), hybrid polyethers **6**, **29** and **30** were scored inactive at all but the highest concentration (12.5 μM), compound **32** had an active profile also at 4.2 μM, and epimer **31** was inactive at all tested concentrations.

In contrast to the hybrid polyethers, salinomycin and lasalocid were both active at lower concentrations (by 9-27 fold, Figure 6a). The full bioactivity profiles were plotted (Figure 6b) and a Pearson correlation matrix was calculated for all compound treatments exceeding the activity threshold (Figure 6c). We were quite surprised by the outcome of this analysis: The activity profiles of salinomycin and lasalocid over several concentrations were clustered (P 0.83-0.94) whereas the hybrid ionophores – at the highest concentration – formed a distinct cluster (Figure 6c). Interestingly, high concentrations of both lasalocid and salinomycin also afforded profiles with significant correlations ($P > 0.63$) to this cluster as did a subset of a reference panel of different growth inhibitory compounds (Figure S7) suggestive of a general toxicity profile. In contrast, the bioactivity profiles associated with the first cluster (low concentration Sal and Las) did not show significant correlations with profiles in our reference panel.

Given the recent strong interest in the cellular activity of salinomycin[29,30,31] and the significant difference in both the chemical structures and ionophore-properties associated with

salinomycin (a K-ionophore as previously mentioned) and lasalocid (a Ca-ionophore), the apparent mechanistic similarity - which is suggested by our data - demands future attention. Another important observation from these experiments is that the hybrid polyethers appear to be more 'silent' in mammalian (U2OS) cells despite having similar anti-bacterial activity compared to lasalocid and salinomycin.

Discussion

As we consider the potential future role of polyether ionophores in biomedicine the following questions are important: 1) Can polyether ionophores be identified with a sufficiently large therapeutic window to be considered as human antibiotics; 2) Can the activity of these compounds be expanded to also target gram-negative strains; 3) Which aspects of mammalian cell biology can be modulated by polyethers? To answer all of these questions, a large increase in accessible compounds within the overall polyether-class is needed. For instance, systematic tests in expanded bacterial panels may reveal activity patterns that can inform further structural variations and in combination with investigations of cross-resistance to other antibiotics new synthetic lead structures can be identified. The use of unbiased bioactivity profiling in mammalian cells – as we demonstrate here – may both pinpoint polyethers with unusual activity patterns that can be subjected to focused mechanistic investigations as well as variants that appear 'silent' in mammalian cells while maintaining antibacterial activity. Hybrid polyether **29** is a good example of the latter. The compound has a ratio of 0.5 between the average (molar) MIC across the *S. aureus* strains and the first bioactive concentration in U2OS cells whereas the equivalent numbers for salinomycin and lasalocid are 5.8 and 2.4, respectively. However, we currently do not understand the mechanistic and structural factors that underlie these differences. On a similar note, despite having closely related structures, compounds **6** and **29** are less active (up to 64 fold) compared to the remarkably low MIC-values

reported for ecteinamycin (**2**)[36]. The specific reason(s) for this difference is also of strong interest. We e.g. note that in the solid state, the sodium-bound forms of **2** and **6/29** differ subtly due to the structural variations close to the C17-C18 bond (Figure S8). How these changes affect the relative selectivity and efficiency of ion-transport should be addressed in future studies.

In conclusion, it is evident that complex polyethers can affect both eukaryotic and prokaryotic cells in ways that transcend the canonical model of pleiotropic ion-transporters and therefore that a strategic merger of synthesis and biology broadly across this class of compounds is timely. The overall synthesis principle of reusing parts of the abundant polyethers that we outline in this paper - fueled by novel methods (such as MicroED[55]) to expedite structural assignment of complex molecules and methods to study mechanisms-of-action - may therefore contribute to the effective resurrection of this whole class of compounds.

Acknowledgements

TBP acknowledges financial support from the Carlsberg foundation (grant CF17-0800) and Independent Research Fund Denmark (Sapere Aude 2 grant 6110-00600A). We are grateful to Eric Jung and Anja Johnbeck for technical assistance with organic synthesis, Anders Bodholt Nielsen for technical assistance with NMR spectroscopy, and Iben Charlotte Stensgaard Jensen for technical assistance with microbiology.

Author contributions

TBP conceived and supervised the study. TBP, SL, and HL designed experiments. SL, HL, and CNP performed organic synthesis. EBS conducted cell biological experiments and analyzed data. TT supervised microbiology experiments and analyzed data. PN carried out x-ray crystallographic analyses. TBP, SL, HL wrote the manuscript with input from all authors.

Competing financial interests

The authors declare no competing financial interests

Methods

Organic Synthesis

All reactions were conducted in flame-dried glassware under an atmosphere of argon unless otherwise stated. CH_2Cl_2, MeCN, THF and PhMe were dried over aluminium oxide via an MBraun SPS-800 solvent purification system. DCE, DMF, MeOH and pyridine were purchased as anhydrous. The dryness of solvents was controlled via Karl Fischer tritration. Reagents were used as received from commercial suppliers unless otherwise stated (Sigma Aldrich, Merck, AK Scientific, and Fluorochem). Et_3N and DIPEA were dried by stirring for at least 30 minutes over CaH_2 followed by distillation onto preactivated molecular sieves (4 Å). Concentration *in vacuo* was performed using a rotary evaporator with the water bath temperature at 30 °C, or 40 °C, followed by further concentration using a high vacuum pump. TLC analysis was carried out on silica coated aluminum foil plates (Merck Kieselgel 60 F254). The TLC plates were visualized by UV irradiation and/or by staining with either CAM stain ($(NH_4)_6Mo_7O_{24}{\cdot}4H_2O$ (10 g), Cerric ammonium sulfate (4 g), 10% H_2SO_4 (aq., 400 mL)), ninhydrin stain (ninhydrin (12 g) and AcOH (12 mL) in *n*-butanol (400 mL)) or $KMnO_4$ stain ($KMnO_4$ (5.0 g), 5 % NaOH (aq., 8.3 mL) and K_2CO_3 (33.3 g) in H_2O (500 mL)). Molecular sieves were activated by drying in the oven at 120 °C for at least 24 hours, before they were heated in a microwave at maximum power for 2 minute, followed by evaporation of the formed vapour on the high vacuum line. This was repeated 3-4 times, and finished by gently flame-drying the flask containing the molecular sieves. Flash column chromatography (FCC) was carried out using silica gel (230-400 mesh particle size, 60 Å pore size) as stationary phase. Infrared spectra (IR) were acquired on a PerkinElmer Spectrum TwoTM UATR. Mass spectra (HRMS) were recorded on a Bruker Daltonics MicrOTOF time-of-flight spectrometer with positive electrospray ionization, or

428 negative ionization when stated. Nuclear magnetic resonance (NMR) spectra were recorded on
429 a Varian Mercury 400 MHz spectrometer or a Bruker BioSpin GmbH 400 MHz spectrometer,
430 running at 400 and 101 MHz for ^{1}H and ^{13}C, respectively. Chemical shifts (δ) are reported in
431 ppm relative to the residual solvent signals ($CDCl_3$: 7.26 ppm ^{1}H NMR, 77.16 ppm ^{13}C NMR,
432 CD_3OD: 3.31 ppm ^{1}H NMR, 49.00 ppm ^{13}C NMR, ^{6}d-DMSO: 2.50 ppm ^{1}H NMR, 39.52 ppm ^{13}C
433 NMR. Multiplicities are indicated using the following abbreviations: s = singlet, d = doublet, t =
434 triplet, q = quartet, h = heptet, m = multiplet, br = broad. LC-MS and HPLC analysis and
435 purification were performed using a Gilson HPLC system.
436
437 For all remaining methods, see the supplementary information.
438
439 **References**

[1] A. Agtarap, J. Chamberlin, J. W. Pinkerton and L. Steinrauf, *J. Am. Chem. Soc.*, **89**, 5737 (1967).

[2] Westley, J. ed., (1982). *Polyether Antibiotics - Naturally Occurring Acid Ionophores*. 1st ed. New York: Marcel Dekker.

[3] Dutton, C. J., Banks, B. J. & Cooper, C. B. Polyether ionophores. *Nat. Prod. Rep.* **12,** 165–181 (1995).

[4] Nakata, T. *et al.* A Total Synthesis of Lasalocid A. *J. Am. Chem. Soc.* **100,** 2933–2935 (1978).

[5] Fukuyama, T. *et al.* Total Synthesis of Monensin. 3. Stereocontrolled Total Synthesis of Monensin. *J. Am. Chem. Soc.* **101,** 262–263 (1979).

[6] Collum, D. B., McDonald, J. H. & Still, W. C. Synthesis of the Polyether Antibiotic Monensin. 3. Coupling of Precursors and Transformation to Monensin1. *J. Am. Chem. Soc.* **102,** 2120–2121 (1980).

[7] Ireland, R. E., Thaisrivongs, S. & Wilcox, C. S. Total Synthesis of Lasalocid A (X537A). *J. Am. Chem. Soc.* **102,** 1155–1157 (1980).

[8] Evans, D. A., Bender, S. L. & Morris, J. Total Synthesis of the Polyether Antibiotic X-206. *J. Am. Chem. Soc.* **110,** 2506–2526 (1988).

[9] Corey, E. J. & Cheng, X.-M. *The logic of chemical synthesis*. (Wiley, 1995).

[10] Faul, M. M. & Huff, B. E. Strategy and Methodology Development for the Total Synthesis of Polyether Ionophore Antibiotics. *Chem. Rev.* **100,** 2407–2473 (2000).

[11] Song, Z., Lohse, A. G. & Hsung, R. P. Challenges in the synthesis of a unique mono-carboxylic acid antibiotic, (+)-zincophorin. *Nat. Prod. Rep.* **26,** 560–571 (2009).

[12] Liu, H., Lin, S., Jacobsen, K. M. & Poulsen, T. B. Chemical syntheses and chemical genetics of carboxyl polyether ionophores: Recent highlights, *Angew. Chem. Int. Ed.* (2019), doi: 10.1002/anie.201812982

[13] Schwan, J. & Christmann, M. Enabling strategies for step efficient syntheses. *Chem. Soc. Rev.* **47,** 7985–7995 (2018).

[14] Gaich, T. & Baran, P. S. Aiming for the ideal synthesis. *J. Org. Chem.* **75,** 4657–4673 (2010).

[15] Kasun, Z. A., Gao, X., Lipinski, R. M. & Krische, M. J. Direct Generation of Triketide Stereopolyads via Merged Redox-Construction Events: Total Synthesis of (+)-Zincophorin Methyl Ester. *J. Am. Chem. Soc.* **137,** 8900–8903 (2015).

[16] Wang, G. & Krische, M. J. Total Synthesis of (+)-SCH 351448: Efficiency via Chemoselectivity and Redox-Economy Powered by Metal Catalysis. *J. Am. Chem. Soc.* **138,** 8088–8091 (2016).

[17] Chen, L.-A., Ashley, M. A. & Leighton, J. L. Evolution of an Efficient and Scalable Nine-Step (Longest Linear Sequence) Synthesis of Zincophorin Methyl Ester. *J. Am. Chem. Soc.* **139,** 4568–4573 (2017).

[18] Huffman, B. J. & Shenvi, R. A. Natural Products in the 'Marketplace': Interfacing Synthesis and Biology. *J. Am. Chem. Soc.* **141**, 3332–3346 (2019).

[19] Schreiber, S. L. Target-oriented and diversity-oriented organic synthesis in drug discovery. *Science* **287,** 1964–1969 (2000).

[20] Wetzel, S., Bon, R. S., Kumar, K. & Waldmann, H. Biology-oriented synthesis. *Angew. Chem. Int. Ed.* **50,** 10800–10826 (2011).

[21] Könst, Z. A. *et al.* Synthesis facilitates an understanding of the structural basis for translation inhibition by the lissoclimides. *Nat. Chem.* **9,** 1140–1149 (2017).

[22] Wilson, R. M. & Danishefsky, S. J. Small molecule natural products in the discovery of therapeutic agents: the synthesis connection. *J. Org. Chem.* 71, 8329–8351 (2006).

[23] Huigens, R. W. *et al.* A ring-distortion strategy to construct stereochemically complex and structurally diverse compounds from natural products. *Nat. Chem.* **5,** 195–202 (2013).

[24] Abbasov, M. E. *et al.* Simplified immunosuppressive and neuroprotective agents based on gracilin A. *Nat. Chem.* **11,** 342–350 (2019).

[25] Seiple, I. B. *et al.* A platform for the discovery of new macrolide antibiotics. *Nature* **533,** 338–345 (2016).

[26] Richter, M. F. *et al.* Predictive compound accumulation rules yield a broad-spectrum antibiotic. *Nature* **545,** 299–304 (2017).

[27] Focused analogs of polyether ionophores have been made. See especially ref. 2. A recent example for salinomycin: Antoszczak, M. et al. Biological activity of doubly modified salinomycin analogs - Evaluation in vitro and ex vivo, *Eur. J. Med. Chem.* 156, 510–523 (2018).

[28] Versini, A. *et al.* Chemical biology of salinomycin. *Tetrahedron* **74,** 5585–5614 (2018).

[29] Gupta, P. B. *et al.* Identification of selective inhibitors of cancer stem cells by high-throughput screening. *Cell* **138,** 645–659 (2009).

[30] Mai, T. T. *et al.* Salinomycin kills cancer stem cells by sequestering iron in lysosomes. *Nat. Chem.* **9,** 1025–1033 (2017).

[31] Wang, F. *et al.* Nucleolin Is a Functional Binding Protein for Salinomycin in Neuroblastoma Stem Cells. *J. Am. Chem. Soc.* **141**, 3613–3622 (2019).

[32] Chapman, H. D., Jeffers, T. K. & Williams, R. B. Forty years of monensin for the control of coccidiosis in poultry, *Poultry Sci.* **89**, 1788–1801 (2010).

[33] Goodrich, R. D. et al. Influence of monensin on the performance of cattle. *J. Anim. Sci.* **58**, 1484–1498 (1984).

[34] Kevin II, D. A., Meujo, D. A. & Hamann, M. T. Polyether ionophores: broad-spectrum and promising biologically active molecules for the control of drug-resistant bacteria and parasites. *Expert Opin. Drug Discov.* **4**, 109–146 (2009)

[35] Igarashi, Y. *et al.* Nonthmicin, a Polyether Polyketide Bearing a Halogen-Modified Tetronate with Neuroprotective and Antiinvasive Activity from Actinomadura sp. *Org. Lett.* **19,** 1406–1409 (2017).

[36] Wyche, T. P. *et al.* Chemical Genomics, Structure Elucidation, and in Vivo Studies of the Marine-Derived Anticlostridial Ecteinamycin. *ACS Chem. Biol.* **12,** 2287–2295 (2017).

[37] Westley, J. W., Evans, R. H., Williams, T. & Stempel, A. Structure of antibiotic X-537A. *J. Chem. Soc. D*, 71–72 (1970).

[38] Westley, J. W., Evans, R. H., Williams, T. & Stempel, A. Pyrolytic Cleavage of Antibiotic X-537A and Related Reactions. *J. Org. Chem.* **38,** 3431–3433 (1973).

[39] Gruenfeld, N. *et al*. Angiotensin Converting Enzyme Inhibitors: Derivatives l-Glutarylindoline-2-carboxylic Acid. *J. Med. Chem.* **26**, 1277–1282 (1983).

[40] Lautens, M., Colucci, J. T., Hiebert, S. & Smith, N. D. Total Synthesis of Ionomycin Using Ring-Opening Strategies. *Org. Lett.* **4**, 1879–1882 (2002)

[41] Mico, A. D., Margarita, R., Parlanti, L., Vescovi, A. & Piancatelli, G. A Versatile and Highly Selective Hypervalent Iodine (III)/2,2,6,6-Tetramethyl-1-piperidinyloxyl-Mediated Oxidation of Alcohols to Carbonyl Compounds. *J. Org. Chem.* **62,** 6974–6977 (1997).

[42] Zhang, Z. & Tong, R. Synthetic Approaches to 2, 6-*trans*-Tetrahydropyrans. *Synthesis* **49**, 4899–4916 (2017).

[43] Brazeau, J.-F. *et al*. Stereocentrolled Synthesis of C1-C17 Fragment of Narasin via a Free Radical-Based Approach. *Org. Lett.* **12**, 36–39 (2010).

[44] Hiyama, T., Kimura, K. & Nozaki, H. Chromium (II) Mediated Threo Selective Synthesis of Homoallyl Alcohols *Tetrahedron Lett.* **22**, 1037–1040 (1981).

[45] Hansen, T. M. *et al*. Highly Chmoselective Oxidation of 1, 5-diols to δ-lactones with TEMPO/BAIB. *Tetrahedron Lett.* **44**, 57–59 (2003)

[40] Zografos, A. L. & Georgiadis, D. Synthetic strategies towards naturally occurring tetronic acids. *Synthesis* 3157–3188 (2006).

[41] Schobert, R. & Jagusch, C. Solution-phase and solid-phase syntheses of enzyme inhibitor RK-682 and antibiotic agglomerins. *J. Org. Chem.* **79**, 6129–6132 (2005).

[42] Hori, K., Hikage, N., Inagaki, A., Mori, S., Nomura, K. & Yoshii, E. Total synthesis of tetronomycin. *J. Org. Chem.* **57**, 2888–2902 (1992).

[43] Tatsuta, K., Suzuki, Y., Furuyama, A. & Ikegami, H. The first total synthesis of a tetracyclic antibiotic, (-)-tetrodecamycin. *Tetrahedron Lett.* **47**, 3595–3598 (2006).

[44] Markó, I. E., Richardson, P. R., Bailey, M., Maguire, A. R. & Coughlan, N. Selective manganese-mediated transformations using the combination: $KMnO_4/Me_3SiCl$. *Tetrahedron Lett.* **38**, 2339–2342 (1997).

[45] Sabbah, M., Bernollin, M., Doutheau, A., Soulère, L. & Queneau, Y. *Med. Chem. Commun.* **4**, 363–366 (2013).

[46] Roush, W. R. Concerning the Diastereofacial Selectivity of the Aldol Reactions of α-Methyl Chiral Aldehydes and Lithium and Boron Propionate Enolates. *J. Org. Chem.* **56,** 4151–4157 (1991).

[47] Masamune, S., Choy, W., Petersen, J. S. & Sita, L. R. Double Asymmetric Synthesis and a New Strategy for Stereochemical Control in Organic Synthesis. *Angew. Chem. Int. Ed.* **24,** 1–30 (1985).

[48] Heathcock, C. H. & Flippin, L. A. Acyclic Stereoselection. 16. High Diastereofacial Selectivity in Lewis Acid Mediated Additions of Enolsilanes to Chiral Aldehydes. *J. Am. Chem. Soc.* **105,** 1667–1668 (1983).

[49] Evans, D. A., Yang, M. G., Dart, M. J., Duffy, J. L. & Kim, A. S. Double Stereodifferentiating Lewis Acid-Promoted (Mukaiyama) Aldol Bond Constructions. *J. Am. Chem. Soc.* **117,** 9598–9599 (1995).

[50] Nicolaou, K. C., Estrada, A. A., Zak, M., Lee, S. H., Safina, B. S. A mild and selective method for the hydrolysis of esters with trimethyltin hydroxide, *Angew. Chem. Int. Ed.* **44**, 1378–1382 (2005)

[51] Hoffmann, R. W., Conformation design of open-chain compounds, *Angew. Chem. Int. Ed.* **39**, 2054–2070 (2000)

[52] Evans, D., Chapman, K. & Carreira, E. Directed reduction of β-hydroxy ketones employing tetramethylammonium triacetoxylborohydride. *J. Am. Chem. Soc.* **110**, 3560–3578 (1988).

[53] Bray, M.-A. *et al.* Cell Painting, a high-content image-based assay for morphological profiling using multiplexed fluorescent dyes. *Nat. Protoc.* **11,** 1757–1774 (2016).

[54] Svenningsen, E. B. & Poulsen, T. B. Establishing cell painting in a smaller chemical biology lab – A report from the frontier. *Bioorg. Med. Chem.* **27**, 2609–2615 (2019).

[55] Nannenga, B. L. & Gonen, T. The cryo-EM method microcrystal electron diffraction (MicroED). *Nat. Meth.* **16,** 369–379 (2019).

Diversity focused semisyntheses of tetronate polyether ionophores

Shaoquan Lin[1,‡], Han Liu[1,‡], Esben B. Svenningsen[1], Christine N. Pedersen[1], Peter Nørby[1], Thomas Tørring[2], Thomas B. Poulsen[1,*]

[1] Department of Chemistry, Aarhus University, Langelandsgade 140, DK-8000, Aarhus C, Denmark.

[2] Department of Engineering – Microbial Biosynthesis, Aarhus University, Gustav Wieds Vej 10, DK-8000, Aarhus C, Denmark

*e-mail: thpou@chem.au.dk

‡ These authors contributed equally

Supplementary Information

Supplementary Figures

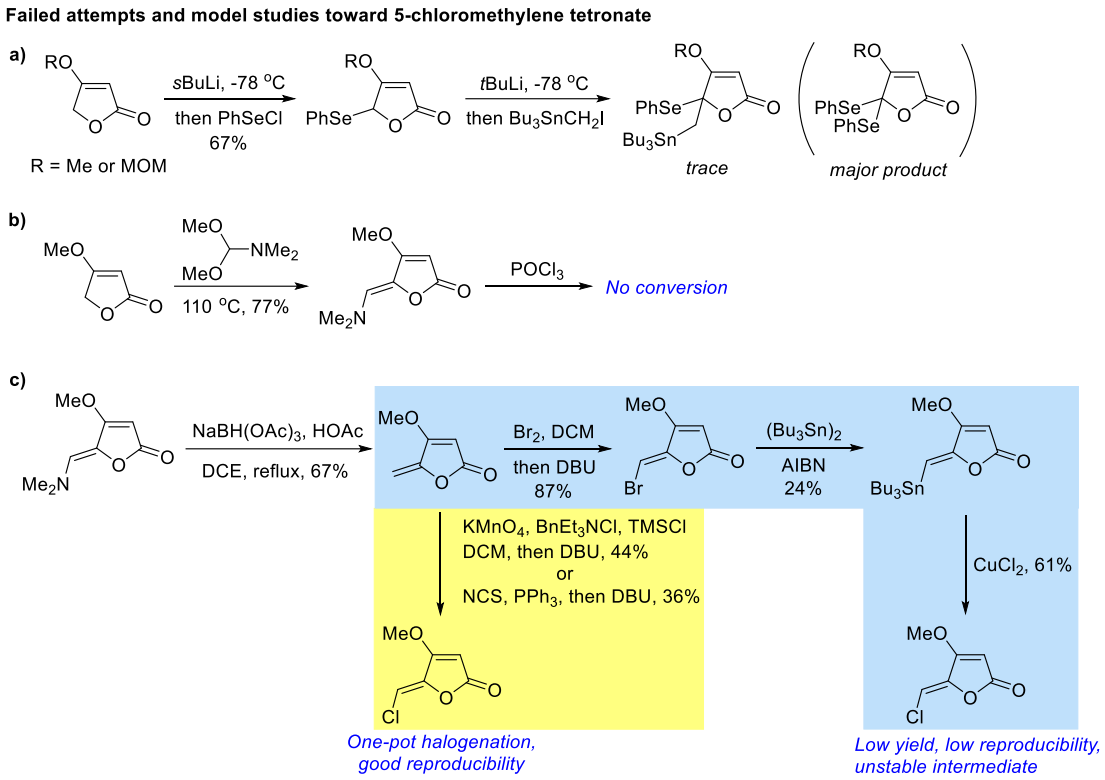

Figure S1 Failed attempts and model studies toward 5-chloromethylidene tetronate. a) Unsuccessful synthesis of 5-tributylstannylmethylidene tetronate. b) Unsuccessful chlorination of 5-dimethylaminomethylidene tetronate. c) Direct and indirect chlorination of 5-methylidene tetronate.

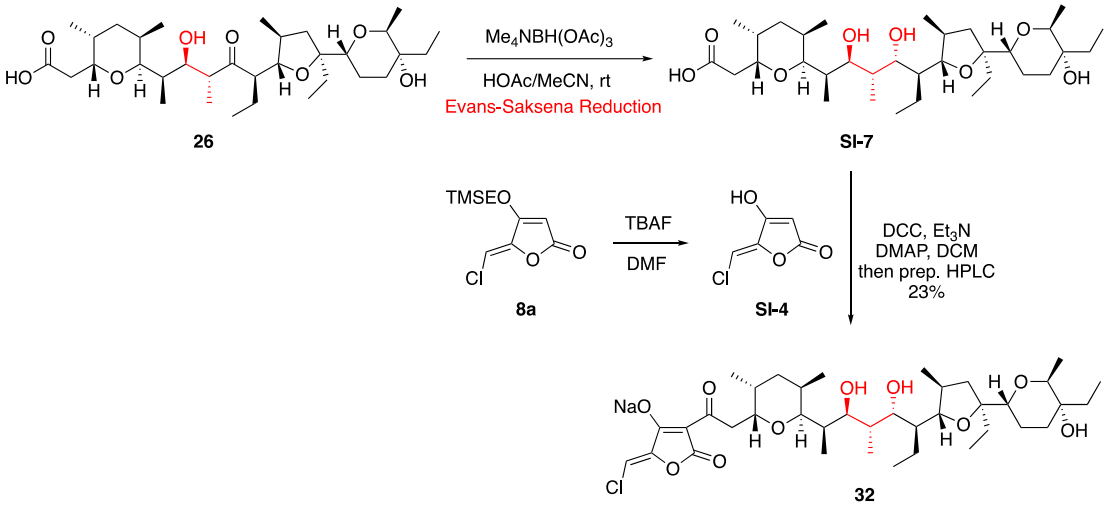

Figure S2 Synthesis of the analog **32** through *anti*-selective reduction followed by coupling with 5-chloromethylidene tetronate.

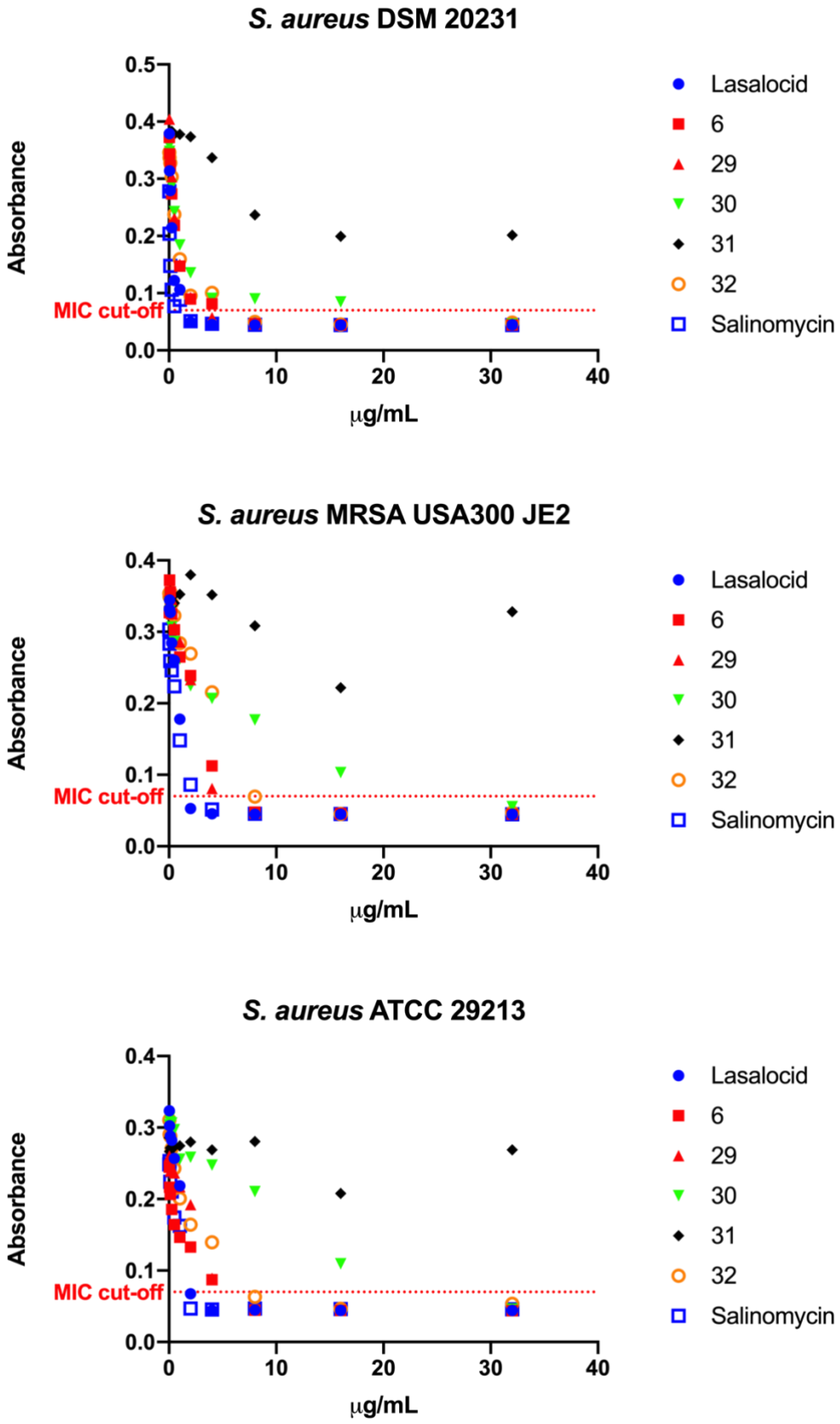

Figure S3. Full dose response curves for MIC determination in *S. aureus*. Vancomycin is omitted from these plots. Data points are means of three replicates.

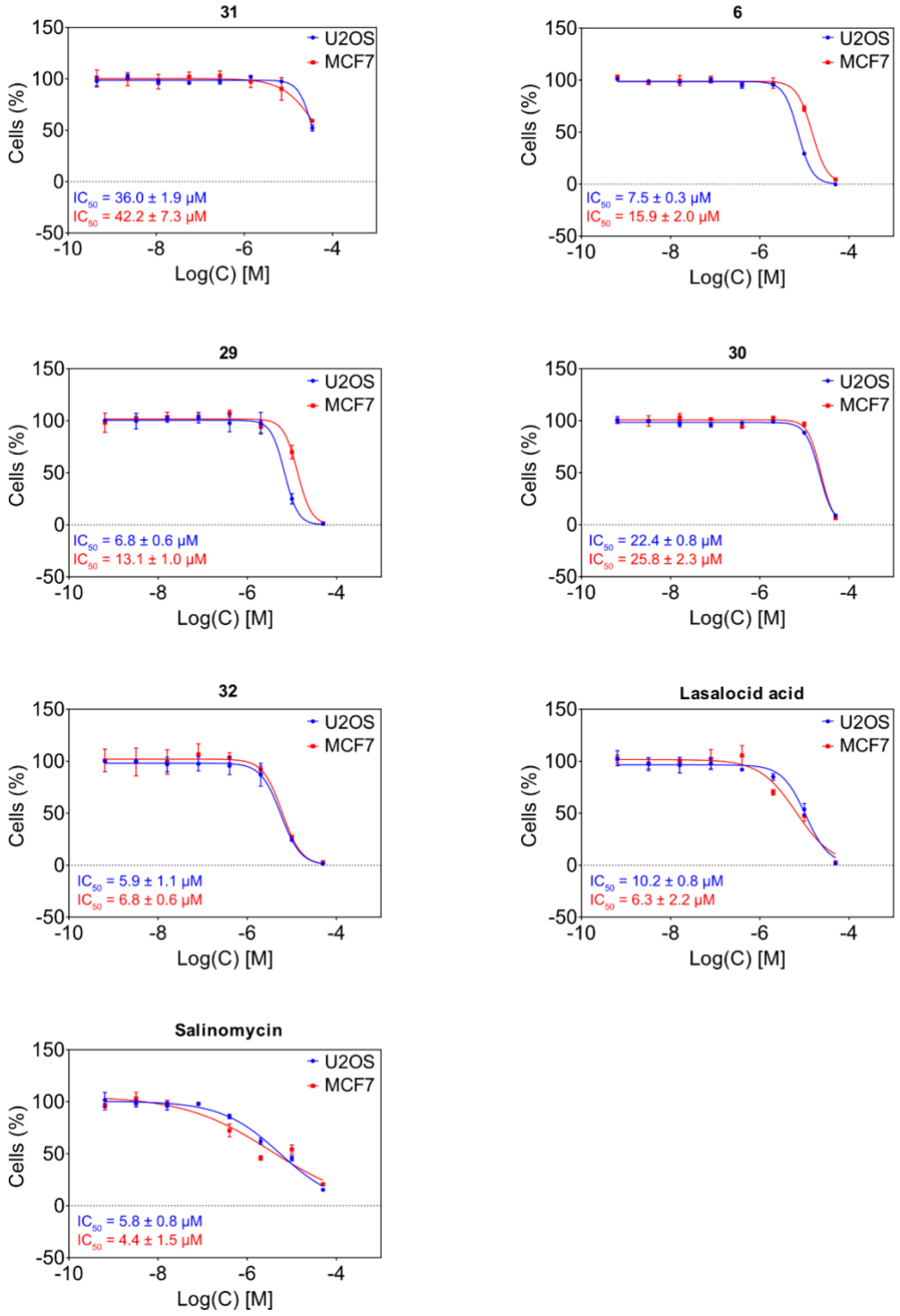

Figure S4 Dose response curves in U2OS and MCF7 cells after 48 h of treatment. IC_{50} is given as average plus/minus one standard deviation of the three repeats. Curves are representative of three repeats, each performed in triplicate. Error bars represent SD.

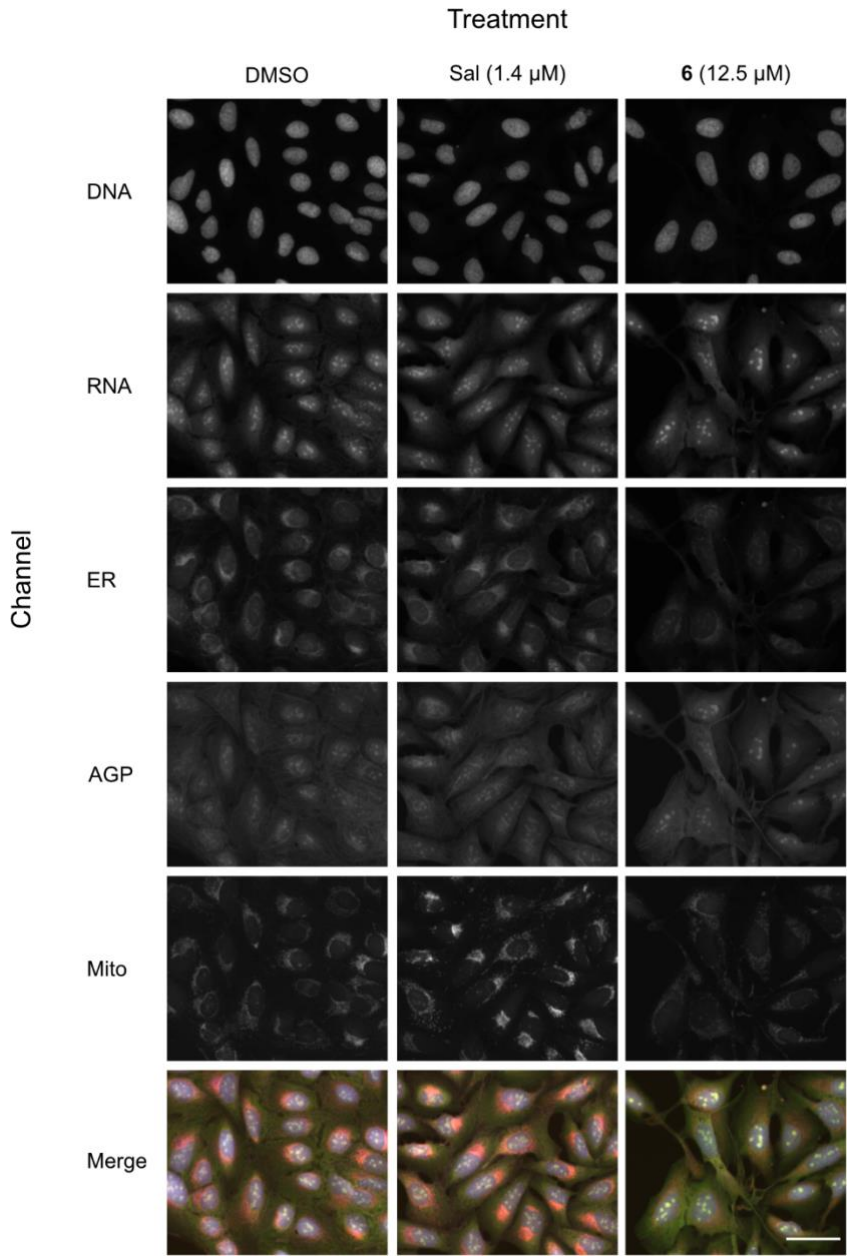

Figure S5 Representative images from the morphological profiling. Images are shown for DMSO treatment, 1.4 µM Salinomycin and 12.5 µM **6** treatment. Scalebar: 50 µM. See the methods section for description of fluorophores in the different channels. Merge: DNA (blue), RNA (yellow), ER (magenta), AGP (green), Mito (red)

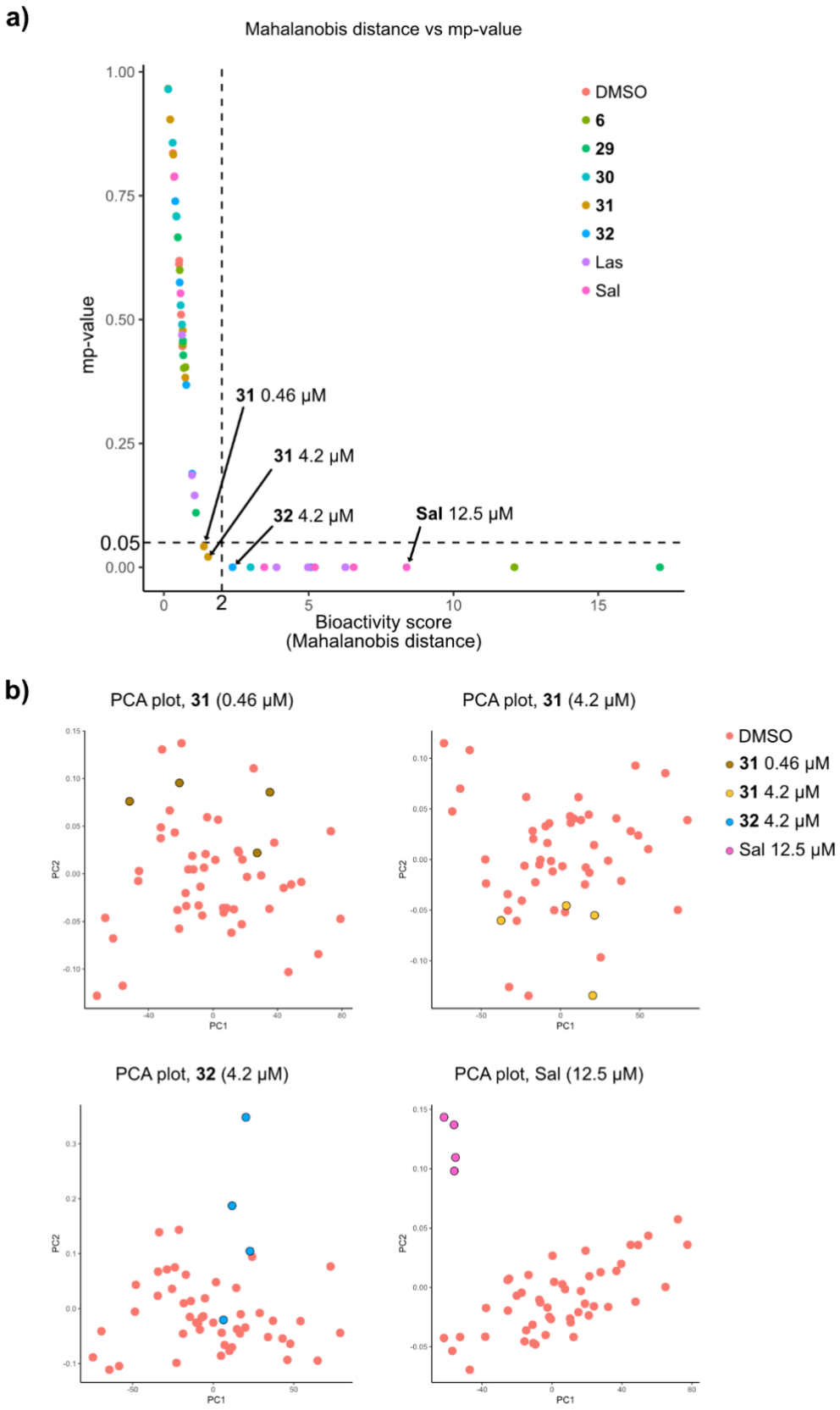

Figure S6 Determination of active compounds. a) Plot of Mahalanobis distance versus mp-value. b) PCA plots for selected compounds close to the activity score cutoff (**31** (0.46 µM), **31** (4.2 µM), **32** (4.2 µM)) and one clearly active compound

(Sal (12.5 µM)). **31** at 0.46 µM and 4.2 µM is deemed inactive as all points are within the DMSO controls. **32** at 4.2 µM is deemed active as some of the replicates differ significantly from the DMSO controls.

Supplemental discussion for Figure S6

To determine which compounds were active we used the method developed by Hutz et al.[1] to calculate the mp-value and the Mahalanobis distance from the per-well non-normalized profiles. Even though Hutz et al. describes that compounds with a mp-value lower than 0.05 should be deemed active, we have found that a stricter cut-off is needed as we sometimes also observe (extra) DMSO controls which exceeds this threshold. To determine when compounds are active we inspect the PCA plots of the first two PCA components for questionable compounds (mp-value ~ 0.05) to determine if they are active (Figure S6). From this, we have observed a general trend that compounds with Mahalanobis distance > 2 differs from DMSO controls. We have used this cuf-off, instead of the mp-value, to determine if compounds were active.

Compound **31** has mp-value = 0.04 at 0.46 µM and mp-value = 0.02 at 4.6 µM. These would be active according to the threshold of 0.05, but by inspected the PCA plots (Figure S6b) all replicates are within the DMSO controls. For compound **32** at 4.2 µM the mp-value is 0 (the lowest possible) and has Mahalanobis distance greater than 2 to DMSO controls. This compound is deemed active as some of the replicates are outside of the DMSO controls. Thus, for this experiment a mp-value cut-off of 0 could also have been applied to distinguish active compounds from inactive compounds.

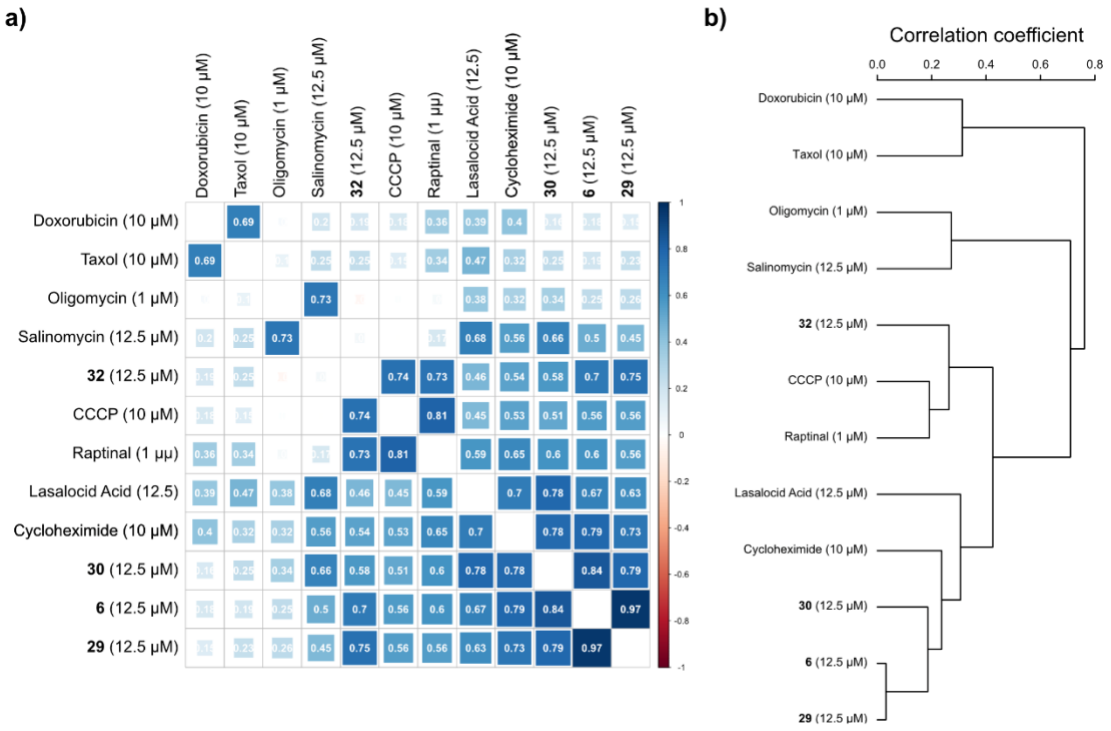

Figure S7 Comparison of high concentrations of hybrid ionophores **6, 29, 30 and 32** and salinomycin and lasalocid acid with reference compounds reveals a general toxic effect. a) Pearson correlation matrix ordered by hierarchical clustering. Profiles from high concentrations of hybrid ionophores correlates highly ($P > 0.7$) with some generally toxic compounds such as carbonyl cyanide 3-chlorophenylhydrazone (CCCP), raptinal and cycloheximide, while some other toxic compunds such as taxol and doxorubicin shows distinct profiles. The color and size of squares indicates the Pearson correlation coefficient. The coefficient is also presented by the number in each square. b) Cluster dendrogram showing the hierarchical clustering. **32** clusters with CCCP and raptinal while **6, 29 and 30** clusters with cycloheximide and lasalocid acid. Doxorubicin and taxol shows similar effects, despite their very different mechanism of action; this indicates a general toxic effect at these concentrations.

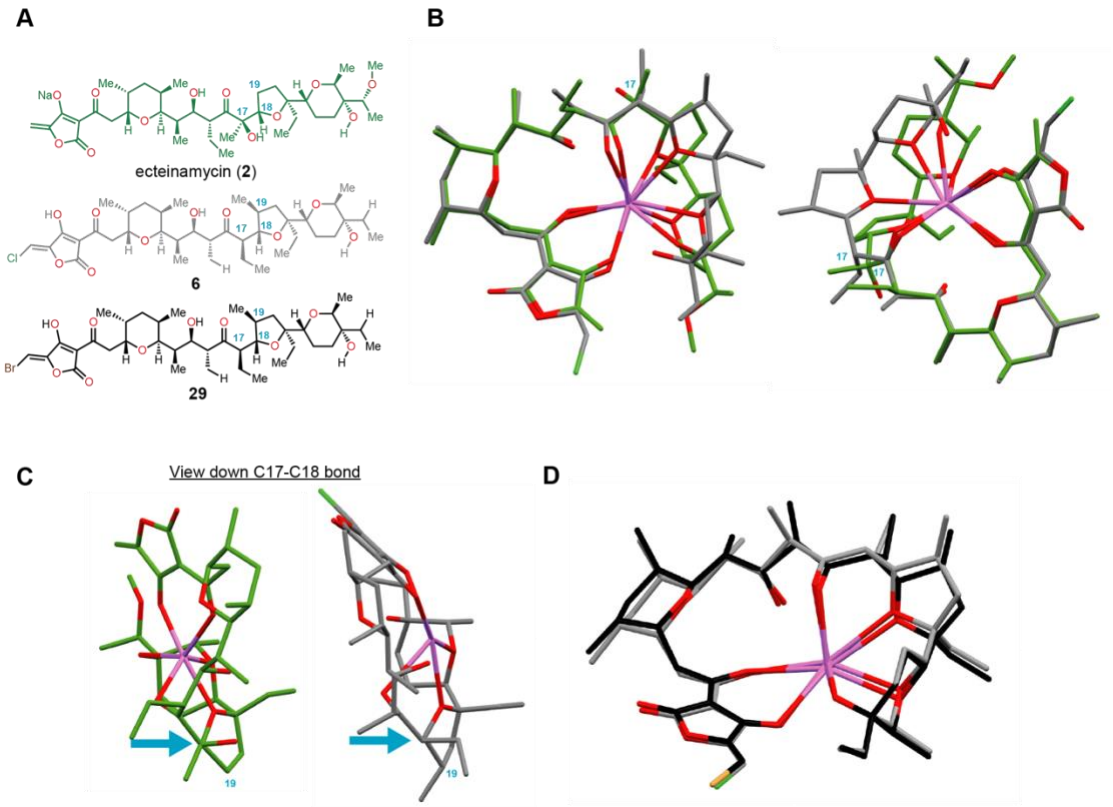

Figure S8 Comparison of X-ray structures of ecteinamycin and hybrid polyethers **6** and **29**. (a) Chemical structures, key carbon atoms indicated with blue numbers. (b) Overlay of X-ray structures of ecteinamycin and **6** reveals a shared ability to encapsulate a single sodium ion, but a different overall topology stemming mainly from deviations in dihedral angles around C17-C19. (c) View down the C17-C18 bond. C17 is quaternary in ecteinamycin but tertiary in **6**. (d) Overlay of X-ray structures of **6** and **29** demonstrates a very high degree of similarity.

Organic synthesis – general methods

All reactions were conducted in flame-dried glassware under an atmosphere of argon unless otherwise stated. CH_2Cl_2, MeCN, THF and PhMe were dried over aluminium oxide via an MBraun SPS-800 solvent purification system. DCE, DMF, MeOH and pyridine were purchased as anhydrous. The dryness of solvents was controlled via Karl Fischer tritration. Reagents were used as received from commercial suppliers unless otherwise stated (Sigma Aldrich, Merck, AK Scientific, and Fluorochem). Et_3N and DIPEA were dried by stirring for at least 30 minutes over CaH_2 followed by distillation onto preactivated molecular sieves (4 Å). Concentration in vacuo was performed using a rotary evaporator with the water bath temperature at 30 °C, or 40 °C, followed by further concentration using a high vacuum pump. TLC analysis was carried out on silica coated aluminum foil plates (Merck Kieselgel 60 F254). The TLC plates were visualized by UV irradiation and/or by staining with either CAM stain ($(NH_4)_6Mo_7O_{24}\cdot 4H_2O$ (10 g), Cerric ammonium sulfate (4 g), 10% H_2SO_4 (aq., 400 mL)), ninhydrin stain (ninhydrin (12 g) and AcOH (12 mL) in *n*-butanol (400 mL)) or $KMnO_4$ stain ($KMnO_4$ (5.0 g), 5 % NaOH (aq., 8.3 mL) and K_2CO_3 (33.3 g) in H_2O (500 mL)). Molecular sieves were activated by drying in the oven at 120 °C for at least 24 hours, before they were heated in a microwave at maximum power for 2 minute, followed by evaporation of the formed vapor on the high vacuum line. This was repeated 3-4 times, and finished by gently flame-drying the flask containing the molecular sieves. Flash column chromatography (FCC) was carried out using silica gel (230-400 mesh particle size, 60 Å pore size) as stationary phase. Infrared spectra (IR) were acquired on a PerkinElmer Spectrum TwoTM UATR. Mass spectra (HRMS) were recorded on a Bruker Daltonics MicrOTOF time-of-flight spectrometer with positive electrospray ionization, or negative ionization when stated. Nuclear magnetic resonance (NMR) spectra were recorded on a Varian Mercury 400 MHz spectrometer or a Bruker BioSpin GmbH 400 MHz spectrometer, running at 400 and 101 MHz for ^1H and ^{13}C, respectively. Chemical shifts (δ) are reported in ppm relative to the residual solvent signals ($CDCl_3$: 7.26 ppm ^1H NMR, 77.16 ppm ^{13}C NMR, CD_3OD: 3.31 ppm ^1H NMR, 49.00 ppm ^{13}C NMR, ^{6}d-DMSO: 2.50 ppm ^1H NMR, 39.52 ppm ^{13}C NMR. Multiplicities are indicated using the following abbreviations: s = singlet, d = doublet, t = triplet, q = quartet, h = heptet, m = multiplet, br = broad. LC-MS and

HPLC analysis and purification were performed using a Gilson HPLC system and a PerkinElmer Flexar SQ 300 MS detector.

X-ray crystallography

Crystal structure **6-Na**, **14**, **24** and **31-Na**

Crystallographic single crystal X-ray data for three structures were collected on a Bruker Kappa *Apex2* diffractometer equipped with a Ag source (**6-Na**, **14** and **31-Na**). The crystals were cooled to 100(1) K using an Oxford Cryosystems liquid nitrogen Cryostream device. Crystallographic single crystal X-ray data for **24** was collected on a different Bruker Kappa *Apex2* diffractometer equipped with a Mo source at room temperature. Absorption correction for all four structures were done with SADABS. Cell refinement and data reduction were done in SAINT-plus.[2] The structures were solved and refined with SHELXT and SHELXL, respectively, in Olex2.[3–5]

Crystal structure **29-Na**

Crystallographic single crystal X-ray data was collected using an Oxford Diffraction Supernova instrument equipped with a Mo micro-focus X-ray source, an Atlas charge-coupled device detector, and a four-circle goniometer. The crystal was cooled to 100(1) K using an Oxford Cryosystems liquid nitrogen Cryostream device. The intensities were empirically corrected for absorption using SCALE3 ABSPACK implemented in CrysAlisPRO.[6] The unit cell parameters were determined, and the Bragg intensities were integrated using CrysAlisPRO. The structure was solved and refined with SHELXT and SHELXL, respectively, in Olex2.[3–5]

Crystallographic details:

	6-Na	**14**	**24**	**29-Na**	**31-Na**
Molecular formula	C38 H58 Cl Na O10	C14 H24 O3	C34 H60 O8	C38 H58 Br Na O10	C38 H58 Cl Na O10, 2(C2 H3 N), H2O
Formula weight	733.28	240.33	596.82	777.74	833.4
Crystal system	orthorhombic	monoclinic	monoclinic	orthorhombic	orthorhombic
Space Group	P 21 21 21	P 1 21 1	P 1 21 1	P 21 21 21	P 21 21 21

a (Å)	17.3673	8.5919	8.8767	17.5111	11.9272
b (Å)	18.6159	9.104	10.3495	18.5108	13.616
c (Å)	53.386	9.673	19.4472	53.5509	27.774
α (°)	90	90	90	90	90
β (°)	90	114.391	91.299	90	90
γ (°)	90	90	90	90	90
Volume ($Å^3$)	17260	689.1	1786.14	17358.2	4510.7
Z	16	2	2	16	4
T (K)	100	100	296	100	100
ρ ($g\ cm^{-1}$)	1.129	1.158	1.11	1.19	1.227
λ (Å)	0.56086	0.56086	0.71073	0.71073	0.56086
μ (mm^{-1})	0.084	0.05	0.077	1.006	0.087
# measured refl	110795	11684	28112	35203	25547
# unique refl	19216	2616	6640	17560	6250
R_{int}	0.0694	0.0486	0.0273	0.0443	0.0474
# parameters	1834	158	391	1759	532
$R(F^2)$, all refl	0.0925	0.0511	0.0584	0.0977	0.0538
$R_w(F^2)$, all refl	0.2365	0.103	0.1278	0.2421	0.121
Goodness of fit	1.007	1.048	1.047	1.04	1.045

Determination of MIC values

The strains tested are *staphylococcus aureus* DSM 20231, *staphylococcus aureus* USA 300 JE2 (MRSA), *staphylococcus aureus* ATCC 29213 (weak β-lactamase producer), *Escherichia. coli* DSM 498, *Pseudomonas aeruginosa* PAO1 DSM 19880. The MIC values are tested in 96-well microtiter plates using a microbroth dilution method in Mueller Hinton broth, inoculating each test well with 5 x 10^5 CFU and incubating at 37°C overnight. The inoculation CFU is validated in parallel using agar plate counts. Stocks of the compounds screened are prepared in DMSO (final conc. <2%). Growth is measured as absorbance at 600 nm using a Tecan Nanoquant infinite M200Pro plate reader. The absorbance value correlating to a difference seen by the unaided eye is determined to be 0.07. Measurements above this value is deemed as growth when determining the MIC values.

Mammalian cell culture and cell viability assay

U2OS cells (ATCC HTB-96) were cultured in McCoy's 5A (Sigma cat. no. M9309) supplemented with fetal bovine serum (FBS, 10%) and penicillin/streptomycin (1%). MCF7 cells (ATCC HTB-22) were cultured in DMEM (Gibco, cat. no. 21969035) supplemented with GlutaMAX (Gibco, cat. no. 35050061), 10 μg/mL human recombinant insulin (Sigma, cat. No. I9278), FBS (10%) and penicillin/streptomycin (1%).

Cells were cultured at 37 °C in a humidified atmosphere containing 5% CO2. Every third day, the cells were washed in PBS (2 × 5 mL, Sigma, cat. no. D8537) and dissociated from the culture flask by trypsin-EDTA (Sigma, cat. no. T4049) and one-fifth of the cells were reseeded in fresh complete medium in a T75 flask (Thermo Scientific, cat. no. 130190)

Cell viability assay

Cells were seeded in black 96-well plates (Thermo Scientific, cat. no. 137101) at a density of 2000 cells/well in complete medium (75 μL/well) and were left to adhere to the substratum overnight. Compounds were dosed in the designated culture plates in triplicates as 4× solutions in 25 μL medium with a normalized DMSO concentration (0.5%) in all treatments, and the plates were placed at 37 °C in a humidified atmosphere containing 5% CO2. After 46.5 h, plates were added CellTiter-Blue (Promega G8080) (20 μL/well) and incubated for 90 min after which the plates were analyzed in a Tecan Spark 10 M multimode plate reader for fluorescence (552 ± 10 nm excitation; 598 ± 10 nm emission). Average growth of treated cells was calculated by correcting fluorescence values for background fluorescence and subsequently normalized to the average of the two lowest treatments of the compound in question. Data was plotted and fitted to a four-parameter dose−response curve using Prism 7.05 for Windows (GraphPad Software, La Jolla, CA, www.graphpad.com) with the following constraints: Bottom = 0, HillSlope > -3.

Morphological profiling

The cell painting protocol is adapted from Bray et al 2016[7] to a 96-well plate format. In brief:

U2OS cells were seeded into the inner 60 wells of a 96-well plate with optical bottom (Corning cat. no. 3603) at a density of 4000 cells/well in complete medium (75 µL) and incubated (37 °C, 5% CO_2, humid) for 24 h. Compounds or DMSO were dosed in the designated culture plates in quadruplicates, distributed over 4 plates, as 4× solutions in 25 µL medium with a normalized DMSO concentration (0.5%). A total of 48 DMSO control wells were included plus 24 DMSO controls wells which were kept out of the normalization to measure background signal. After 24 h, 75 µL medium was removed and replaced with 75 µL complete medium containing 500 nM MitoTracker Deep Red (final C = 325 nM) and plates were incubated in the dark for 30 min. Wells were then aspirated and 75 µL medium were added, before adding 25 µL 16% paraformaldehyde (Electron Microscopy Sciences 15710-S) (final PFA = 4%) and incubating in the dark for 20 min. Plates were washed once with 1X HBSS (Invitrogen 14065-056) and 75 µL 0.1% (vol/vol) Triton X-100 (BDH 306324N) in 1X HBSS was added and incubated for 15 min in the dark. Plates were washed twice with 1X HBSS before addition of 75 µL multiplex staining solution (final concentrations: 1.5 µg/mL WGA-AF555; 35 µg/mL Concanavalin-AF488; 5 µL/mL Phalloidin-AF568; 3 µM SYTO 14; 5 µg/mL Hoechst 33342 in 1% (wt/vol) BSA (Sigma-Aldrich A9647)) and incubation for 30 min in the dark. Plates were then washed three times with 1X HBSS with no final aspiration and imaged immediately in a Zeiss Celldiscoverer 7 automated microscope.

Imaging

The following imaging settings were used on a Zeiss Celldiscoverer 7 microscope:

Channel	**Dyes**	**Excitation LED**	**Beamsplitter**	**Emission filter**
DNA	Hoechst 33342	385 nm	RTBS 405 + 493 + 610	TBP 425/30 + 524/50 + 688/154
ER	Concanavalin-AF488	470 nm	RTBS 405 + 493 + 610	TBP425/30 + 524/50 + 688/145
RNA	SYTO 14 green fluorescent nucleic acid stain	511 nm	RTBS 450 + 538 + 610	TBP 467/24 + 555/25 + 687/145
AGP	Phalloidin-AF568 +	567 nm	RQBS 405 +	QBP 425/30 +

	Wheat-germ agglutinin-AF555		493 + 575 + 653	514/30 + 592/25 + 709/100
Mito	MitoTracker Deep Red	625 nm	RQBS 405 + 493 + 575 + 653	QBP 425/30 + 514/30 + 592/25 + 709/100

AF: Alexa Fluor

9 images are acquired in each well with 2x2 binning using the AxioCam 702 CMOS 12-bit camera with 4x analog gain.

Computational

To generate the bioactivity profiles the workflow outlined in Svenningsen & Poulsen[8] was followed. In short, CellProfiler 2.1.1[9] was used to correct images for uneven illumination followed by image segmentation and extraction of 1476 features across nuclei, cytoplasm and the whole cell on a per-cell basis. Features were then averaged to per-well profiles after which the data was normalized on a per-plate basis followed by per-treatment aggregation which affords the final profiles.

The heatmap of morphological profiles is visualized with heatmap.2 in the gplots package[10]. The Pearson correlation matrix is calculated using the stats package in R 3.6.0[11] and visualized using the corrplot 0.84 package[12].

Hierarchical clustering is performed using the stats package using Pearson correlation coefficients as distance metric and average linkage method.

Synthesis protocols and characterization data

(*R*)-4-((2*S*,3*S*,5*S*)-5-ethyl-5-((2*R*,5*R*,6*S*)-5-ethyl-5-hydroxy-6-methyltetrahydro-2*H*-pyran-2-yl)-3-methyltetrahydrofuran-2-yl)hexan-3-one (4)

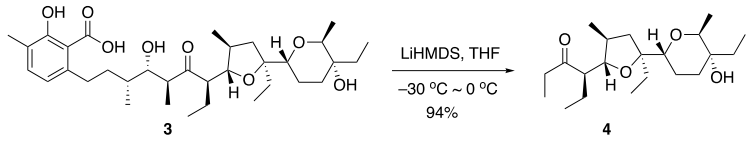

3 4

Lasalocid acid **3** was extracted from the commercial product Bovatec. To a solution of the Lasalocid acid (11.8 g, 20 mmol, 1 eq.) in 200 mL of THF was added LiHMDS (120 mL, 1.0 M in THF, 6 eq.) slowly at -30 °C under Ar. The resulting mixture was slowly warmed to 0 °C and stirred for 6 d. It was quenched with sat. NH_4Cl and extracted with ether. The combined organic phases were washed with brine and dried with Na_2SO_4. The solvent was removed, and the crude mixture was purified by flash column chromatography to afford the product **4** as a pale yellow oil (6.64 g, 94%).

R_f: 0.22 (EtOAc/pentane 1:9).

^{1}H NMR (400 MHz, $CDCl_3$): δ 3.76 (q, *J* = 6.9 Hz, 1H), 3.57 – 3.54 (m, 1H), 3.49 – 3.46 (m, 1H), 2.63 – 2.53 (m, 3H), 2.44 (dq, *J* = 18.4, 7.2 Hz, 1H), 2.02 – 1.92 (m, 1H), 1.83 (dd, *J* = 12.5, 8.1 Hz, 1H), 1.78 – 1.69 (m, 1H), 1.66 – 1.25 (m, 10H), 1.19 (d, *J* = 6.9 Hz, 3H), 1.00 (t, *J* = 7.2 Hz, 3H), 0.89 (m, 6H), 0.81 (t, *J* = 7.4 Hz, 6H).

^{13}C NMR (101 MHz, $CDCl_3$): δ 214.1, 86.0, 84.4, 77.0, 73.0, 71.1, 57.6, 40.8, 37.4, 37.0, 30.5, 29.4, 28.7, 21.4, 21.2, 16.8, 14.2, 12.6, 8.2, 7.5, 6.6.

(2*R*,4*R*)-5-((tert-Butyldimethylsilyl)oxy)-2,4-dimethylpentan-1-ol (10)

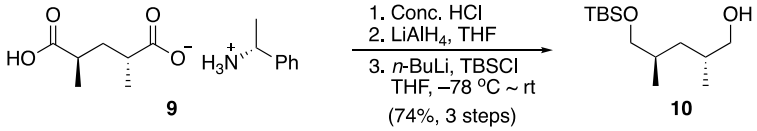

9 10

The optically active salt **9** (5.39 g, 19.2 mmol, 1.0 eq.) was dissolved in conc. HCl (50 mL), and the resulting clear solution was stirred for 5 mins before solvent was removed. The residue was extracted with ether. The combined organic layers were dried with Na_2SO_4, and then solvent was removed. The crude product was used directly in the next step.

The crude product was dissolved in 120 mL dry THF under Ar and cooled to 0 °C, $LiAlH_4$ (2.91 g, 76.8 mmol, 4 eq.) was added in small portions. Then the mixture was

warmed to room temperature and stirred overnight. It was quenched with water (2.91 g), 10% NaOH (2.91 g), and water (8.73 g). The white precipitate was filtered off and washed with EtOAc. The crude product was used directly in the next step.

To a solution of crude diol in dry THF (35 mL) at -78 °C under Ar, *n*-BuLi (7.3 mL, 2.5 N, 0.95 eq.) was added dropwise and the resulting solution was stirred for 1 h at -78 °C. Then, a solution of TBSCl (2.75 g, 18.2 mmol, 0.95 eq.) in THF (5 mL) was added rapidly, and the resulting mixture was stirred at -78 °C for 10 min before it was warmed to room temperature and stirred for another 3 h. The reaction mixture was quenched with sat. NH_4Cl and extracted with ether. The combined organic layers were washed with brine and dried with Na_2SO_4. Then the solvent was removed and the crude product was purified by flash column chromatography to yield the product **10** as a clear oil (3.48 g, 74%).

R_f: 0.25 (EtOAc/pentane= 1/9).

$[\alpha]_D^{296.6\,K}$ 18.6 (c = 1, $CHCl_3$).

IR ν_{max} (cm^{-1}): 3308 (br), 2955, 2928, 2857, 1472, 1388, 1254, 1095, 1036.

^1H NMR (400 MHz, $CDCl_3$): δ 3.50 –3.39 (m, 4H), 1.79 – 1.68 (m, 2H), 1.47 (s, 1H), 1.25 – 1.10 (m, 2H), 0.92 – 0.85 (m, 15H), 0.04 (s, 6H).

^{13}C NMR (101 MHz, $CDCl_3$): δ 69.2, 69.1, 37.0, 33.2, 33.1, 26.1, 18.5, 16.8, 16.6, -5.2.

HRMS (ESI) *m/z* $[M+H]^+$ calc. for $C_{13}H_{31}O_2Si$: 247.2088; found 247.2092.

(2*R*,4*R*)-5-((tert-butyldimethylsilyl)oxy)-2,4-dimethylpentanal (11)

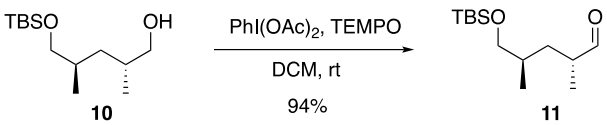

To a solution of mono-TBS protected diol **10** (3.48 g, 14.1 mmol, 1 eq.) in dry DCM (70 mL) under Ar, $PhI(OAc)_2$ (6.81 g, 21.2 mmol, 1.5 eq.) and TEMPO (443 mg, 2.82 mmol, 0.2 eq.) were added. The mixture was stirred until SM disappeared (6 h) at room temperature under Ar. Then, the reaction was quenched with aq. $Na_2S_2O_3$ and extracted with DCM. The combined organic phases were washed with sat. aq.

$NaHCO_3$, brine and dried over Na_2SO_4, filtered, and concentrated under reduced pressure. The crude product was purified by flash column chromatography to yield the aldehyde **11** as a clear oil (3.24 g, 94%).

R_f: 0.50 (EtOAc/pentane = 1/19).

IR ν_{max} (cm^{-1}): 2956, 2929, 2857, 1728, 1462, 1252, 1093, 836, 765.

^1H NMR (400 MHz, $CDCl_3$): δ 9.62 (d, *J* = 2.0 Hz, 1H), 3.47 – 3.40 (m, 2H), 2.48 – 2.39 (m, 1H), 1.75 – 1.66 (m, 1H), 1.53 – 1.38 (m, 2H), 1.08 (d, *J* = 7.0 Hz, 3H), 0.89 – 0.87 (m, 12H), 0.04 (s, 6H).

^{13}C NMR (101 MHz, $CDCl_3$): δ 205.5, 68.3, 44.3, 34.1, 33.4, 26.1, 18.5, 16.6, 13.6, -5.3.

HRMS (ESI) *m/z* $[M+H]^+$ calc. for $C_{13}H_{29}O_2Si$: 245.1931; found 245.1929.

(3*R*,5*R*)-6-(But-3-en-2-yl)-3,5-dimethyltetrahydro-2*H*-pyran-2-one (12)

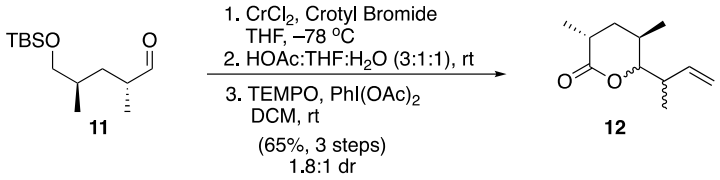

To $CrCl_2$ (3.613 g, 29.4 mmol, 4 eq.) at 0 °C under Ar was added dry THF (40 mL) with vigorous stirring. After 30 min, aldehyde **11** (1.796 g, 7.35 mmol, 1 eq.) in THF (4.0 mL) and 1-bromo-2-butene (2.27 mL, 22.1 mmol, 3 eq.) in THF (2 mL) were added dropwise. The mixture was stirred at 0 °C for 20 h after which it was poured into ice-cold water (150 mL) and extracted with ether. Then, the solvent was removed, and the crude mixture was used in the next step without further purification.

The crude mixture was dissolved in 10 mL of HOAc-THF-H_2O (3:1:1) and was stirred until SM disappeared (overnight). The reaction mixture was diluted with water and quenched with solid $NaHCO_3$. The mixture was extracted with ether and the combined organic phases were dried over Na_2SO_4, filtered, and concentrated under reduced pressure to afford a crude mixture that was used without further purification.

To a solution of the crude mixture in DCM (45 mL) at room temperature under Ar, TEMPO (230 mg, 1.47 mmol, 0.2 eq.) and $PhI(OAc)_2$ (4.735 g, 14.7 mmol, 2.0 eq)

were added. After 12 h, the reaction mixture was partitioned between aq. $Na_2S_2O_3$ and DCM. The combined organic phases were washed with sat. aq. $NaHCO_3$, brine and dried with Na_2SO_4, filtered, and concentrated under reduced pressure. The crude product mixture was purified by flash column chromatography to obtain the product **12** as a clear oil (867 mg, 65%, *dr*: 1.8:1). NMR data are reported for the major diastereomer.

R_f: 0.26 (EtOAc/pentane 1:9).

$[\alpha]_D^{296.6\ K}$ 69.4 (c = 1, $CHCl_3$).

IR ν_{max} (cm^{-1}): 3090, 2968, 2934, 2850, 1734, 1460, 1378, 1199, 1101, 989, 737.

^1H NMR (400 MHz, $CDCl_3$): δ 5.94 (ddd, *J* = 17.4, 10.4, 7.1 Hz, 1H), 5.15 – 5.05 (m, 2H), 4.02 (dd, *J* = 9.7, 2.6 Hz, 1H), 2.67 – 2.57 (m, 1H), 2.46 – 2.37 (m, 1H), 2.19 – 2.12 (m, 1H), 1.94 (ddd, *J* = 13.6, 7.2, 3.4 Hz, 1H), 1.68 (td, *J* = 12.8, 3.9 Hz, 1H), 1.29 (d, *J* = 7.1 Hz, 3H), 1.03 (d, *J* = 7.1 Hz, 3H), 1.00 (d, *J* = 6.9 Hz, 3H).

^{13}C NMR (101 MHz, $CDCl_3$): δ 174.2, 140.4, 115.1, 87.1, 39.5, 36.4, 31.3, 28.1, 18.0, 15.5, 10.8.

HRMS (ESI) *m/z* $[M+Na]^+$ calc. for $C_{11}H_{18}O_2Na$: 205.1199; found 205.1209.

(2*S*,3*R*,5*R*,6*S*)-6-((*R*)-But-3-en-2-yl)-3,5-dimethyltetrahydro-2*H*-pyran-2-yl acetate (13)

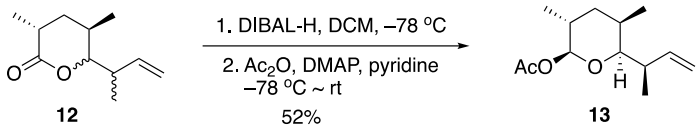

12 13

To a solution of lactone **12** (403 mg, 2.21 mmol, 1 eq.) in DCM (22 mL) under Ar was cooled to -78 °C, DIBAL-H (2.87 mL, 1.0 M in cyclohexane, 1.3 eq.) was added dropwise. After 5 h, acetic anhydride (2.07 mL, 22.1 mmol, 10 eq.), pyridine (1.43 mL, 17.7 mmol, 8 eq.), and DMAP (351 mg, 3.87 mmol, 1.3 eq.) were added. The reaction mixture was slowly warm to room temperature and stirred for overnight. Sat. aq. NH_4Cl was added and the DCM was removed. The aqueous phase was extracted with Et_2O. The combined organic layers were washed with sat. aq. Na_2HPO_4 twice, NaH_2PO_4 twice, and sat. aq. $CuSO_4$ twice. The organic phase was dried over Na_2SO_4, filtered,

and concentrated under reduced pressure. The crude mixture was purified by column chromatography to afford the major product **13** as a clear solid (259 mg, 52%).

R_f: 0.42 (EtOAc/pentane 1:15).

$[\alpha]_D^{296.8\,K}$ -27.4 (c = 1, $CHCl_3$).

IR ν_{max} (cm^{-1}): 3081, 2968, 2921,1757, 1462, 1228, 1105, 1044, 902.

^1H NMR (400 MHz, $CDCl_3$): δ 5.92 (ddd, *J* = 17.1, 10.4, 6.3 Hz, 1H), 5.22 (d, *J* = 9.2 Hz, 1H), 5.07 – 4.96 (m, 2H), 3.27 (dd, *J* = 10.0, 2.2 Hz, 1H), 2.36 – 2.25 (m, 1H), 2.11 (s, 3H), 1.88 – 1.83 (m, 2H), 1.74 – 1.69 (m, 1H), 1.45 (td, *J* = 13.2, 5.2 Hz, 1H), 1.00 (d, *J* = 7.0 Hz, 3H), 0.93 (d, *J* = 6.9 Hz, 3H), 0.83 (d, *J* = 6.5 Hz, 3H).

^{13}C NMR (101 MHz, $CDCl_3$): δ 170.0, 141.9, 113.7, 99.7, 83.1, 39.0, 38.5, 29.6, 29.0, 21.3, 16.2, 15.5, 12.1.

HRMS (ESI) *m/z* $[M+Na]^+$ calc. for $C_{13}H_{22}O_3Na$: 249.1461; found 249.1464.

Methyl 2-((2*R*,3*R*,5*R*,6*S*)-6-((*R*)-but-3-en-2-yl)-3,5-dimethyltetrahydro-2*H*-pyran-2-yl)acetate (14)

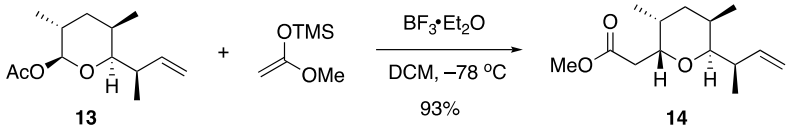

To a solution of acetal **13** (326 mg, 1.44 mmol, 1 eq.) in DCM (14 mL) under Ar at -78 °C, ((1-methoxyvinyl)oxy)trimethylsilane (2.46 mL, 14.4 mmol, 10 eq.) was added. Then BF3•OEt2 (274 uL, 2.16 mmol, 1.5 eq.) was added dropwise. The resulting mixture was stirred at -78 °C for 22 h. Then, sat. aq. $NaHCO_3$ was added at -78 °C and the mixture was allowed to warmed to room temperature. The mixture was extracted with DCM, dried over Na_2SO_4, filtered, and concentrated under reduced pressure. The crude product was purified by flash column chromatography to afford the product **14** as a clear solid (323 mg, 93%). The single crystal sample for XRD analysis was obtained via the single-tube method using acetone/MeOH as solvent.

R_f: 0.31 (EtOAc/pentane 1:15).

$[\alpha]_D^{296.6\,K}$ 71 (c = 1, $CHCl_3$).

IR ν_{max} (cm^{-1}): 3092, 2961, 2913, 1741, 1436, 1378, 1288, 1213, 1070, 966, 906.

^{1}H NMR (400 MHz, $CDCl_3$): δ 5.72 (ddd, *J* = 17.7, 10.4, 7.8 Hz, 1H), 5.00 – 4.89 (m, 2H), 4.35 (dt, *J* = 10.8, 5.1 Hz, 1H), 3.68 (s, 3H), 3.30 (dd, *J* = 9.8, 2.5 Hz, 1H), 2.79 (dd, *J* = 14.3, 11.4 Hz, 1H), 2.30 (dd, *J* = 14.3, 4.5 Hz, 1H), 2.27 – 2.13 (m, 2H), 1.90 – 1.84 (m, 1H), 1.56 – 1.42 (m, 2H), 0.98 (d, *J* = 7.0 Hz, 3H), 0.90 (d, *J* = 6.8 Hz, 3H), 0.75 (d, *J* = 6.9 Hz, 3H).

^{13}C NMR (101 MHz, $CDCl_3$): δ 172.5, 143.3, 113.1, 75.1, 75.0, 51.8, 39.9, 34.9, 31.9, 29.0, 26.8, 17.6, 16.1, 11.8.

HRMS (ESI) *m/z* $[M+Na]^+$ calc. for $C_{14}H_{24}O_3Na$: 263.1618; found 263.1633.

Methyl 2-((2*R*,3*R*,5*R*,6*S*)-3,5-dimethyl-6-((*S*)-1-oxopropan-2-yl)tetrahydro-2*H*-pyran-2-yl)acetate (7)

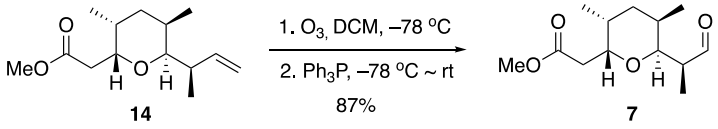

A stream of ozone was bubbled through a solution of alkene **14** (305 mg, 1.27 mmol, 1.0 eq.) in DCM (30 mL) at -78 °C until the blue color persisted. Excess ozone was removed with a stream of oxygen (until solution becomes colorless) and then a stream of nitrogen (30 min) at -78 °C. Ph_3P (1.666 g, 6.35 mmol, 5.0 eq.) was added and the reaction mixture was stirred for 2 h at -78 °C. Then, it was allowed to warm to room temperature and stirred for 18 h. The solvent was removed, and the crude mixture was purified by flash column chromatography to afford the product **7** as a white solid (269 mg, 87%).

R_f: 0.42 (EtOAc/pentane 1:9).

$[\alpha]_D^{296.6\ K}$ 106 (c = 1, $CHCl_3$).

IR ν_{max} (cm^{-1}): 2960, 2917, 2879, 2857, 2726, 1736, 1462, 1438, 1261, 1289, 1176, 1077, 968, 856.

^{1}H NMR (400 MHz, $CDCl_3$): δ 9.53 (d, *J* = 3.5 Hz, 1H), 4.31 (dt, *J* = 10.9, 5.0 Hz, 1H), 3.81 (dd, *J* = 10.3, 2.6 Hz, 1H), 3.67 (s, 3H), 2.81 (dd, *J* = 14.0, 11.6 Hz, 1H), 2.39 – 2.23 (m, 3H), 1.88 – 1.84 (m, 1H), 1.61 – 1.46 (m, 2H), 0.99 (d, *J* = 7.0 Hz, 3H), 0.95 (d, *J* = 7.0 Hz, 3H), 0.77 (d, *J* = 6.9 Hz, 3H).

^{13}C NMR (101 MHz, $CDCl_3$): δ 205.3, 172.4, 75.3, 72.0, 52.0, 48.3, 34.4, 31.8, 28.6, 26.8, 17.5, 11.9, 9.8.

HRMS (ESI) *m/z* $[M+Na]^+$ calc. for $C_{13}H_{22}O_4Na$: 265.1410; found 265.1415.

2-Trimethylsilylethyl 2,2-dimethyl-1,3-dioxolane-4-carboxylate (16):

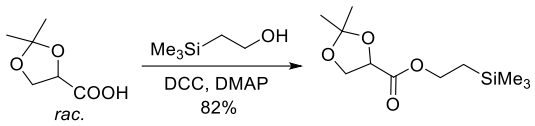

15 **16**

To the solution of racemic acid **15** (2.294 g, 15.7 mmol, 1.0 equiv) in anhydrous DCM (20 mL), 2-trimethylsilylethanol (2.93 mL, 20.4 mmol, 1.3 equiv) was added. The mixture was cooled to 0 °C, then the solution of DCC (4.21 g, 20.4 mmol, 1.3 equiv) in DCM (10 mL) was added, followed by DMAP (96 mg, 0.78 mmol, 0.05 equiv). The white precipitate DCU was generated immediately. After 5 h reaction, the mixture was diluted with pentane and filtered through celite to remove DCU. The filtrate was concentrated and the residue was purified by silica gel column chromatography using pentane/ethyl acetate 50:1 *v*/*v* as eluent. The product **16** was obtained as colorless oil (3.179 g, 82%).

R_f: 0.34 (Pentane/EtOAc 20:1).

^{1}H NMR (400 MHz, $CDCl_3$): δ 4.57 (dd, *J* = 7.2, 5.2 Hz, 1H), 4.32 – 4.22 (m, 3H), 4.10 (dd, *J* = 8.8, 5.2 Hz, 1H), 1.51 (s, 3H), 1.42 (s, 3H), 1.04 (t, *J* = 8.8 Hz, 2H), 0.06 (s, 9H).

^{13}C NMR (101 MHz, $CDCl_3$): δ 171.4, 111.4, 74.4, 67.4, 63.9, 26.0, 25.7, 17.5, -1.4.

The synthetic compound showed identical spectroscopic data to the reported one.[13]

2-Trimethylsilylethyl 2,3-dihydroxypropionate (SI-1):

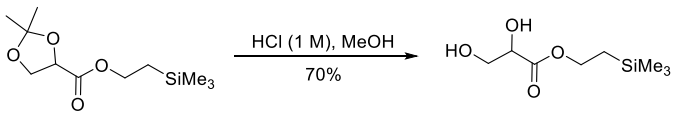

16 **SI-1**

To the solution of acetonide protected ester **16** (6.93 g, 28.1 mmol, 1.0 equiv) in MeOH (24 mL), the solution of 1 M HCl (aq, 35.1 mL, 35.1 mmol, 1.25 equiv) was

added. The mixture was stirred at r.t. for 12 h. After full conversion, the reaction was quenched by Et_3N (6 mL) and concentrated under vacuum. The residue was then purified by silica gel column chromatography using pentane/ethyl acetate 3:1 to 2:1 as eluent. The product **SI-1** was obtained as colorless oil (4.027 g, 70%).

R_f: 0.60 (Pentane/EtOAc 1:2).

^{1}H NMR (400 MHz, $CDCl_3$): δ 4.35 – 4.30 (m, 2H), 4.24 (dd, *J* = 8.0, 3.6 Hz, 1H), 3.93 – 3.81 (m, 2H), 3.19 (d, *J* = 4.4 Hz, 1H), 2.17 (dd, *J* = 8.0, 5.2 Hz, 1H), 1.08 – 1.04 (m, 2H), 0.06 (s, 9H).

^{13}C NMR (101 MHz, $CDCl_3$): δ 173.3, 71.7, 64.8, 64.2, 17.5, -1.4.

The synthetic compound showed identical spectroscopic data to the reported one.[13]

2-Trimethylsilylethyl 3-triphenylmethoxy-2-hydroxypropionate (17):

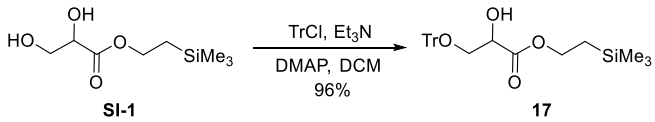

To as stirred solution of **SI-1** (1.50 g, 7.27 mmol, 1.0 equiv) in anhydrous DCM (15 mL) were added Et_3N (1.52 mL, 10.9 mmol, 1.5 equiv) and DMAP (45 mg, 0.36 mmol, 0.05 equiv). The mixture was cooled to 0 °C, then the solution of trityl chloride (3.04 g, 7.27 mmol, 1.0 equiv) in anhydrous DCM (5 mL) was added dropwise. After addition, the mixture was stirred at 0 °C to r.t. for 20 h. When full conversion was achieved, the mixture was concentrated under vacuum, and the residue was purified by silica gel column chromatography using pentane/ethyl acetate 40:1 *v*/*v* as eluent. The trityl protection product **17** was obtained as colorless oil (3.14 g, 96%).

R_f: 0.30 (Pentane/EtOAc 15:1).

IR ν_{max} (cm^{-1}): 3059, 2952, 2897, 1733, 1597, 1490, 1449, 1249, 1231, 1118, 1095, 1029, 933, 858, 835.

^{1}H NMR (400 MHz, $CDCl_3$): δ 7.46 – 7.44 (m, 6H), 7.33 – 7.29 (m, 6H), 7.27 – 7.23 (m, 3H), 4.32 – 4.24 (m, 3H), 3.51 (dd, *J* = 9.2, 3.2 Hz, 1H), 3.38 (dd, *J* = 9.2, 3.2 Hz, 1H), 3.27 (d, *J* = 7.6 Hz, 1H), 0.96–1.00 (m, 2H), 0.05 (s, 9H).

^{13}C NMR (101 MHz, $CDCl_3$): δ 173.3, 143.7, 128.7, 127.9, 127.2, 86.4, 70.9, 65.4, 64.2, 17.6, -1.4.

HRMS (ESI) *m/z* $[M+Na]^+$ calc. for $C_{27}H_{32}NaO_4Si$: 471.1962; found 471.1983.

2-Triphenylmethoxy-3-(2-trimethylsilylethoxy)-2*H*-furan-5-one (18):

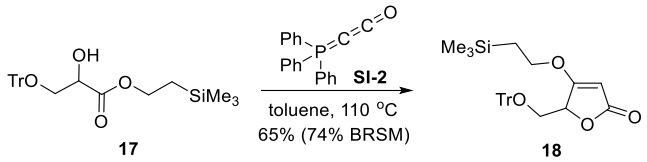

To a stirred solution of of **17** (1.46 g, 3.24 mmol, 1.0 equiv) in anhydrous toluene (35 mL) was added Bestmann reagent (**SI-2**) (1.76 g, 5.83 mmol, 1.8 equiv, prepared according to published procedure). The mixture was heated under argon to 110 °C for 24 h. After being cooled to r.t., the mixture was concentrated under vacuum, and the residue was purified by silica gel column chromatography. The recovered starting material **17** was eluted by pentane/ethyl acetate 40:1 *v*/*v* (192 mg, 13%), then the product **18** was eluted by pentane/ethyl acetate 6:1 and obtained as white solid (989 mg, 64%, 74% BRSM).

R_f: 0.44 (Pentane/EtOAc 6:1).

IR ν_{max} (cm^{-1}): 3058, 2951, 1760, 1628, 1490, 1448, 1350, 1292, 1248, 1232, 1151, 1115, 1077, 1033, 930, 836.

^{1}H NMR (400 MHz, $CDCl_3$): δ 7.45 – 7.43 (m, 6H), 7.33 – 7.29 (m, 6H), 7.28 – 7.23 (m, 3H), 5.14 (s, 1H), 4.84 – 4.82 (m, 1H), 4.16 – 4.05 (m, 2H), 3.59 (dd, *J* = 10.4, 2.8 Hz, 1H), 3.28 (dd, *J* = 10.4, 4.4 Hz, 1H), 1.10 – 1.06 (m, 2H), 0.03 (s, 9H).

^{13}C NMR (101 MHz, $CDCl_3$): δ 179.0, 173.2, 143.5, 128.7, 128.0, 127.2, 89.6, 86.6, 78.7, 71.2, 62.0, 17.3, -1.3.

HRMS (ESI) *m/z* $[M+Na]^+$ calc. for $C_{29}H_{32}NaO_4Si$: 495.1962; found 495.1971.

2-Hydroxymethyl-3-(2-trimethylsilylethoxy)-2*H*-furan-5-one (SI-3):

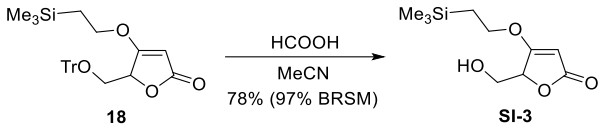

The solid **18** (941 mg, 1.99 mmol, 1.0 equiv) was dissolved in MeCN (18 mL) and then formic acid (6.0 mL, excess amount) was added. The mixture was stirred at r.t. for 5 h, then was diluted by ethyl acetate (300 mL). The organic phase was thoroughly washed with sat. $NaHCO_3$ (aq) and brine, dried over anhydrous Na_2SO_4, and concentrated under vacuum. The residue was purified by silica gel column chromatography. The recovered starting material was eluted by pentane/ethyl acetate *v*/*v* 6:1 (184 mg, 20%), then the deprotection product **SI-3** was eluted by pentane/ethyl acetate 1:1 *v*/*v* and obtained as white solid (356 mg, 78%, 97% BRSM).

R_f: 0.16 (Pentane/EtOA 2:1).

IR ν_{max} (cm^{-1}): 3428 (br), 3122, 2954, 2892, 1738, 1678, 1620, 1463, 1449, 1403, 1379, 1354, 1313, 1246, 1196, 1161, 1100, 1058, 1031, 946, 923, 836.

^1H NMR (400 MHz, $CDCl_3$): δ 5.08 (s, 1H), 4.80 – 4.79 (m, 1H), 4.14 (dd, *J* = 9.6, 7.6 Hz, 2H), 4.04 (ddd, *J* = 12.4, 6.0, 2.8 Hz, 1H), 3.80 (ddd, *J* = 12.4, 8.0, 4.0 Hz, 1H), 2.59 (dd, *J* = 8.0, 6.0 Hz, 1H), 1.19 – 1.13 (m, 2H), 0.07 (s, 9H).

^{13}C NMR (101 MHz, $CDCl_3$): δ 178.8, 173.3, 89.8, 79.9, 71.5, 61.2, 17.4, -1.4.

HRMS (ESI) *m/z* $[M+Na]^+$ calc. for $C_{10}H_{18}NaO_4Si$: 253.0867; found 253.0874.

2-Methylene-3-(2-trimethylsilylethoxy)-2*H*-furan-5-one (19):

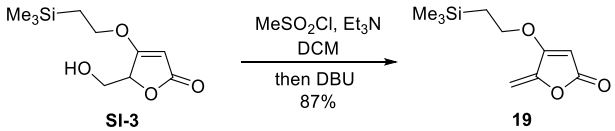

To a stirred solution of **SI-3** (357 mg, 1.55 mmol, 1.0 equiv) in anhydrous DCM (18 mL) was added Et_3N (0.54 mL, 3.88 mmol, 2.5 equiv). The mixture was cooled to 0 °C, then $MeSO_2Cl$ (0.18 mL, 2.33 mmol, 1.5 equiv) was added dropwise. The mixture was stirred at 0 °C to r.t. for 2 h, and full mesylation of **SI-3** was achieved. However, the elimination of the mesylate was incomplete (> 20% mesylate left). To facilitate complete elimination, DBU (0.046 mL, 0.31 mmol, 0.2 equiv) was added. The

mixture was further stirred at r.t. for 2 h, then was diluted with ethyl acetate. The organic phase was washed with water and brine, dried over anhydrous Na_2SO_4, and concentrated under vacuum. The residue was purified by silica gel column chromatography using pentane/ethyl acetate 20:1 *v*/*v* as eluent. The product **19** was obtained as white solid (287 mg, 87%).

R_f: 0.36 (Pentane/EtOA 15:1).

IR ν_{max} (cm^{-1}): 3128, 2953, 2897, 1783, 1669, 1603, 1466, 1415, 1372, 1348, 1260, 1229, 1176, 1097, 1065, 1038, 969, 935, 857, 838, 797.

^1H NMR (400 MHz, $CDCl_3$): δ 5.19 (d, *J* = 1.2 Hz, 1H), 5.04 – 5.02 (m, 2H), 4.17 (t, *J* = 8.4 Hz, 2H), 1.18 (t, *J* = 8.4 Hz, 2H), 0.09 (s, 9H).

^{13}C NMR (101 MHz, $CDCl_3$): δ 168.8, 168.7, 150.2, 92.3, 89.8, 71.1, 17.3, -1.3.

HRMS (ESI) *m/z* $[M+Na]^+$ calc. for $C_{10}H_{16}NaO_3Si$: 235.0761; found 235.0763.

2-Chloromethylene-3-(2-trimethylsilylethoxy)-2*H*-furan-5-one (8a):

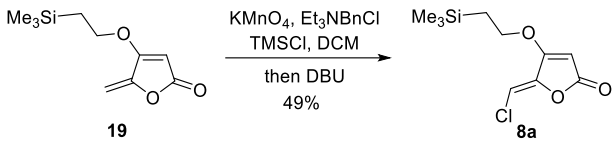

To a flame dried Schlenk flask were added $KMnO_4$ (174 mg, 1.10 mmol, 1.0 equiv), triethylbenzylammonium chloride (251 mg, 1.10 mmol, 1.0 equiv) and anhydrous DCM (20 mL). The mixture was stirred at r.t. for 40 min to generate a homogeneous solution. Then the mixture was cooled to 0 °C and TMSCl (0.56 mL, 4.40 mmol, 4.0 equiv) was added. The mixture was stirred at 0 °C for 20 min to generate a dark green colored solution. To this mixture, the solution of **19** (234 mg, 1.10 mmol, 1.0 equiv) in anhydrous DCM (5 mL) was added at 0 °C dropwise. After addition, the mixture was stirred at 0 °C to r.t. overnight to achieve full conversion. To this mixture, DBU (0.82 mL, 5.50 mmol, 5.0 equiv) was added to facilitate elimination of the dichloride intermediate. After full conversion of the intermediate (ca. 5 h), the mixture was quenched with sat. $NaHCO_3$ (aq) and filtered through celite to remove precipitate. The filtrate was washed with water and brine, dried over anhydrous Na_2SO_4, and concentrated under vacuum. The residue was purified by silica gel column

chromatography using pentane/ethyl acetate 20:1 *v*/*v* as eluent. The product **8a** was obtained as white solid (132 mg, 49%).

R_f: 0.38 (Pentane/EtOA 15:1).

IR ν_{max} (cm^{-1}): 3098, 2954, 2901, 1769, 1588, 1461, 1432, 1401, 1356, 1295, 1248, 1236, 1172, 1067, 942, 922, 882, 836.

^1H NMR (400 MHz, $CDCl_3$): δ 6.06 (s, 1H), 5.20 (s, 1H), 4.18 (t, *J* = 8.4 Hz, 2H), 1.17 (t, *J* = 8.4 Hz, 2H), 0.09 (s, 9H).

^{13}C NMR (101 MHz, $CDCl_3$): δ 168.0, 167.3, 145.4, 100.0, 89.3, 71.6, 17.4, -1.3.

HRMS (ESI) *m/z* $[M+Na]^+$ calc. for $C_{10}H_{15}ClNaO_3Si$: 269.0371; found 269.0371.

2-Bromomethylene-3-(2-trimethylsilylethoxy)-2*H*-furan-5-one (8b):

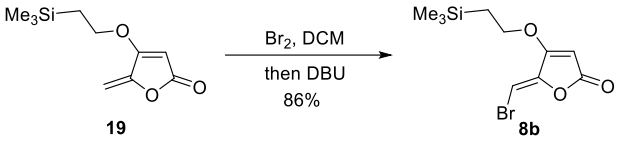

To a flame dried Schlenk flask were added **19** (110 mg, 0.516 mmol, 1.0 equiv) and anhydrous DCM (8 mL). To this solution, Br_2 (0.026 mL, 0.516 mmol, 1.0 equiv) was added dropwise. The mixture was stirred at r.t. overnight, and full conversion of **19** was achieved accompanied by the disappearance of the color of Br_2. To this mixture, DBU (0.085, 0.568 mmol, 1.1 equiv) was added to facilitate elimination of the dibromide intermediate. After 2 h, the mixture was diluted with ethyl acetate, and successively washed with $Na_2S_2O_3$ (aq), water and brine. The organIc phase was dried over anhydrous Na_2SO_4 and concentrated under vacuum. The residue was purified by silica gel column chromatography using pentane/ethyl acetate 20:1 *v*/*v* as eluent. The product **8b** was obtained as white solid (129 mg, 86%).

R_f: 0.32 (Pentane/EtOA 15:1).

IR ν_{max} (cm^{-1}): 3097, 2954, 2901, 1764, 1725, 1589, 1460, 1432, 1398, 1353, 1248, 1233, 1161, 1068, 941, 916, 860, 836.

^1H NMR (400 MHz, $CDCl_3$): δ 6.16 (s, 1H), 5.23 (s, 1H), 4.18 (t, *J* = 8.4 Hz, 2H), 1.17 (t, *J* = 8.4 Hz, 2H), 0.09 (s, 9H).

^{13}C NMR (101 MHz, $CDCl_3$): δ 167.7, 167.3, 147.4, 89.6, 87.8, 71.6, 17.4, -1.3.

HRMS (ESI) *m/z* $[M+Na]^+$ calc. for $C_{10}H_{15}BrNaO_3Si$: 312.9866; found 312.9870.

Triethyl(((*R*,*Z*)-4-((2*S*,3*S*,5*S*)-5-ethyl-5-((2*R*,5*R*,6*S*)-5-ethyl-6-methyl-5-((triethylsilyl)oxy)tetrahydro-2*H*-pyran-2-yl)-3-methyltetrahydrofuran-2-yl)hex-2-en-3-yl)oxy)silane (20a):

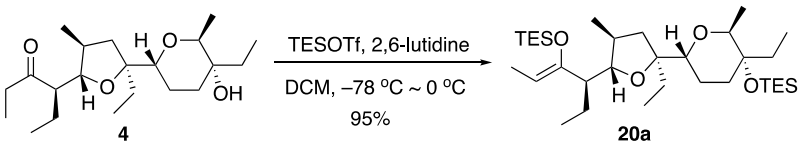

4 **20a**

To a solution of alcohol **4** (3.02 g, 8.52 mmol, 1 eq.) in 35 ml dry DCM cooled to -78 °C, 2,6-lutidine (9.9 mL, 85.2 mmol, 10 eq.) was added under Ar. Then TESOTf (4.8 mL, 21.3 mmol, 2.5 eq.) was added dropwise. The obtained mixture was warmed to 0 °C and stirred overnight. The mixture was diluted with ether and then was washed with water, brine and dried with Na_2SO_4. The solvent was removed, and the crude mixture was purified by flash column chromatography to afford the product **20a** as colorless oil (4.73 g, 95%). The *Z* and *E* configurations are determined by NOE.

R_f: 0.90 (EtOAc/pentane 1:9).

$[\alpha]_D^{299.2\ K}$ +7.8 (c = 1, $CHCl_3$).

IR ν_{max} (cm^{-1}): 2954, 2912, 2876, 1669, 1458, 1240, 1096, 1064, 1046, 1007, 723.

^{1}H NMR (400 MHz, $CDCl_3$): δ 4.53 (q, *J* = 6.6 Hz, 1H), 3.79 (q, *J* = 6.9 Hz, 1H), 3.41 (d, *J* = 9.3 Hz, 1H), 3.35 (t, *J* = 7.8 Hz, 1H), 1.93 – 1.84 (m, 2H), 1.81 – 1.73 (m, 2H), 1.70 – 1.63 (m, 2H), 1.60 – 1.28 (m, 10H), 1.15 (d, *J* = 6.8 Hz, 3H), 1.01 – 0.84 (m, 31H), 0.71 – 0.59 (m, 12H).

^{13}C NMR (101 MHz, $CDCl_3$): δ 151.1, 101.9, 87.7, 84.4, 76.7, 75.2, 74.9, 53.5, 41.9, 38.6, 31.0, 30.9, 28.4, 22.8, 21.8, 17.6, 15.5, 12.5, 11.0, 8.3, 7.5, 7.13, 7.08, 7.0, 6.1.

HRMS (ESI) *m/z* $[M+H]^+$ calc. for $C_{33}H_{67}O_4Si_2$: 583.4572; found 583.4587.

Triethyl(((*R*,*E*)-4-((2*S*,3*S*,5*S*)-5-ethyl-5-((2*R*,5*R*,6*S*)-5-ethyl-6-methyl-5-((triethylsilyl)oxy)tetrahydro-2*H*-pyran-2-yl)-3-methyltetrahydrofuran-2-yl)hex-2-en-3-yl)oxy)silane (20b):

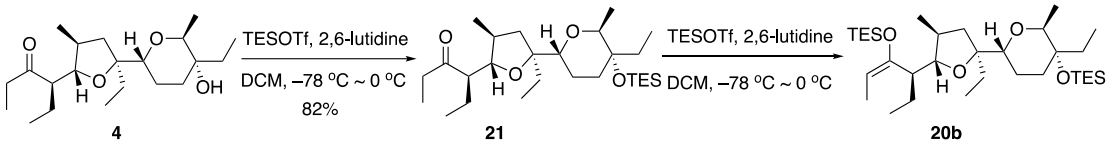

To a solution of alcohol **4** (520 mg, 1.468 mmol, 1 eq.) in 15 ml DCM (0.1 M) cooled to -78 °C under Ar, 2,6-lutidine (850 uL, 7.34 mmol, 5 eq.) was added. Then TESOTf (400 uL, 1.76 mmol, 1.2 eq.) was added slowly. The resulting mixture was slowly warmed to -10 °C and stirred overnight. The mixture was diluted with ether and then was washed with 2 N HCl, sat. aq. $NaHCO_3$, brine and dried with Na_2SO_4. The solvent was removed, and the crude mixture was purified by flash column chromatography to afford the product **21** as colorless oil (562 mg, 82%).

To a solution of mono-TES protected ketone **21** (1.0 eq.) in DCM (0.1 M) was added TESOTf (10 eq.) slowly at -78 °C under Ar. The mixture was stirred at -78 °C for another 2 h before pyridine (10 eq.) was added dropwise. The resulting mixture was warmed to 0 °C and stirred until the ketone disappeared. The mixture was diluted with ether and then was washed with cold sat. aq. $NaHCO_3$, brine and dried with Na_2SO_4. The solvent was removed, and the crude mixture was purified by flash column chromatography to afford the product (**20a**/**20b** ratio 1:2.3) as colorless oil (Note: the *Z*/*E* isomers are very difficult to separate by flash column chromatography. To get acceptable amount of enolate, a mixture of **20a**/**20b** (ratio range from 1:1.7 to 1:3.0) was collected). The total yield is more then 90%.

Only the ^{1}H NMR characteristic peaks were reported here, **20a**/**20b** (*Z*/*E*) ratio 1:2.3:

^{1}H NMR (400 MHz, $CDCl_3$): δ 4.61 (q, *J* = 6.7 Hz, 2.3H) (*E* enolate), 4.53 (q, *J* = 6.7 Hz, 1.0H) (Z enolate), 2.33 (ddd, *J* = 11.1, 8.5, 3.1 Hz, 2.4H) (*E* enolate).

General protocol for the Mukaiyama-aldol reaction:

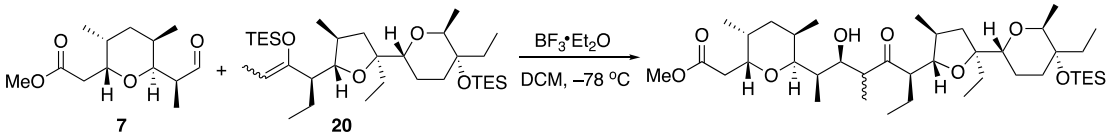

To a solution of aldehyde **7** (1.0 eq) and enolate **20** (2.0-3.0 eq.) in DCM (0.05 M) at -78 °C, $BF_3{\cdot}OEt_2$ (1.5 eq.) was added slowly. The obtained mixture was stirred at -78 °C until the enolate disappeared. The reaction was quenched with sat. aq. $NaHCO_3$ at -78

°C and the mixture was extracted with DCM and dried with Na_2SO_4. The solvent was removed and the crude mixture was purified by flash column chromatography to afford the products.

Using pure *Z*-enolate **20a** (3.0 eq.), 60 h: P2 (442.5 mg, 56%), P3 (232.7 mg, 30%)

Using a mixture of *Z*/*E*-enolate **20a/22b** (*Z*/*E*=1/2.3, 2.0 eq.), 36 h: P2 (41.2 mg, 7%), P3 (457.2 mg, 81%)

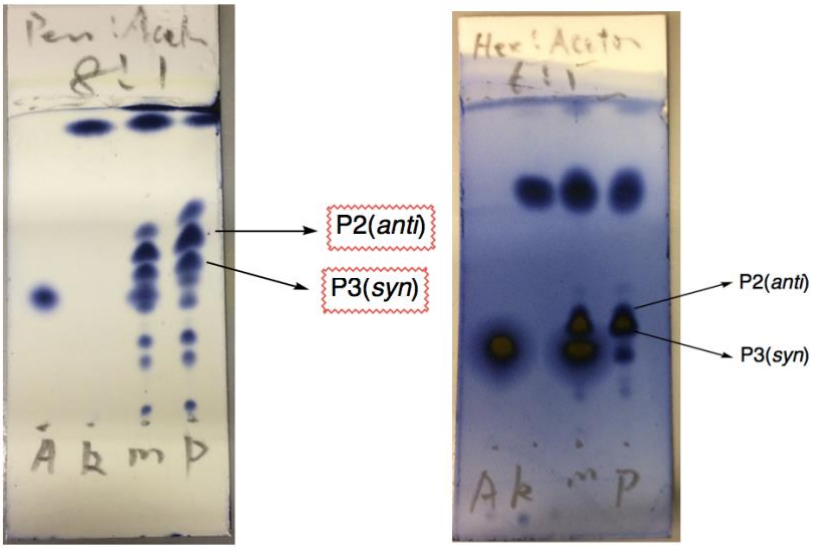

Using pure *Z*-enolate Using a mixture of *Z*/*E*-enolate (*Z*/*E*=1/2.3)

Methyl 2-((2*R*,3*R*,5*R*,6*S*)-6-((2*R*,3*R*,4*R*,6*R*)-6-((2*S*,3*S*,5*S*)-5-ethyl-5-((2*R*,5*R*,6*S*)-5-ethyl-6-methyl-5-((triethylsilyl)oxy)tetrahydro-2*H*-pyran-2-yl)-3-methyltetrahydrofuran-2-yl)-3-hydroxy-4-methyl-5-oxooctan-2-yl)-3,5-dimethyltetrahydro-2*H*-pyran-2-yl)acetate (22)

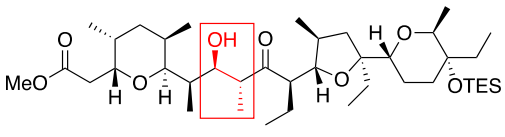

22

22: P2 (*anti*-aldol product)

R_f: 0.58 (Pentane/Acetone= 8/1).

$[\alpha]_D^{296.8\ K}$ -12.8 (c = 1, $CHCl_3$).

IR ν_{max} (cm^{-1}): 3533 (br), 2957, 2876, 1723, 1458, 1377, 1291, 1132, 1072, 1047, 1010, 985, 957.

^{1}H NMR (400 MHz, $CDCl_3$): δ 4.29 (dt, *J* = 12.2, 4.7 Hz, 1H), 3.95 (ddd, *J* = 10.3, 5.9, 1.5 Hz, 1H), 3.83 (dd, *J* = 9.9, 3.4 Hz, 1H), 3.77 – 3.71 (m, 4H), 3.52 (dd, *J* = 10.0, 2.2 Hz, 1H), 3.45 (dd, *J* = 11.3, 2.5 Hz, 1H), 3.19 (d, *J* = 5.9 Hz, 1H), 2.94 – 2.90 (m, 1H), 2.81 (t, *J* = 12.7 Hz, 1H), 2.70 (dt, *J* = 9.8, 3.3 Hz, 1H), 2.30 (dd, *J* = 13.2, 4.0 Hz, 1H), 2.24 (dt, *J* = 12.1, 6.0 Hz, 1H), 2.02 – 1.71 (m, 5H), 1.63 – 1.35 (m, 9H), 1.32 – 1.25 (m, 3H), 1.12 (d, *J* = 6.8 Hz, 3H), 0.99 – 0.82 (m, 27H), 0.76 (d, *J* = 6.9 Hz, 6H), 0.66 – 0.52 (m, 6H).

^{13}C NMR (101 MHz, $CDCl_3$): δ 215.8, 174.7, 84.6, 83.8, 76.7, 75.4, 75.0, 74.0, 72.0, 70.4, 57.8, 52.7, 47.2, 40.1, 37.0, 36.3, 35.0, 32.3, 31.8, 30.3, 29.1, 28.9, 27.0, 22.2, 17.8, 17.6, 16.1, 15.5, 13.6, 12.5, 11.7, 8.0, 7.5, 7.2, 7.1, 7.0, 6.7, 6.4, 5.9.

HRMS (ESI) *m/z* $[M+Na]^+$ calc. for $C_{40}H_{74}NaO_8Si$: 733.5045; found 733.5088.

Methyl 2-((2*R*,3*R*,5*R*,6*S*)-6-((2*R*,3*R*,4*S*,6*R*)-6-((2*S*,3*S*,5*S*)-5-ethyl-5-((2*R*,5*R*,6*S*)-5-ethyl-6-methyl-5-((triethylsilyl)oxy)tetrahydro-2*H*-pyran-2-yl)-3-methyltetrahydrofuran-2-yl)-3-hydroxy-4-methyl-5-oxooctan-2-yl)-3,5-dimethyltetrahydro-2*H*-pyran-2-yl)acetate (23)

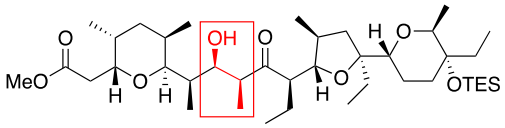

23

23: P3 (*syn*-aldol product)

R_f: 0.50 (Pentane/Acetone= 8/1).

$[\alpha]_D^{296.8\ K}$ -1.0 (c = 1, $CHCl_3$).

IR ν_{max} (cm^{-1}): 3542 (br), 2959, 2935, 2876, 1726, 1458, 1378, 1290, 1132, 1062, 984.

^{1}H NMR (400 MHz, $CDCl_3$): δ 4.24 (ddd, *J* = 9.2, 6.0, 3.1 Hz, 1H), 4.02 – 3.96 (m, 1H), 3.75 – 3.65 (m, 5H), 3.51 – 3.47 (m, 1H), 3.45 – 3.39 (m, 2H), 2.94 – 2.89 (m, 1H), 2.81 (td, *J* = 12.7, 2.5 Hz, 1H), 2.58 (dq, *J* = 9.5, 3.4 Hz, 1H), 2.27 – 2.14 (m, 2H), 1.91 – 1.77 (m, 4H), 1.71 – 1.68 (m, 1H), 1.65 – 1.55 (m, 2H), 1.52 – 1.36 (m, 4H), 1.34 – 1.25 (m, 3H), 1.22– 1.18 (m, 3H), 1.12 (dd, *J* = 6.9, 2.5 Hz, 3H), 0.96 – 0.71 (m, 33H), 0.63 – 0.50 (m, 6H).

^{13}C NMR (101 MHz, $CDCl_3$): δ 215.1, 174.5, 84.9, 83.9, 76.7, 75.2, 75.0, 73.9, 71.3, 69.4, 55.7, 52.2, 48.2, 40.9, 37.9, 37.6, 35.0, 31.61, 31.59, 30.4, 28.9, 28.5, 27.0, 21.8, 18.9, 17.7, 16.8, 15.5, 15.4, 12.3, 11.8, 8.6, 8.1, 7.4, 7.0, 6.9.

HRMS (ESI) *m/z* $[M+Na]^+$ calc. for $C_{40}H_{74}NaO_8Si$: 733.5045; found 733.5089.

General protocol for the TES deprotection:

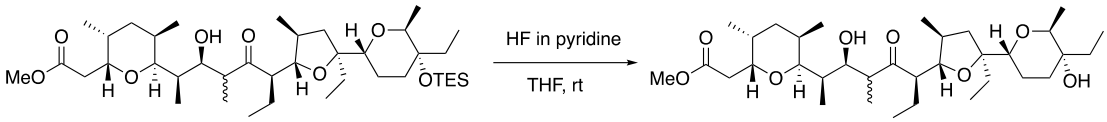

To a solution of the ester (1.0 eq.) in dry THF (0.1 M) in a plastic vial under Ar at room temperature, hydrogen fluoride in pyridine (1.0 mL per 1.0 mmol) was added dropwise. The resulting mixture was stirred until SM disappeared (~24 h). The mixture was diluted with water and extracted with ether. The combined organic layers were washed with 1N HCl and dried with Na_2SO_4. The solvent was removed, and the crude mixture was purified by flash column chromatography to afford the product.

Methyl 2-((2*R*,3*R*,5*R*,6*S*)-6-((2*R*,3*R*,4*R*,6*R*)-6-((2*S*,3*S*,5*S*)-5-ethyl-5-((2*R*,5*R*,6*S*)-5-ethyl-5-hydroxy-6-methyltetrahydro-2*H*-pyran-2-yl)-3-methyltetrahydrofuran-2-yl)-3-hydroxy-4-methyl-5-oxooctan-2-yl)-3,5-dimethyltetrahydro-2*H*-pyran-2-yl)acetate (24)

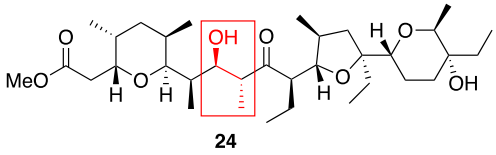

24

24: from *anti* isomer: 81%. The single crystal sample for XRD analysis was obtained via the single-tube method using EtOAc/Pentane as solvent.

R_f: 0.13 (Pentane/EtOAc 4:1).

$[\alpha]_D^{296.7\ K}$ -4.2 (c = 1, $CHCl_3$).

IR ν_{max} (cm^{-1}): 3530 (br), 2961, 2936, 2877, 1720, 1458, 1378, 1291, 1215, 1179, 1131, 1072, 1050, 984, 956.

^1H NMR (400 MHz, $CDCl_3$): δ 4.29 (dt, *J* = 11.9, 4.8 Hz, 1H), 3.95 (ddd, *J* = 10.3, 6.5, 1.5 Hz, 1H), 3.83 – 3.72 (m, 5H), 3.54 – 3.48 (m, 2H), 3.26 (d, *J* = 6.0 Hz, 1H), 2.93 (dq, *J* = 10.2, 6.8 Hz, 1H), 2.81 (t, *J* = 12.7 Hz, 1H), 2.70 – 2.66 (m, 2H), 2.31 (dd, *J* = 13.2, 4.1 Hz, 1H), 2.24 (dt, *J* = 11.8, 6.0 Hz, 1H), 2.06 – 1.78 (m, 4H), 1.66 – 1.25 (m, 13H), 1.17 (d, *J* = 6.9 Hz, 3H), 0.99 (d, *J* = 6.4 Hz, 3H), 0.95 (d, *J* = 7.0 Hz, 3H), 0.92 – 0.88 (m, 9H), 0.84 (t, *J* = 7.4 Hz, 3H), 0.77 – 0.75 (m, 6H).

^{13}C NMR (101 MHz, $CDCl_3$): δ 215.6, 174.7, 84.5, 84.0, 76.9, 75.4, 73.0, 72.0, 71.0, 70.4, 57.7, 52.7, 47.1, 40.1, 36.8, 36.3, 35.0, 32.3, 30.5, 29.5, 29.2, 28.9, 27.0, 21.8, 17.7, 17.6, 16.3, 14.2, 13.8, 12.4, 11.7, 8.1, 7.3, 6.6.

HRMS (ESI) *m/z* $[M+Na]^+$ calc. for $C_{34}H_{60}NaO_8$: 619.4180; found 619.4181.

Methyl 2-((2*R*,3*R*,5*R*,6*S*)-6-((2*R*,3*R*,4*S*,6*R*)-6-((2*S*,3*S*,5*S*)-5-ethyl-5-((2*R*,5*R*,6*S*)-5-ethyl-5-hydroxy-6-methyltetrahydro-2*H*-pyran-2-yl)-3-methyltetrahydrofuran-2-yl)-3-hydroxy-4-methyl-5-oxooctan-2-yl)-3,5-dimethyltetrahydro-2*H*-pyran-2-yl)acetate (25)

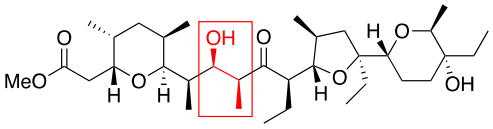

25

25: from *syn* isomer: 93%

R_f: 0.13 (Pentane/EtOAc 4:1).

$[\alpha]_D^{296.4\ K}$ 4.0 (c = 1, $CHCl_3$).

IR ν_{max} (cm^{-1}): 3539 (br), 2961, 2935, 2876, 1725, 1457, 1379, 1290, 1214, 1177, 1132, 1050, 985, 956.

^{1}H NMR (400 MHz, $CDCl_3$): δ 4.25 (dt, *J* = 12.4, 4.2 Hz, 1H), 3.99 (dd, *J* = 9.0, 4.9 Hz, 1H), 3.77 – 3.65 (m, 5H), 3.52 – 3.45 (m, 3H), 2.95 – 2.88 (m, 1H), 2.82 (t, *J* = 12.6 Hz, 1H), 2.62 – 2.56 (m, 2H), 2.27 (dd, *J* = 13.1, 3.7 Hz, 1H), 2.24 – 2.16 (m, 1H), 1.93 – 1.84 (m, 3H), 1.82 – 1.76 (m, 1H), 1.62 – 1.40 (m, 11H), 1.38 – 1.26 (m, 2H), 1.21 – 1.18 (m, 6H), 0.95 (d, *J* = 5.7 Hz, 3H), 0.92 – 0.79 (m, 12H), 0.77 (d, *J* = 6.9 Hz, 3H), 0.74 (d, *J* = 6.9 Hz, 3H).

^{13}C NMR (101 MHz, $CDCl_3$): δ 214.9, 174.5, 84.6, 84.0, 77.1, 75.3, 73.1, 71.3, 71.1, 69.6, 55.7, 52.3, 48.2, 41.1, 37.9, 37.6, 35.0, 31.6, 30.5, 29.4, 28.9, 28.3, 27.0, 21.4, 18.9, 17.7, 17.0, 15.5, 14.2, 12.2, 11.8, 8.7, 8.2, 6.6.

HRMS (ESI) *m/z* $[M+Na]^+$ calc. for $C_{34}H_{60}NaO_8$: 619.4180; found 619.4198.

General protocol for the methyl ester hydrolysis:

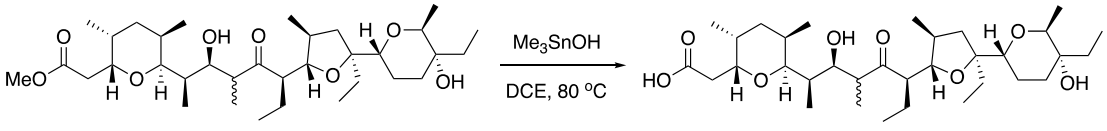

To a solution of the ester (1 eq.) and Me_3SnOH (5 eq.) in DCE (0.025 M) was heated to 80 °C until TLC analysis indicated a complete reaction (48 h). Then solvent was removed and the residue was taken up in EtOAc. The organic layer was then washed with aq. HCl (5%), brine and dried over Na_2SO_4. The solvent was removed, and the crude mixture was purified by flash column chromatography to afford the product.

2-((2*R*,3*R*,5*R*,6*S*)-6-((2*R*,3*R*,4*R*,6*R*)-6-((2*S*,3*S*,5*S*)-5-Ethyl-5-((2*R*,5*R*,6*S*)-5-ethyl-5-hydroxy-6-methyltetrahydro-2*H*-pyran-2-yl)-3-methyltetrahydrofuran-2-yl)-3-hydroxy-4-methyl-5-oxooctan-2-yl)-3,5-dimethyltetrahydro-2*H*-pyran-2-yl)acetic acid (26)

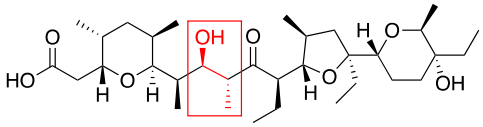

26

26: from *anti* isomer derivative: quantitative yield.

R_f: 0.40 (DCM/MeOH/AcOH 20:1:0.01).

$[\alpha]_D^{296.2\ K}$ -10.8 (c = 1, MeOH).

IR ν_{max} (cm^{-1}): 3484 (br), 2961, 2935, 2879, 1711, 1598 (br), 1458, 1379, 1288, 1130, 1108, 1071, 1053, 988, 956.

^{1}H NMR (400 MHz, CD_3OD): δ 4.27 (dt, *J* = 10.5, 4.3 Hz, 1H), 4.03 (dd, *J* = 10.4, 1.7 Hz, 1H), 3.88 (dd, *J* = 10.0, 2.7 Hz, 1H), 3.77 (q, *J* = 6.9 Hz, 1H), 3.62 – 3.54 (m, 2H), 3.02 (dq, *J* = 10.4, 7.1 Hz, 1H), 2.79 – 2.73 (m, 2H), 2.34 (dd, *J* = 13.1, 3.8 Hz, 1H), 2.27 – 2.21 (m, 1H), 2.07 – 2.00 (m, 1H), 1.93 – 1.83 (m, 3H), 1.78 (dd, *J* = 12.3, 8.0 Hz, 1H), 1.65 – 1.28 (m, 12H), 1.19 (d, *J* = 6.9 Hz, 3H), 1.03 (d, *J* = 6.3 Hz, 3H), 0.98 (d, *J* = 7.0 Hz, 3H), 0.92 – 0.85 (m, 12H), 0.80 – 0.77 (m, 6H).

^{13}C NMR (101 MHz, CD_3OD): δ 218.5, 177.7, 86.5, 85.6, 77.2, 74.0, 73.6, 72.2, 71.5, 58.9, 48.0, 40.3, 37.6, 37.4, 35.9, 32.6, 32.4, 30.7, 30.6, 30.2, 28.5, 22.7, 18.2, 17.8, 16.0, 14.9, 14.1, 13.2, 12.0, 8.4, 7.6, 6.7.

HRMS (ESI) *m/z* $[M-H]^-$ calc. for $C_{33}H_{57}O_8$: 581.4059; found 581.4064.

2-((2*R*,3*R*,5*R*,6*S*)-6-((2*R*,3*R*,4*S*,6*R*)-6-((2*S*,3*S*,5*S*)-5-Ethyl-5-((2*R*,5*R*,6*S*)-5-ethyl-5-hydroxy-6-methyltetrahydro-2*H*-pyran-2-yl)-3-methyltetrahydrofuran-2-yl)-3-h

ydroxy-4-methyl-5-oxooctan-2-yl)-3,5-dimethyltetrahydro-2*H*-pyran-2-yl)acetic acid (27)

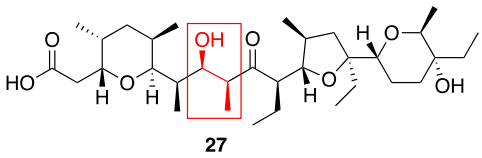

27

27: from *syn* isomer derivative: 89%

R_f: 0.24 (DCM/MeOH/AcOH 20:1:0.01).

$[\alpha]_D^{296.2\ K}$ 6.0 (c = 1, MeOH).

IR ν_{max} (cm^{-1}): 3474 (br), 2963, 2937, 2879, 1710, 1618 (br), 1458, 1379, 1284, 1215, 1176, 1132, 1095, 1077, 1050, 986, 954.

^{1}H NMR (400 MHz, CD_3OD): δ 4.31 – 4.26 (m, 1H), 4.10 (d, *J* = 9.4 Hz, 1H), 3.80 – 3.71 (m, 2H), 3.60 – 3.46 (m, 3H), 2.99 – 2.91 (m, 1H), 2.72 (t, *J* = 12.3 Hz, 1H), 2.69 (dq, *J* = 12.3 Hz, 1H), 2.37 (d, *J* = 13.6 Hz, 1H), 2.26 – 2.18 (m, 1H), 2.04 – 1.95 (m, 1H), 1.90 – 1.83 (m, 3H), 1.74 – 1.40 (m, 12H), 1.36 – 1.29 (m, 3H), 1.21 – 1.16 (m, 6H), 1.01 (d, *J* = 6.3 Hz, 3H), 0.92 – 0.83 (m, 12H), 0.80 – 0.78 (m, 6H).

^{13}C NMR (101 MHz, CD_3OD): δ 216.5, 178.0 (br), 86.5, 85.0, 77.4, 76.9, 74.2, 72.5, 72.2, 71.0, 66.9, 64.2, 56.8, 49.5, 41.4, 39.0, 38.6, 36.0, 32.8 (br), 32.4, 30.7, 30.2, 29.7, 28.5, 22.3, 19.6, 17.9, 17.1, 15.9, 15.5, 15.0, 12.4, 12.3, 8.9, 8.6, 6.8.

HRMS (ESI) *m/z* $[M-H]^-$ calc. for $C_{33}H_{57}O_8$: 581.4059; found 581.4068.

Sodium (*Z*)-2-(chloromethylene)-4-(2-((2*R*,3*R*,5*R*,6*S*)-6-((2*R*,3*R*,4*R*,6*R*)-6-((2*S*,3*S*,5*S*)-5-ethyl-5-((2*R*,5*R*,6*S*)-5-ethyl-5-hydroxy-6-methyltetrahydro-2*H*-pyran-2-yl)-3-methyltetrahydrofuran-2-yl)-3-hydroxy-4-methyl-5-oxooctan-2-yl)-3,5-dimethyltetrahydro-2*H*-pyran-2-yl)acetyl)-5-oxo-2,5-dihydrofuran-3-olate (6)

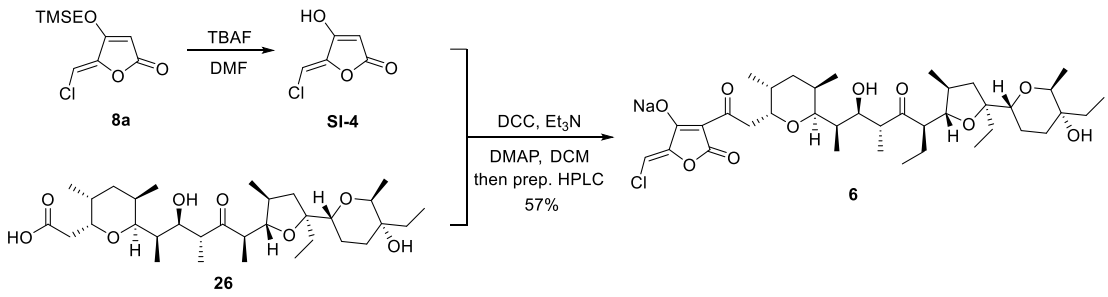

8a SI-4 26 6

To a stirred solution of TMSE protected tetronate **8a** (49 mg, 0.20 mmol, 2.0 equiv) in DMF (3.6 mL) was added TBAF (1 M solution in THF, 0.40 mL, 0.40 mmol, 4.0 equiv). The mixture was stirred at r.t. for 4 h, then was acidified with 1 M HCl (aq) and diluted with ethyl acetate. The organic phase was thoroughly washed with water and brine, dried over anhydrous Na_2SO_4, and concentrated under vacuum. The crude tetronic acid **SI-4** was obtained as white solid almost quantitatively and directly used in the next coupling reaction without further purification.

To a flame dried Schlenk tube were added tetronic acid **SI-4** (crude solid, 0.20 mmol, 2.0 equiv) and acid **26** (58 mg, 0.10 mmol, 1.0 equiv). To this mixture, anhydrous DCM (4 mL) was added, followed by Et_3N (0.028 mL, 0.20 mmol, 2.0 equiv) to give a clear solution. To this solution, DCC (41 mg, 0.20 mmol, 2.0 equiv) was added, followed by DMAP (4.0 mg, 0.033 mmol, 0.33 equiv). After 1 h, DCU started to precipitate. The mixture was stirred at r.t. for 24 h, till the full conversion of the acid **26**. The mixture was then diluted with ethyl acetate, and the organic phase was washed with 1 M HCl (aq) to remove DMAP and Et_3N. Then the organic phase was washed with sat. $NaHCO_3$ (aq) to removed excess amount of tetronic acid **SI-4**, and the product **6** with ionophore property was transformed to its sodium salt and retained in the organic phase. The organic phase was dried over anhydrous Na_2SO_4 and concentrated under vacuum. The residue was treated with MeCN, and the insoluble DCU was removed by filtration. The filtrate was concentrated again, and the residue was dissolved into MeCN/10 mM $NaHCO_3$ (aq) 1:1 *v*/*v* (10 mL in total) and filtered through PTFE membrane to give the sample solution for preparative HPLC separation (concentration of product ~ 10 mM). The sample was then separated on C18 preparative HPLC column using MeCN/10 mM NH_4HCO_3 (aq) as eluent (40% to 50% MeCN gradient, multiple injections). The peak with strong UV absorption was eluted at 14 min and was collected. The collected solutions from all injections were combined and concentrated under vacuum to remove most of the MeCN, and the water phase was thoroughly extracted with DCM (5 × 100 mL). The combined organic phase was dried over anhydrous Na_2SO_4 and concentrated under vacuum. The product **6** (in sodium salt form as shown in the XRD structure) was obtained as colorless solid (42.1 mg, 57%). The single crystal sample for XRD analysis was obtained via the single-tube method using MeCN as solvent.

R_f: 0.52 (pentane/ethyl acetate 1:1).

$[\alpha]_D^{296.7\ K}$ +114.3 (c = 0.46, DCM).

IR ν_{max} (cm^{-1}): 3409 (br), 2964, 2909, 2880, 1760, 1705, 1663, 1626, 1555, 1454, 1424, 1379, 1308, 1055, 988, 964, 949, 834.

^{1}H NMR (500 MHz, ^{6}d-DMSO): δ 6.04 (s, 1H), 4.46 (d, *J* = 6.0 Hz, 1H), 4.16 – 4.12 (m, 1H), 3.91 (s, 1H), 3.79 – 3.75 (m, 2H), 3.66 (q, *J* = 7.0 Hz, 1H), 3.50 (d, *J* = 9.5 Hz, 1H), 3.40 (d, *J* = 11.0 Hz, 1H), 3.35 (dd, *J* = 13.5, 4.5 Hz, 1H), 2.88 – 2.81 (m, 1H), 2.63 – 2.61 (m, 1H), 2.47 (dd, *J* = 13.0, 9.0 Hz, 1H), 2.06 – 2.03 (m, 1H), 1.95 – 1.89 (m, 1H), 1.78 – 1.67 (m, 4H), 1.59 – 1.52 (m, 2H), 1.50 – 1.26 (m, 8H), 1.21 – 1.16 (m, 2H), 1.07 (d, *J* = 7.0 Hz, 3H), 0.95 (d, *J* = 6.0 Hz, 3H), 0.86 (d, *J* = 7.0 Hz, 3H), 0.83 (t, *J* = 7.5 Hz, 3H), 0.80 – 0.77 (m, 6H), 0.74 (d, *J* = 6.5 Hz, 6H), 0.66 (d, *J* = 6.5 Hz, 3H).

^{13}C NMR (101 MHz, ^{6}d-DMSO): δ 214.5, 193.1, 178.4, 167.9, 148.9, 94.2, 94.1, 84.1, 83.7, 75.4, 74.7, 72.5, 70.8, 69.6, 69.5, 56.3, 46.1, 35.9, 35.7, 35.4, 34.9, 31.4, 29.3, 28.9, 28.4, 27.5, 21.2, 17.4, 16.9, 15.7, 14.6, 13.3, 12.8, 11.9, 7.8, 7.3, 6.4.

HRMS (ESI) *m/z* [M-Na]$^-$ calc. for $C_{38}H_{58}ClO_{10}$: 709.3724; found 709.3765.

Sodium (*Z*)-2-(bromomethylene)-4-(2-((2*R*,3*R*,5*R*,6*S*)-6-((2*R*,3*R*,4*R*,6*R*)-6-((2*S*,3*S*,5*S*)-5-ethyl-5-((2*R*,5*R*,6*S*)-5-ethyl-5-hydroxy-6-methyltetrahydro-2*H*-pyran-2-yl)-3-methyltetrahydrofuran-2-yl)-3-hydroxy-4-methyl-5-oxooctan-2-yl)-3,5-dimethyltetrahydro-2*H*-pyran-2-yl)acetyl)-5-oxo-2,5-dihydrofuran-3-olateNonthmicin analog (29)

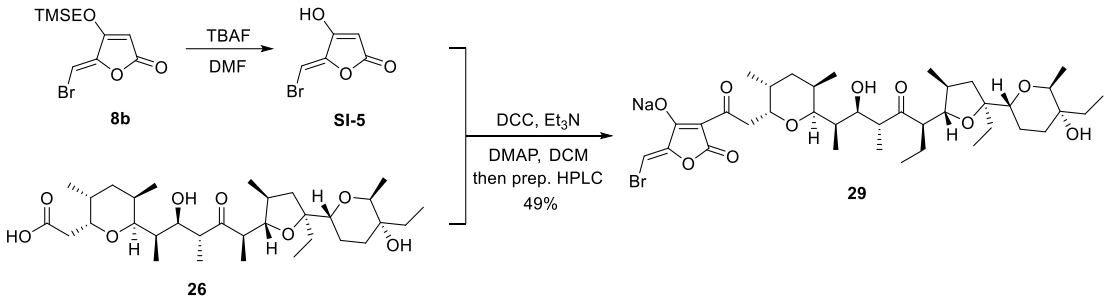

To a stirred solution of TMSE protected tetronate **8b** (23 mg, 0.080 mmol, 2.0 equiv) in DMF (1.6 mL) was added TBAF (1 M solution in THF, 0.16 mL, 0.16 mmol, 4.0

equiv). The mixture was stirred at r.t. for 4 h, then was acidified with 1 M HCl (aq) and diluted with ethyl acetate. The organic phase was thoroughly washed with water and brine, dried over anhydrous Na_2SO_4, and concentrated under vacuum. The crude tetronic acid **SI-5** was obtained as white solid almost quantitatively and directly used in the next coupling reaction without further purification.

To a flame dried Schlenk tube were added tetronic acid **SI-5** (crude solid, 0.080 mmol, 2.0 equiv) and acid **26** (23 mg, 0.040 mmol, 1.0 equiv). To this mixture, anhydrous DCM (2 mL) was added, followed by Et_3N (0.011 mL, 0.080 mmol, 2.0 equiv) to give a clear solution. To this solution, DCC (16 mg, 0.080 mmol, 2.0 equiv) was added, followed by DMAP (1.6 mg, 0.013 mmol, 0.33 equiv). After 1 h, DCU started to precipitate. The mixture was stirred at r.t. for 24 h, till the full conversion of the acid **26**. The mixture was then diluted with ethyl acetate, and the organic phase was washed with 1 M HCl (aq) to removed DMAP and Et_3N. Then the organic phase was washed with sat. $NaHCO_3$ (aq) to removed excess amount of tetronic acid **SI-5**, and the product **29** with ionophore property was transformed to its sodium salt and retained in the organic phase. The organic phase was dried over anhydrous Na_2SO_4 and concentrated under vacuum. The residue was treated with MeCN, and the insoluble DCU was removed by filtration. The filtrate was concentrated again, and the residue was dissolved into MeCN/10 mM $NaHCO_3$ (aq) 1:1 *v*/*v* (10 mL in total) and filtered through PTFE membrane to give the sample solution for preparative HPLC separation (concentration of product ~ 10 mM). The sample was then separated on C18 preparative HPLC column using MeCN/10 mM NH_4HCO_3 (aq) as eluent (30% to 50% MeCN gradient, multiple injections). The peak with strong UV absorption was eluted at 18 min and was collected. The collected solutions from all injections were combined and concentrated under vacuum to remove most of the MeCN, and the water phase was thoroughly extracted with DCM (5 × 100 mL). The combined organic phase was dried over anhydrous Na_2SO_4 and concentrated under vacuum. The product **29** (in sodium salt form as shown in the XRD structure) was obtained as colorless solid (15.2 mg, 49%). The single crystal sample for XRD analysis was obtained via the single-tube method using MeCN as solvent.

R_f: 0.55 (pentane/ethyl acetate 1:1).

$[\alpha]_D^{296.7\ K}$ +137.8 (c = 0.50, DCM).

IR ν_{max} (cm^{-1}): 3418 (br), 2962, 2933, 2876, 1761, 1705, 1683, 1625, 1555, 1450, 1424, 1381, 1298, 1091, 988, 964, 949.

^{1}H NMR (500 MHz, ^{6}d-DMSO): δ 6.06 (s, 1H), 4.46 (d, *J* = 6.0 Hz, 1H), 4.16 – 4.12 (m, 1H), 3.90 (s, 1H), 3.78 – 3.75 (m, 2H), 3.65 (q, *J* = 7.0 Hz, 1H), 3.50 (d, *J* = 9.0 Hz, 1H), 3.40 (d, *J* = 11.0 Hz, 1H), 3.36 – 3.32 (m, 1H), 2.88 – 2.81 (m, 1H), 2.64 – 2.61 (m, 1H), 2.46 (dd, *J* = 13.0, 8.5 Hz, 1H), 2.07 – 2.01 (m, 1H), 1.95 – 1.88 (m, 1H), 1.78 – 1.67 (m, 4H), 1.58 – 1.50 (m, 2H), 1.47 – 1.26 (m, 8H), 1.21 – 1.16 (m, 2H), 1.07 (d, *J* = 6.5 Hz, 3H), 0.95 (d, *J* = 6.5 Hz, 3H), 0.86 (d, *J* = 7.0 Hz, 3H), 0.82 (t, *J* = 7.0 Hz, 3H), 0.81 – 0.77 (m, 6H), 0.74 (d, *J* = 6.5 Hz, 6H), 0.66 (d, *J* = 6.5 Hz, 3H).

^{13}C NMR (101 MHz, ^{6}d-DMSO): δ 214.7, 193.4, 178.0, 168.0, 151.0, 94.3, 84.2, 83.7, 82.8, 75.4, 74.7, 72.4, 70.7, 69.6, 69.5, 56.2, 46.1, 35.8, 35.7, 35.4, 34.9, 31.4, 29.3, 28.9, 28.4, 27.5, 21.1, 17.3, 16.7, 15.7, 14.5, 13.3, 12.9, 11.9, 7.9, 7.3, 6.4.

HRMS (ESI) m/z [M-Na]$^{-}$: calcd. for $C_{38}H_{58}BrO_{10}$: 753.3219; found: 753.3261.

Sodium 4-(2-((2*R*,3*R*,5*R*,6*S*)-6-((2*R*,3*R*,4*R*,6*R*)-6-((2*S*,3*S*,5*S*)-5-ethyl-5-((2*R*,5*R*,6*S*)-5-ethyl-5-hydroxy-6-methyltetrahydro-2*H*-pyran-2-yl)-3-methyltetrahydrofuran-2-yl)-3-hydroxy-4-methyl-5-oxooctan-2-yl)-3,5-dimethyltetrahydro-2*H*-pyran-2-yl)acetyl)-2-methylene-5-oxo-2,5-dihydrofuran-3-olate (30)

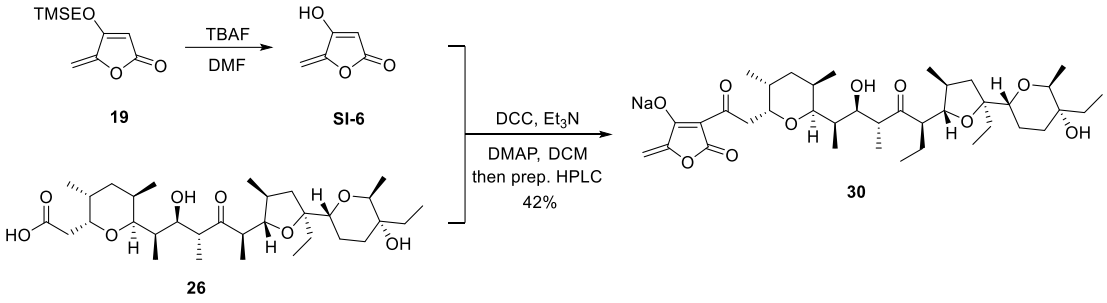

To a stirred solution of TMSE protected tetronate **19** (29 mg, 0.14 mmol, 3.0 equiv) in DMF (2.7 mL) was added TBAF (1 M solution in THF, 0.28 mL, 0.28 mmol, 6.0 equiv). The mixture was stirred at r.t. for 4 h, then was acidified with 1 M HCl (aq) and diluted with ethyl acetate. The organic phase was thoroughly washed with water and brine, and dried over anhydrous Na_2SO_4. During the workup process, some white

precipitate was observed, which was attributed to the partial dimerization of the tetronic acid **SI-6** via hetero-Diels-Alder reaction. The amount of **SI-6** consumed in the side reaction was lower than 1/3, so the amount of **SI-6** obtained should be around 0.092 mmol (2.0 equiv). The precipitate was removed via filtration, and the filtrate was concentrated under vacuum. The crude tetronic acid **SI-6** was obtained as white solid and directly used in the next coupling reaction without further purification.

To a flame dried Schlenk tube were added tetronic acid **SI-6** (crude solid, 0.092 mmol, 2.0 equiv) and acid **26** (27 mg, 0.046 mmol, 1.0 equiv). To this mixture, anhydrous DCM (3 mL) was added, followed by Et_3N (0.013 mL, 0.092 mmol, 2.0 equiv) to give a clear solution. To this solution, DCC (19 mg, 0.092 mmol, 2.0 equiv) was added, followed by DMAP (1.8 mg, 0.015 mmol, 0.33 equiv). After 1 h, DCU started to precipitate. The mixture was stirred at r.t. for 24 h, till the full conversion of the acid **26**. The mixture was then diluted with ethyl acetate, and the organic phase was washed with 1 M HCl (aq) to remove DMAP and Et_3N. Then the organic phase was washed with sat. $NaHCO_3$ (aq) to remove excess amount of tetronic acid **SI-6**, and the product **30** with ionophore property was transformed to its sodium salt and retained in the organic phase. The organic phase was dried over anhydrous Na_2SO_4 and concentrated under vacuum. The residue was treated with MeCN, and the insoluble DCU was removed by filtration. The filtrate was concentrated again, and the residue was dissolved into MeCN/10 mM $NaHCO_3$ (aq) 1:1 *v*/*v* (10 mL in total) and filtered through PTFE membrane to give the sample solution for preparative HPLC separation (concentration of product ~ 10 mM). The sample was then separated on C18 preparative HPLC column using MeCN/10 mM NH_4HCO_3 (aq) as eluent (40% to 50% MeCN gradient, multiple injections). The peak with strong UV absorption was eluted at 14 min and was collected. The collected solutions from all injections were combined and concentrated under vacuum to remove most of the MeCN, and the water phase was thoroughly extracted with DCM (5 × 100 mL). The combined organic phase was dried over anhydrous Na_2SO_4 and concentrated under vacuum. The product **30** (in sodium salt form) was obtained as colorless solid (15.2 mg, 49%).

R_f: 0.34 (pentane/ethyl acetate 1:1).

$[\alpha]_D^{296.7\ K}$ +107.0 (c = 0.34, DCM).

IR ν_{max} (cm^{-1}): 3411 (br), 2964, 2935, 2911, 2878, 1752, 1705, 1679, 1633, 1557, 1453, 1426, 1379, 1292, 1053, 988, 972, 949.

^{1}H NMR (400 MHz, ^{6}d-DMSO): δ 4.74 (s, 1H), 4.57 (d, *J* = 6.0 Hz, 1H), 4.48 (s, 1H), 4.16 – 4.12 (m, 1H), 3.92 (s, 1H), 3.81 – 3.75 (m, 2H), 3.66 (q, *J* = 6.8 Hz, 1H), 3.50 (d, *J* = 10.0 Hz, 1H), 3.43 – 3.39 (m, 2H), 2.89 – 2.81 (m, 1H), 2.63 – 2.59 (m, 1H), 2.44 (dd, *J* = 12.8, 8.8 Hz, 1H), 2.08 – 2.01 (m, 1H), 1.96 – 1.88 (m, 1H), 1.79 – 1.70 (m, 4H), 1.62 – 1.52 (m, 2H), 1.48 – 1.16 (m, 10H), 1.07 (d, *J* = 6.8 Hz, 3H), 0.95 (d, *J* = 6.0 Hz, 3H), 0.87 – 0.74 (m, 18H), 0.66 (d, *J* = 6.8 Hz, 3H).

^{13}C NMR (101 MHz, ^{6}d-DMSO): δ 214.7, 193.3, 180.0, 169.3, 154.2, 94.7, 85.5, 84.2, 83.7, 75.5, 74.8, 72.5, 70.7, 69.6, 69.5, 56.2, 46.1, 35.8, 35.7, 35.2, 35.0, 31.4, 29.3, 28.9, 28.4, 27.5, 21.1, 17.4, 16.7, 15.7, 14.5, 13.3, 13.0, 11.9, 7.9, 7.3, 6.4.

HRMS (ESI) m/z [M-Na]$^{-}$: calcd. for $C_{38}H_{59}O_{10}$: 675.4114; found: 675.4149.

Sodium
(*Z*)-2-(chloromethylene)-4-(2-((2*R*,3*R*,5*R*,6*S*)-6-((2*R*,3*R*,4*S*,6*R*)-6-((2*S*,3*S*,5*S*)-5-ethyl-5-((2*R*,5*R*,6*S*)-5-ethyl-5-hydroxy-6-methyltetrahydro-2*H*-pyran-2-yl)-3-methyltetrahydrofuran-2-yl)-3-hydroxy-4-methyl-5-oxooctan-2-yl)-3,5-dimethyltetrahydro-2*H*-pyran-2-yl)acetyl)-5-oxo-2,5-dihydrofuran-3-olate (31)

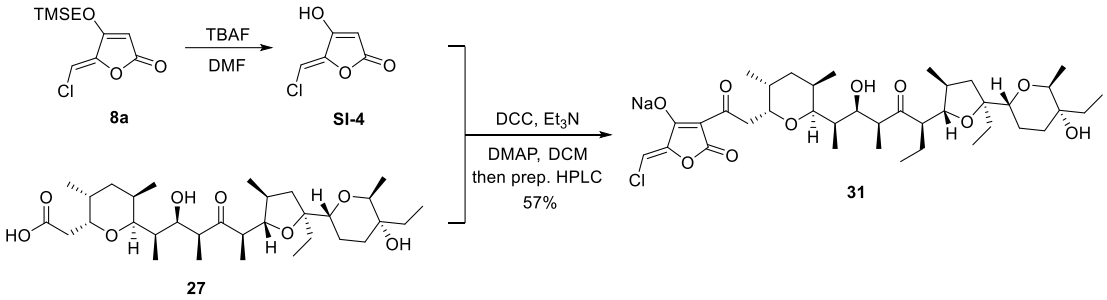

The product **31** was synthesized following the same procedure as product **6**, using acid **27** (undesired epimer of **26**) as the coupling partner. After workup, the crude mixture was dissolved into MeCN/10 mM $NaHCO_3$ (aq) 1:1 *v*/*v* (10 mL in total) and filtered through PTFE membrane to give the sample solution for preparative HPLC separation (concentration of product ~ 10 mM). The sample was then separated on C18 preparative HPLC column using MeCN/10 mM NH_4HCO_3 (aq) as eluent (35% to 45% MeCN gradient, multiple injections). The peak with strong UV absorption

was eluted at 13 min and was collected. The collected solutions from all injections were combined and concentrated under vacuum to remove most of the MeCN, and the water phase was thoroughly extracted with DCM (5 × 100 mL). The combined organic phase was dried over anhydrous Na_2SO_4 and concentrated under vacuum. The product **31** (in sodium salt form as shown in the XRD structure) was obtained as colorless solid (42.2 mg, 57%). The single crystal sample for XRD analysis was obtained via single-tube method using MeCN as solvent.

R_f: 0.69 (ethyl acetate).

$[\alpha]_D^{296.7\ K}$ –1.4 (c = 0.71, DCM).

IR ν_{max} (cm^{-1}): 3408 (br), 2962, 2933, 2876, 1755, 1694, 1662, 1623, 1563, 1454, 1379, 1310, 1222, 1105, 1051, 1029, 989, 948, 833.

^{1}H NMR (500 MHz, ^{6}d-DMSO): δ 6.08 (s, 1H), 4.63 (s, 1H), 4.16 (s, 1H), 3.87 (s, 1H), 3.76 (t, *J* = 8.0 Hz, 1H), 3.65 – 3.59 (m, 2H), 3.48 (d, *J* = 10.0 Hz, 1H), 3.38 – 3.33 (m, 1H), 2.80 – 2.74 (m, 1H), 2.54 – 2.50 (m, 1H), 2.44 – 2.36 (m, 1H), 2.06 – 2.00 (m, 1H), 1.89 – 1.82 (m, 1H), 1.80 – 1.70 (m, 3H), 1.63 – 1.51 (m, 3H), 1.47 – 1.32 (m, 6H), 1.24 – 1.16 (m, 5H), 1.08 (d, *J* = 7.0 Hz, 3H), 1.60 (d, *J* = 6.5 Hz, 3H), 0.91 (d, *J* = 6.0 Hz, 3H), 0.81 – 0.71 (m, 15H), 0.65 (d, *J* = 7.0 Hz, 3H).

^{13}C NMR (101 MHz, ^{6}d-DMSO): δ 213.4, 94.2, 84.2, 82.5, 75.6, 74.4, 73.1, 70.4, 69.5, 68.5, 54.8, 47.5, 40.6, 37.2, 37.0, 36.2, 34.9, 31.4, 29.4, 28.3, 27.7, 27.3, 20.9, 17.7, 17.2, 16.7, 15.9, 14.6, 11.6(2), 11.5(6), 8.1, 7.9, 6.4. (The absence of four peaks from the 3-acyl tetronic acid unit and some broaden peaks were observed after > 20000 scans for 20 mg sample, due to the conformational flexibility.)

HRMS (ESI) m/z $[M\text{-}Na]^-$: calcd. for $C_{38}H_{58}ClO_{10}$: 709.3724; found: 709.3773.

Sodium (*Z*)-2-(chloromethylene)-4-(2-((2*R*,3*R*,5*R*,6*S*)-6-((2*R*,3*S*,4*R*,5*S*,6*S*)-6-((2*S*,3*S*,5*S*)-5-ethyl-5-((2*R*,5*R*,6*S*)-5-ethyl-5-hydroxy-6-methyltetrahydro-2*H*-pyran-2-yl)-3-methyltetrahydrofuran-2-yl)-3,5-dihydroxy-4-methyloctan-2-yl)-3,5-dimethyltetrahydro-2*H*-pyran-2-yl)acetyl)-5-oxo-2,5-dihydrofuran-3-olate (32)

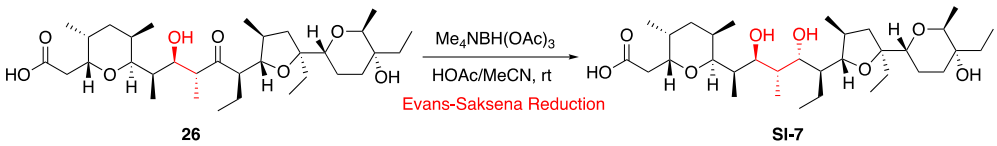

26 **SI-7**

To a solution of $Me_4NBH(OAc)_3$ (132 mg, 0.5 mmol, 10 eq.) in MeCN (1.0 mL) was added HOAc (1.0 mL). The solution was stirred for 30 min at rt and then cooled to 0 ^oC before the ketone **26** (29.1 mg, 0.05 mmol, 1.0 eq.) in MeCN/AcOH (1:1) (1.0 mL) was added dropwise. The obtained mixture was warmed to rt and stirred for 72 h at rt. The reaction mixture was diluted with EtOAc and poured into sat. $NaHCO_3$. Solid $NaHCO_3$ was added until pH>7. Then Rochelles salt solution was added and the mixture was stirred for another 2 h. The layers were separated and the aqueous layer was extracted with EtOAc. The combined organic layers were washed with sat. aq. $NaHCO_3$, aq. 0.1 N HCl, brine and dried over Na_2SO_4, filtered, and concentrated to give the crude product which was used directly in the next step.

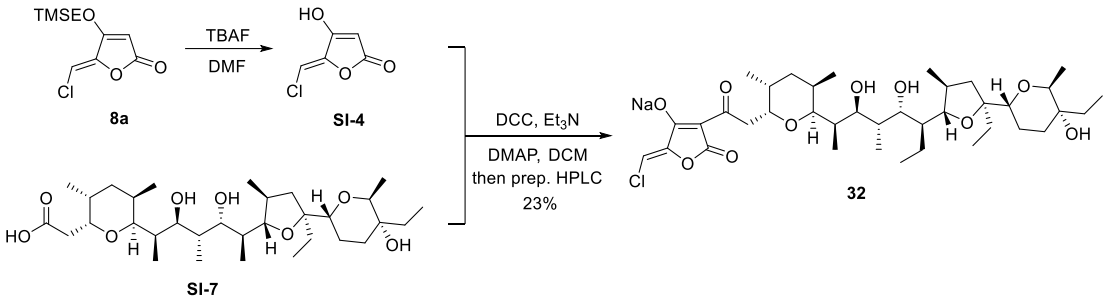

The product **32** was synthesized following the same procedure as product **6**, using crude acid **SI-7** (obtained via 1,3-*anti* reduction of acid **26** on 0.05 mmol scale) as the coupling partner. After workup, the crude mixture was dissolved into MeCN/10 mM $NaHCO_3$ (aq) 1:1 *v*/*v* (10 mL in total) and filtered through PTFE membrane to give the sample solution for preparative HPLC separation (concentration of product ~ 10 mM). The sample was then separated on a C18 preparative HPLC column using MeCN/10 mM NH_4HCO_3 (aq) as eluent (40% to 50% MeCN gradient, multiple injections). The peak with strong UV absorption was eluted at 18 min and was collected. The collected solutions from all injections were combined and concentrated under vacuum to remove most of the MeCN, and the water phase was thoroughly extracted with DCM (5 × 100 mL). The combined organic phase was dried over anhydrous Na_2SO_4 and concentrated under vacuum. The product **32** (in sodium salt form) was obtained as colorless solid (8.4 mg, 23%).

R_f: 0.67 (pentane/ethyl acetate 1:1).

$[\alpha]_D^{296.7\ K}$ +83.8 (c = 0.42, DCM).

IR ν_{max} (cm^{-1}): 3435 (br), 2961, 2935, 2878, 1741, 1661, 1626, 1557, 1453, 1422, 1380, 1310, 1221, 1091, 1083, 990, 964, 947, 834.

^{1}H NMR (400 MHz, ^{6}d-DMSO): δ 6.06 (s, 1H), 4.18 – 4.16 (m, 1H), 4.12 (d, *J* = 6.4 Hz, 1H), 3.86 (s, 1H), 3.90 – 3.83 (m, 1H), 3.78 (d, *J* = 10.0 Hz, 1H), 3.66 (q, *J* = 6.8 Hz, 1H), 3.56 – 3.48 (m, 2H), 3.44 – 3.35 (m, 2H), 2.46 – 2.40 (m, 1H), 2.08 – 2.00 (m, 1H), 1.96 – 1.88 (m, 1H), 1.86 (dd, *J* = 12.4, 8.0 Hz, 1H), 1.73 (br, 1H), 1.66 – 1.33 (m, 13H), 1.26 – 1.17 (m, 4H), 1.11 (d, *J* = 6.8 Hz, 3H), 0.91 – 0.78 (m, 15H), 0.72 (d, *J* = 6.8 Hz, 3H), 0.61 (d, *J* = 6.8 Hz, 3H), 0.58 (d, *J* = 6.8 Hz, 3H).

^{13}C NMR (100 MHz, ^{6}d-DMSO): δ 194.0, 178.4, 168.7, 148.8, 94.5, 94.4, 84.2, 83.7, 75.7, 74.1, 72.8, 70.3, 69.8, 69.6, 67.7, 42.6, 37.6, 37.0, 36.0, 34.90, 34.86, 31.2, 29.5, 28.3, 28.0, 27.2, 20.7, 17.8, 17.2, 15.8, 14.6, 13.9, 11.7, 9.6, 8.2, 7.3, 6.4.

HRMS (ESI) m/z $[M\text{-}Na]^-$: calcd. for $C_{38}H_{60}ClO_{10}$: 711.3880; found: 711.3919.

References

1. Hutz, J. E. *et al.* The multidimensional perturbation value: A single metric to measure similarity and activity of treatments in high-throughput multidimensional screens. *J. Biomol. Screen.* **18**, 367–377 (2013).
2. Bruker. Apex2, SADABS (2016/2) and SAINT (Version 8.38A). (2016).
3. Sheldrick, G. M. SHELXT – Integrated space-group and crystal-structure determination. *Acta Crystallogr. Sect. A Found. Adv.* **A71**, 3–8 (2015).
4. Sheldrick, G. M. Crystal structure refinement with SHELXL. *Acta Crystallogr. Sect. C Struct. Chem.* **C71**, 3–8 (2015).
5. Dolomanov, O. V., Bourhis, L. J., Gildea, R. J., Howard, J. A. K. & Puschmann, H. OLEX2 : a complete structure solution, refinement and analysis program. *J. Appl. Crystallogr.* **42**, 339–341 (2009).
6. Rigaku Oxford Diffraction. CrysAlisPro 1.171.39.46. (2018).
7. Bray, M. A. *et al.* Cell Painting, a high-content image-based assay for morphological profiling using multiplexed fluorescent dyes. *Nat. Protoc.* **11**, 1757–1774 (2016).
8. Svenningsen, E. B. & Poulsen, T. B. Establishing cell painting in a smaller chemical biology lab – A report from the frontier. *Bioorg. Med. Chem.* **27**, 2609–2615 (2019).
9. Lamprecht, M. R., Sabatini, D. M. & Carpenter, A. E. CellProfiler™: free, versatile software for automated biological image analysis. *Biotechniques* **42**, 71–75 (2007).
10. Warnes, G. R. *et al.* gplots: Various R Programming Tools for Plotting Data. (version 3.0.1.1). Available at: https://cran.r-project.org/package=gplots.
11. R Core Team. *R: A Language and Environment for Statistical Computing*. (R Foundation for Statistical Computing, 2018).
12. Wei, T. & Simko, V. R package 'corrplot': Visualization of a Correlation Matrix (version 0.84). (2017). Available at: https://github.com/taiyun/corrplot.
13. Schobert, R. & Jagusch, C. Solution-phase and solid-phase syntheses of enzyme inhibitor RK-682 and antibiotic agglomerins. *J. Org. Chem.* **70**, 6129–6132 (2005).

Compound 4

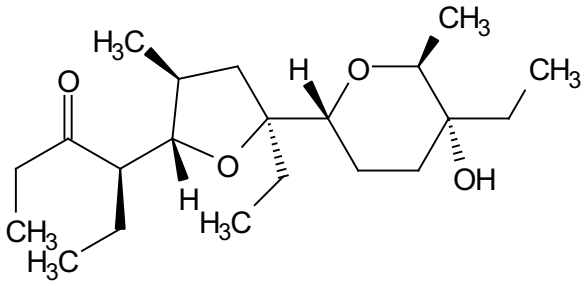

3.7642 3.7471 3.5672 3.5539 3.5431 3.4890 3.4668 2.6251 2.6132 2.5997 2.5953 2.5902 2.5857 2.5771 2.5736 2.5668 2.5603 2.5495 2.4689 2.4509 2.4229 1.8547 1.8343 1.8234 1.8032 1.7538 1.7358 1.7277 1.6243 1.6141 1.6108 1.6071 1.5972 1.5897 1.5735 1.5676 1.5588 1.5450 1.5407 1.5325 1.5275 1.5153 1.5084 1.5007 1.4938 1.4901 1.4740 1.4693 1.4623 1.4552 1.4463 1.4356 1.4151 1.3968 1.3837 1.3797 1.3662 1.3623 1.3484 1.3404 1.3296 1.3217 1.3109 1.3036 1.2858 1.1970 1.1797 1.0207 1.0027 0.9847 0.9088 0.8984 0.8902 0.8824 0.8715 0.8327 0.8143 0.7957

Compound 4

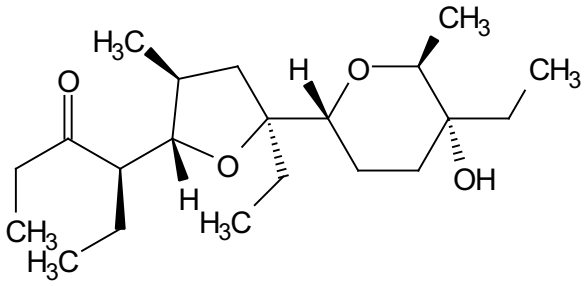

214.1463

85.9790
84.4197
77.4780
77.1600
76.9802
76.8416
73.0083
71.0595

57.5702

40.8321
37.3610
37.0394
30.4575
29.3856
28.6525
21.3692
21.2420
16.8021
14.2465
12.5901
8.1714
7.5124
6.5505

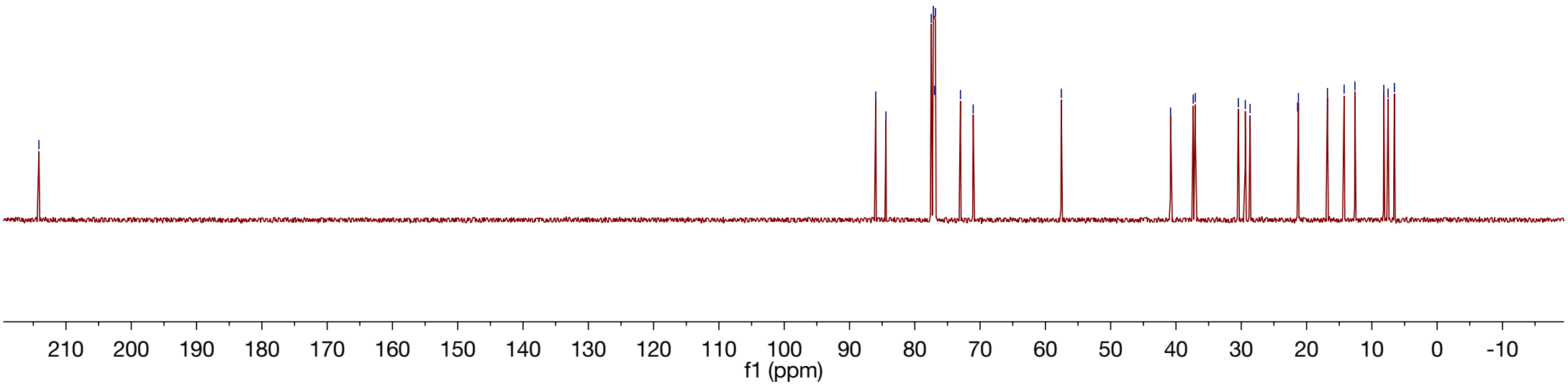

Compound 10

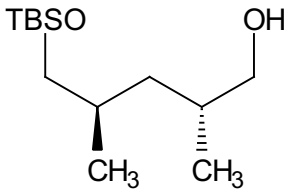
TBSO
OH
CH3
CH3

3.5017
3.4863
3.4756
3.4599
3.4524
3.4368
3.4253
3.4154
3.4110
3.3995
3.3954
3.3864
1.7916
1.7753
1.7627
1.7580
1.7525
1.7474
1.7410
1.7363
1.7308
1.7249
1.7203
1.7143
1.7092
1.6977
1.6819
1.5428
1.4726
1.2494
1.2375
1.2155
1.2039
1.1933
1.1813
1.1652
1.1528
1.1424
1.1307
1.1089
0.9022
0.8960
0.8855
0.8671
0.8505
4.30
2.13
1.00
2.19
16.41
6.48
.0
7.5
7.0
6.5
6.0
5.5
5.0
4.5
4.0
3.5
3.0
2.5
2.0
1.5
1.0
0.5
0.0
-0
f1 (ppm)

Compound 10

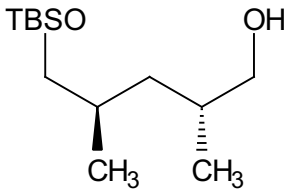

77.4779
77.1604
76.8429
69.1760
69.1416
36.9753
33.2353
33.0867
26.1006
18.5076
16.7764
16.5982
-5.2078

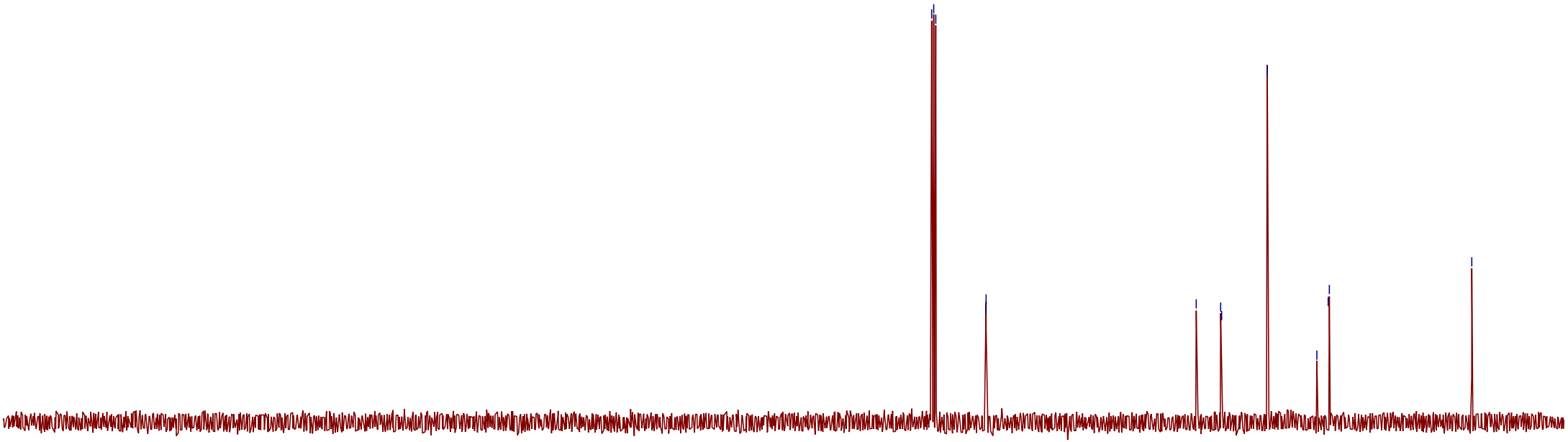

210 200 190 180 170 160 150 140 130 120 110 100 90 80 70 60 50 40 30 20 10 0 -10

f1 (ppm)

Compound 11

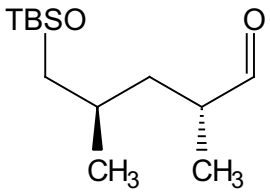

9.6255
9.6206
7.2600
3.4707
3.4561
3.4461
3.4354
3.4315
3.4204
3.4110
3.3958
2.4833
2.4815
2.4676
2.4633
2.4470
2.4303
2.4141
2.4096
2.3971
2.3941
1.7453
1.7301
1.7139
1.7090
1.6990
1.6940
1.6779
1.6629
1.5498
1.5309
1.5160
1.5096
1.4963
1.4818
1.4754
1.4604
1.4494
1.4357
1.4284
1.4149
1.4014
1.3942
1.3804
1.0848
1.0674
0.8948
0.8875
0.8802
0.8728
0.0350

0.90
2.09
1.00
0.99
2.05
3.07
12.15
6.00

f1 (ppm)

Compound 11

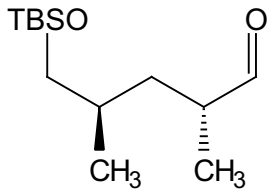
TBSO
O
CH3
CH3

205.5086
77.4786
77.1611
76.8438
68.2843
44.2959
34.1069
33.3817
26.0664
18.4647
16.6352
13.6062
-5.2546
210 200 190 180 170 160 150 140 130 120 110 100 90 80 70 60 50 40 30 20 10 0 -10
f1 (ppm)

Compound 12

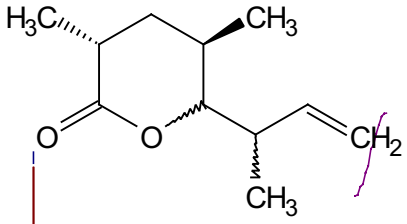

7.2598

5.9840 5.9661 5.9580 5.9405 5.9231 5.9148 5.8970 5.1386 5.1351 5.1316 5.1036 5.1010 5.0970 5.0919 5.0885 5.0775 5.0748 5.0714 4.0398 4.0334 4.0154 4.0090 2.6574 2.6395 2.6273 2.6217 2.6093 2.5915 2.5736 2.4424 2.4237 2.4024 2.3832 2.1775 2.1685 2.1600 2.1512 2.1427 2.1339 2.1252 2.1179 1.9687 1.9604 1.9507 1.9425 1.9347 1.9263 1.9170 1.9085 1.7143 1.7045 1.6829 1.6731 1.6502 1.6404 1.5495 1.3006 1.2828 1.0366 1.0189 1.0126

0.99 2.08 1.00 1.00 1.05 1.04 1.02 1.04 3.25 2.68 3.28

8.0 7.5 7.0 6.5 6.0 5.5 5.0 4.5 4.0 3.5 3.0 2.5 2.0 1.5 1.0 0.5 0.0 -0

f1 (ppm)

Compound 12

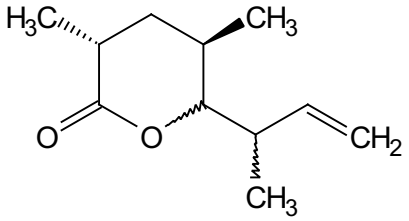
H3C
CH3
O
O
CH2
CH3

174.2021
140.3642
115.1480
87.1455
77.4775
77.1595
76.8412
39.5137
36.4427
31.2932
28.0722
17.9847
15.5138
10.8444
210
200
190
180
170
160
150
140
130
120
110
100
90
80
70
60
50
40
30
20
10
0
-10
f1 (ppm)

Compound 13

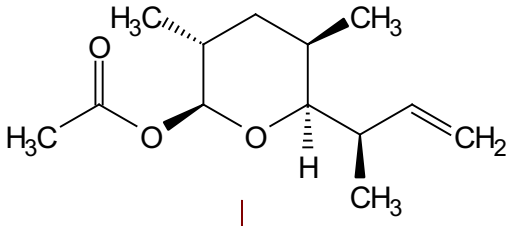

5.9609 5.9451 5.9346 5.9180 5.9015 5.8912 5.8753 5.2345 5.2117 5.0599 5.0559 5.0521 5.0167 5.0128 5.0090 5.0021 4.9985 4.9948 4.9758 4.9716 3.2887 3.2833 3.2636 3.2582 2.3310 2.3135 2.2905 2.2721 2.1127 1.8776 1.8724 1.8551 1.8484 1.8324 1.8251 1.7403 1.7335 1.7236 1.7063 1.6996 1.6899 1.5453 1.4927 1.4811 1.4598 1.4484 1.4302 1.4155 1.0096 0.9922 0.9375 0.9204 0.8359 0.8197 0.0669

1.02 1.00 2.09 1.03 1.02 3.16 2.05 1.09 1.27 3.10 3.13 3.14

.0 8.5 8.0 7.5 7.0 6.5 6.0 5.5 5.0 4.5 4.0 3.5 3.0 2.5 2.0 1.5 1.0 0.5 0.0 -0

f1 (ppm)

Compound 13

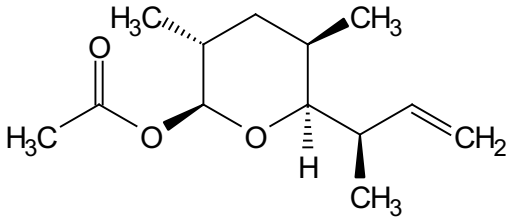

169.9535
141.8777
113.6680
99.6772
83.1048
77.4806
77.1629
76.8450
39.0442
38.5232
29.6018
28.9855
21.3302
16.2024
15.4799
12.0853

f1 (ppm)

Compound 14

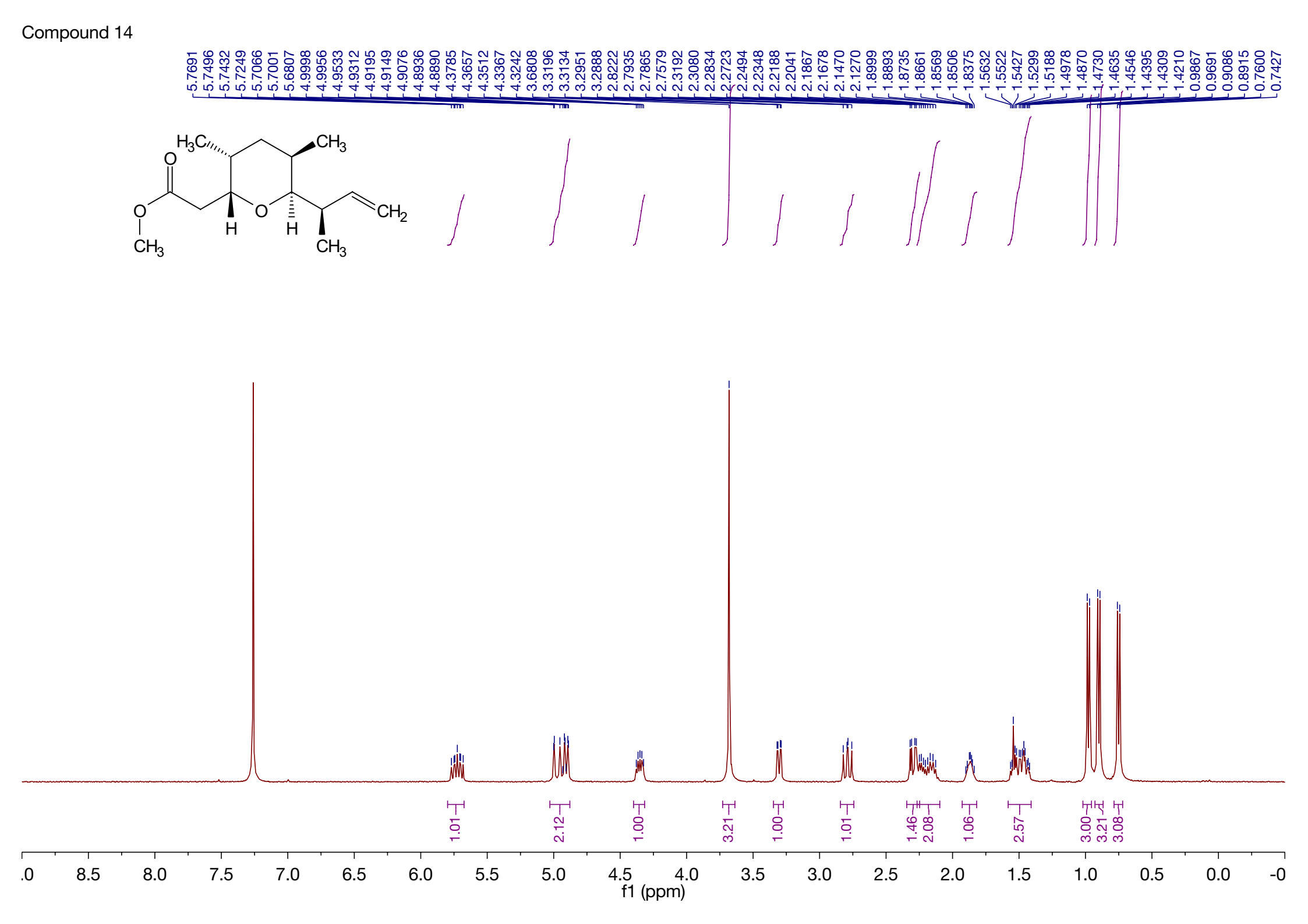
5.7691
5.7496
5.7432
5.7249
5.7066
5.7001
5.6807
4.9998
4.9956
4.9533
4.9312
4.9195
4.9149
4.9076
4.8936
4.8890
4.3785
4.3657
4.3512
4.3367
4.3242
3.6808
3.3196
3.3134
3.2951
3.2888
2.8222
2.7935
2.7865
2.7579
2.3192
2.3080
2.2834
2.2723
2.2494
2.2348
2.2188
2.2041
2.1867
2.1678
2.1470
2.1270
1.8999
1.8893
1.8735
1.8661
1.8569
1.8506
1.8375
1.5632
1.5522
1.5427
1.5299
1.5188
1.4978
1.4870
1.4730
1.4635
1.4546
1.4395
1.4309
1.4210
0.9867
0.9691
0.9086
0.8915
0.7600
0.7427
H3C
CH3
O
O
CH3
O
H
H
CH2
CH3
1.01
2.12
1.00
3.21
1.00
1.01
1.46
2.08
1.06
2.57
3.00
3.21
3.08
.0
8.5
8.0
7.5
7.0
6.5
6.0
5.5
5.0
4.5
4.0
3.5
3.0
2.5
2.0
1.5
1.0
0.5
0.0
-0
f1 (ppm)

Compound 14

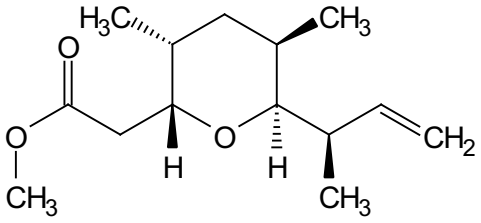
H3C
CH3
O
O
O
H
H
CH3
CH3
CH2

172.4625
143.3232
113.1055
77.4776
77.1604
76.8422
75.1439
74.9580
51.7955
39.9454
34.9390
31.9034
29.0077
26.8324
17.5850
16.1116
11.8257
210
200
190
180
170
160
150
140
130
120
110
100
90
80
70
60
50
40
30
20
10
0
-10
f1 (ppm)

Compound 7

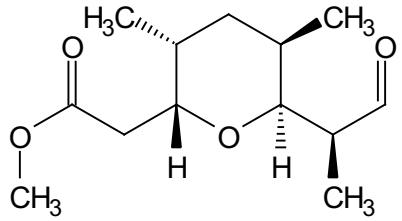

9.5392
9.5304
7.2593
4.3405
4.3280
4.3135
4.2987
4.2862
3.8248
3.8185
3.7991
3.7927
3.6890
3.6810
3.6699
3.6601
2.8378
2.8090
2.8029
2.7738
2.3898
2.3729
2.3644
2.3556
2.3471
2.3388
2.3324
2.3220
2.3119
2.3041
2.2982
2.2873
2.2727
2.2583
2.2427
2.2272
1.8822
1.8741
1.8646
1.8561
1.8468
1.8388
1.6093
1.5982
1.5791
1.5752
1.5646
1.5434
1.5326
1.5160
1.5067
1.4979
1.4822
1.4734
1.4637
0.9977
0.9802
0.9567
0.9393
0.7801
0.7627

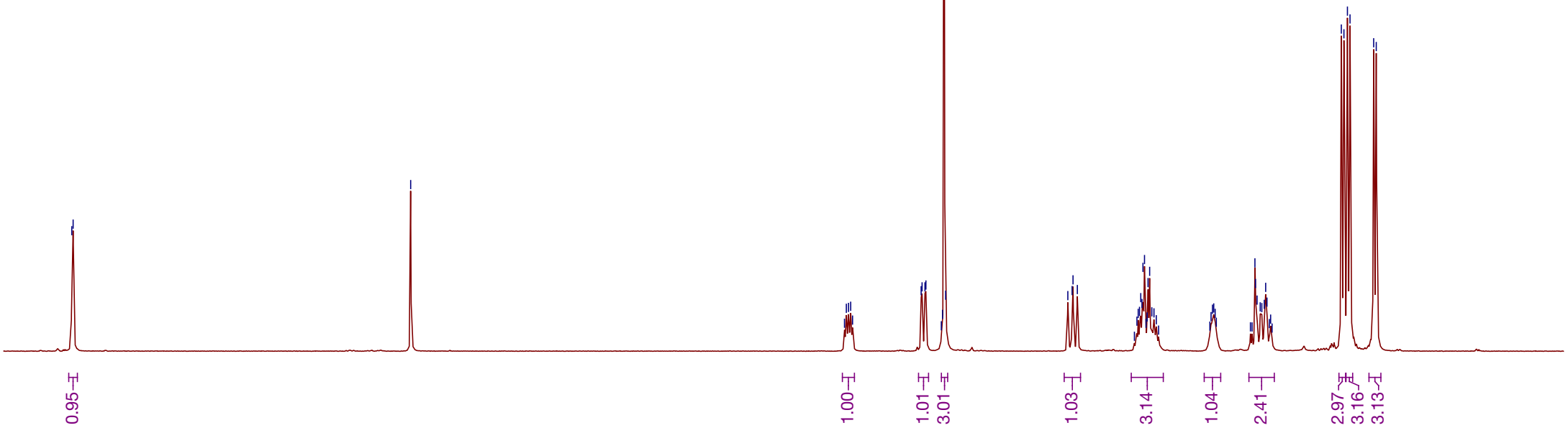

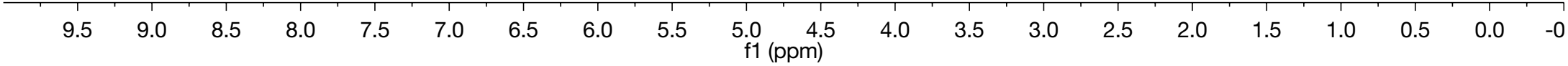

Compound 7

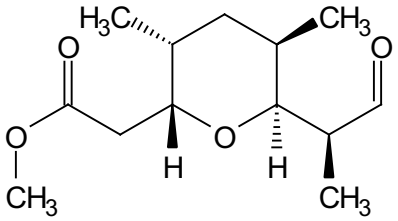

205.3160
172.4413
77.4778
77.1599
76.8420
75.3122
71.9929
51.9986
48.3274
34.3802
31.7709
28.5813
26.8057
17.5395
11.8764
9.7613

210 200 190 180 170 160 150 140 130 120 110 100 90 80 70 60 50 40 30 20 10 0 -1

f1 (ppm)

Compound 17

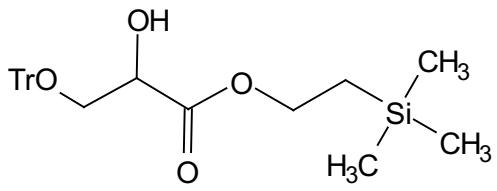
OH
TrO
O
O
Si
CH3
CH3
H3C

7.462
7.458
7.441
7.331
7.314
7.309
7.294
7.273
7.270
7.266
7.258
7.252
7.245
7.234
4.321
4.315
4.298
4.294
4.277
4.272
4.266
4.266
4.258
4.255
4.247
4.240
3.525
3.517
3.501
3.494
3.396
3.388
3.373
3.365
3.277
3.258
1.005
0.999
0.989
0.982
0.978
0.972
0.962
0.956
0.046
6.22
6.16
3.07
3.07
1.03
1.05
1.00
2.00
8.06
9.0
8.5
8.0
7.5
7.0
6.5
6.0
5.5
5.0
4.5
4.0
3.5
3.0
2.5
2.0
1.5
1.0
0.5
0.0
-0
f1 (ppm)

Compound 17

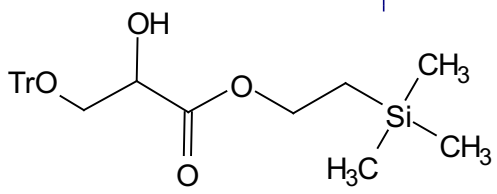
OH
TrO
O
O
Si
CH3
CH3
H3C

173.339
143.689
128.737
127.928
127.195
86.419
77.479
77.161
76.843
70.868
65.420
64.228
17.583
-1.418
230 220 210 200 190 180 170 160 150 140 130 120 110 100 90 80 70 60 50 40 30 20 10 0 -10
f1 (ppm)

Compound 18

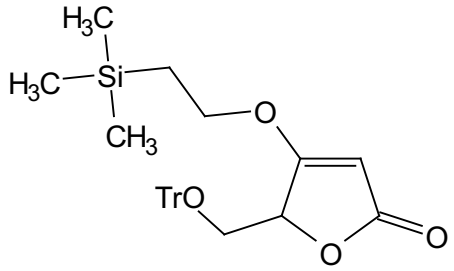
H3C
H3C
Si
CH3
O
TrO
O
O

7.448
7.444
7.427
7.334
7.330
7.325
7.313
7.294
7.276
7.274
7.270
7.267
7.259
7.253
7.251
7.246
7.238
7.234
7.231
5.145
4.837
4.833
4.830
4.826
4.822
4.820
4.163
4.145
4.138
4.118
4.096
4.076
4.069
4.051
3.609
3.602
3.583
3.576
3.294
3.283
3.268
3.257
1.103
1.098
1.083
1.079
1.076
1.061
1.056
0.032
5.97
5.93
3.32
0.99
1.00
2.03
1.00
1.00
2.03
8.99
9.0
8.5
8.0
7.5
7.0
6.5
6.0
5.5
5.0
4.5
4.0
3.5
3.0
2.5
2.0
1.5
1.0
0.5
0.0
-0.5
f1 (ppm)

Compound 18

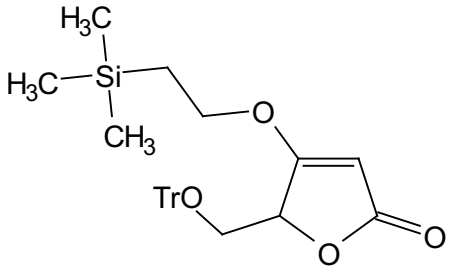
H3C
H3C
Si
CH3
O
TrO
O
O

179.036
173.173
143.515
128.722
127.988
127.248
89.617
86.620
78.677
77.477
77.158
76.840
71.242
61.987
17.343
1.344
210 200 190 180 170 160 150 140 130 120 110 100 90 80 70 60 50 40 30 20 10 0 -10
f1 (ppm)

Compound SI-3

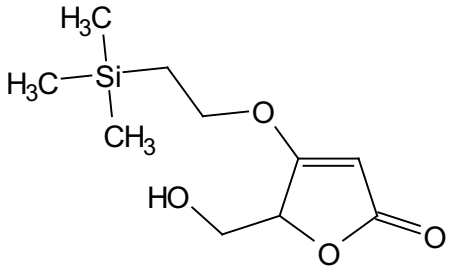

Compound SI-3

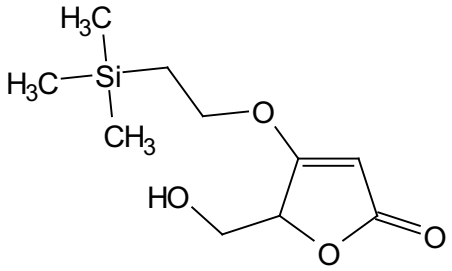

Compound 19

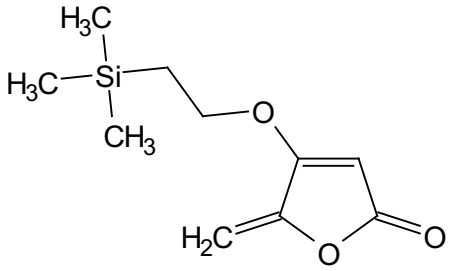
H3C
H3C
Si
CH3
O
H2C
O
O

7.270
5.190
5.187
5.042
5.036
5.032
5.025
5.023
5.018
5.017
4.195
4.174
4.153
1.201
1.180
1.160
0.086
1.00
2.10
2.11
2.09
9.34
9.0
8.5
8.0
7.5
7.0
6.5
6.0
5.5
5.0
4.5
4.0
3.5
3.0
2.5
2.0
1.5
1.0
0.5
0.0
-0.5
f1 (ppm)

Compound 19

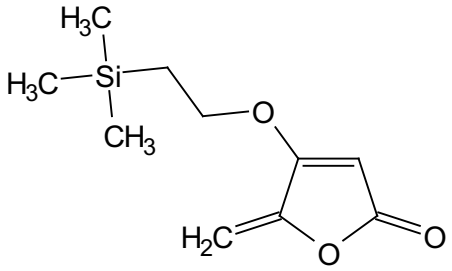
H3C
H3C
Si
CH3
O
H2C
O
O

168.802
168.745
150.217
92.295
89.844
77.479
77.161
76.843
71.105
17.301
1.319
210 200 190 180 170 160 150 140 130 120 110 100 90 80 70 60 50 40 30 20 10 0 -10
f1 (ppm)

Compound 8a

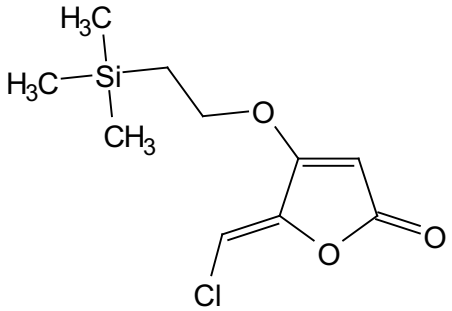
H3C
H3C
Si
CH3
O
O
O
Cl

7.270
6.063
5.205
4.205
4.184
4.163
1.191
1.171
1.150
0.087
1.00
1.03
2.14
2.17
9.31
9.0
8.5
8.0
7.5
7.0
6.5
6.0
5.5
5.0
4.5
4.0
3.5
3.0
2.5
2.0
1.5
1.0
0.5
0.0
-0.5
f1 (ppm)

Compound 8a

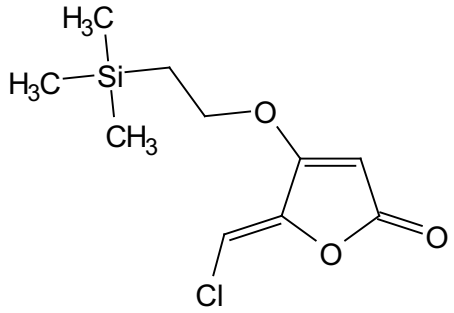

168.045
167.265
145.391
99.951
89.325
77.479
77.160
76.842
71.560
17.368
-1.319

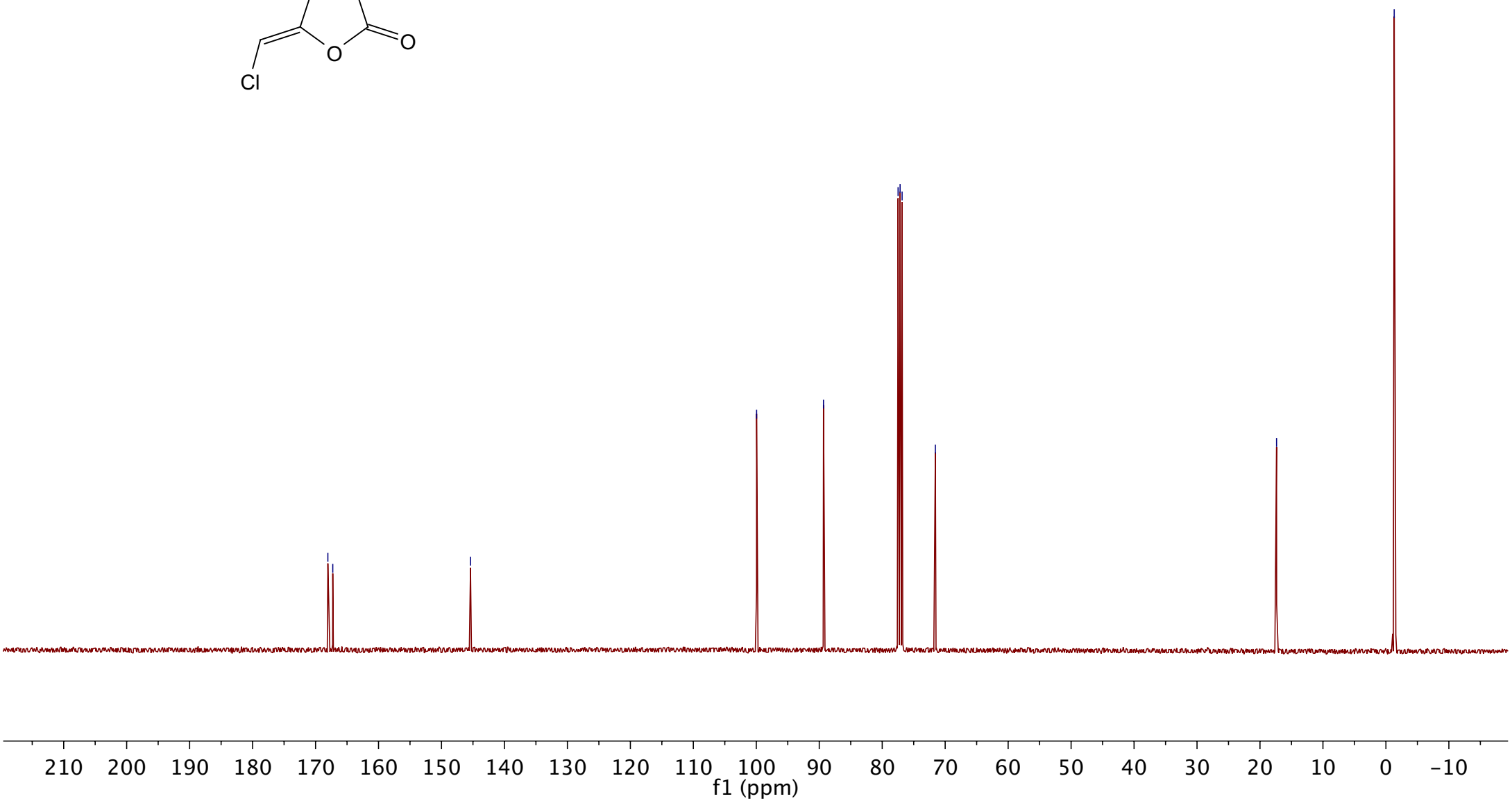

Compound 8b

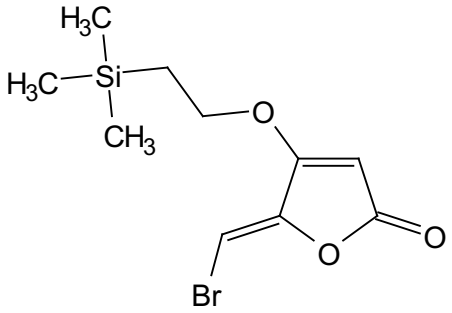
H3C
H3C
Si
CH3
O
O
O
Br

7.270
6.165
5.234
4.199
4.179
4.157
1.192
1.171
1.151
0.088
1.00
1.03
2.11
2.10
9.38
9.0
8.5
8.0
7.5
7.0
6.5
6.0
5.5
5.0
4.5
4.0
3.5
3.0
2.5
2.0
1.5
1.0
0.5
0.0
-0.5
f1 (ppm)

Compound 8b

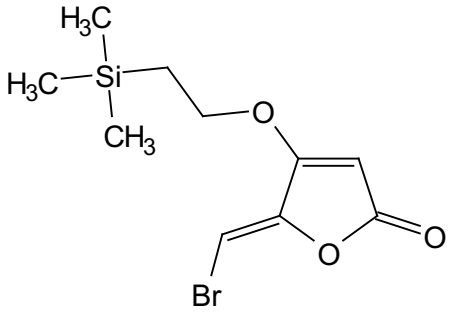
H3C
H3C
Si
CH3
O
O
O
Br

167.690
167.301
147.400
89.558
87.767
77.477
77.161
76.841
71.576
17.362
-1.315
210 200 190 180 170 160 150 140 130 120 110 100 90 80 70 60 50 40 30 20 10 0 -10
f1 (ppm)

Compound 20a

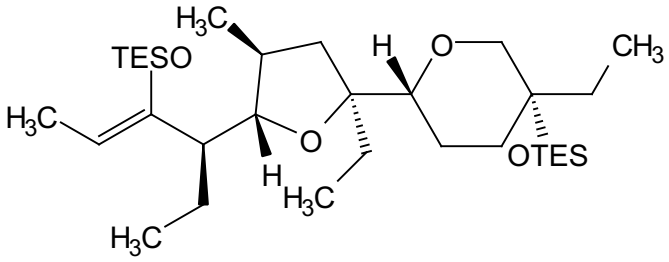

4.5577 4.5411 4.5243 4.5077 3.8122 3.7951 3.7778 3.7607 3.4180 3.3947 3.3660 3.3462 3.3268 1.9305 1.9147 1.9074 1.8840 1.8570 1.8357 1.8135 1.8045 1.7934 1.7854 1.7756 1.7578 1.7388 1.7301 1.6974 1.6700 1.6429 1.6329 1.6047 1.5772 1.5509 1.5311 1.5166 1.4997 1.4713 1.4526 1.4329 1.4163 1.3961 1.3799 1.3616 1.3410 1.3211 1.3021 1.2842 1.1591 1.1422 1.0087 0.9888 0.9705 0.9532 0.9323 0.9136 0.8960 0.8784 0.8632 0.8575 0.8446 0.8378 0.7125 0.6926 0.6728 0.6533 0.6337 0.6137 0.5934

1.04 1.00 1.04 1.00 2.23 2.35 2.16 12.85 3.26 33.35 12.94

.0 8.5 8.0 7.5 7.0 6.5 6.0 5.5 5.0 4.5 4.0 3.5 3.0 2.5 2.0 1.5 1.0 0.5 0.0 -0

f1 (ppm)

Compound 20a

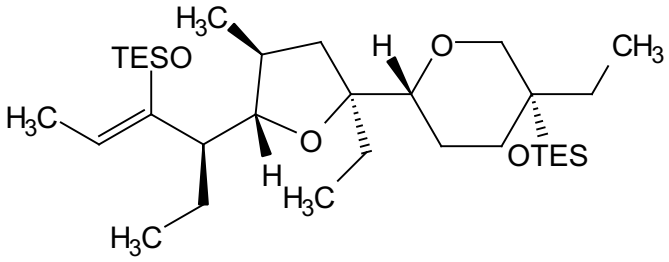

151.1084
101.9469
87.7450
84.4323
77.4781
77.1602
76.8429
76.6731
75.1538
74.9340
53.5193
41.9384
38.6458
30.9956
30.8817
28.3631
22.8474
21.7859
17.6149
15.5228
12.5248
11.0218
8.3052
7.4661
7.1357
7.0804
7.0006
6.1180

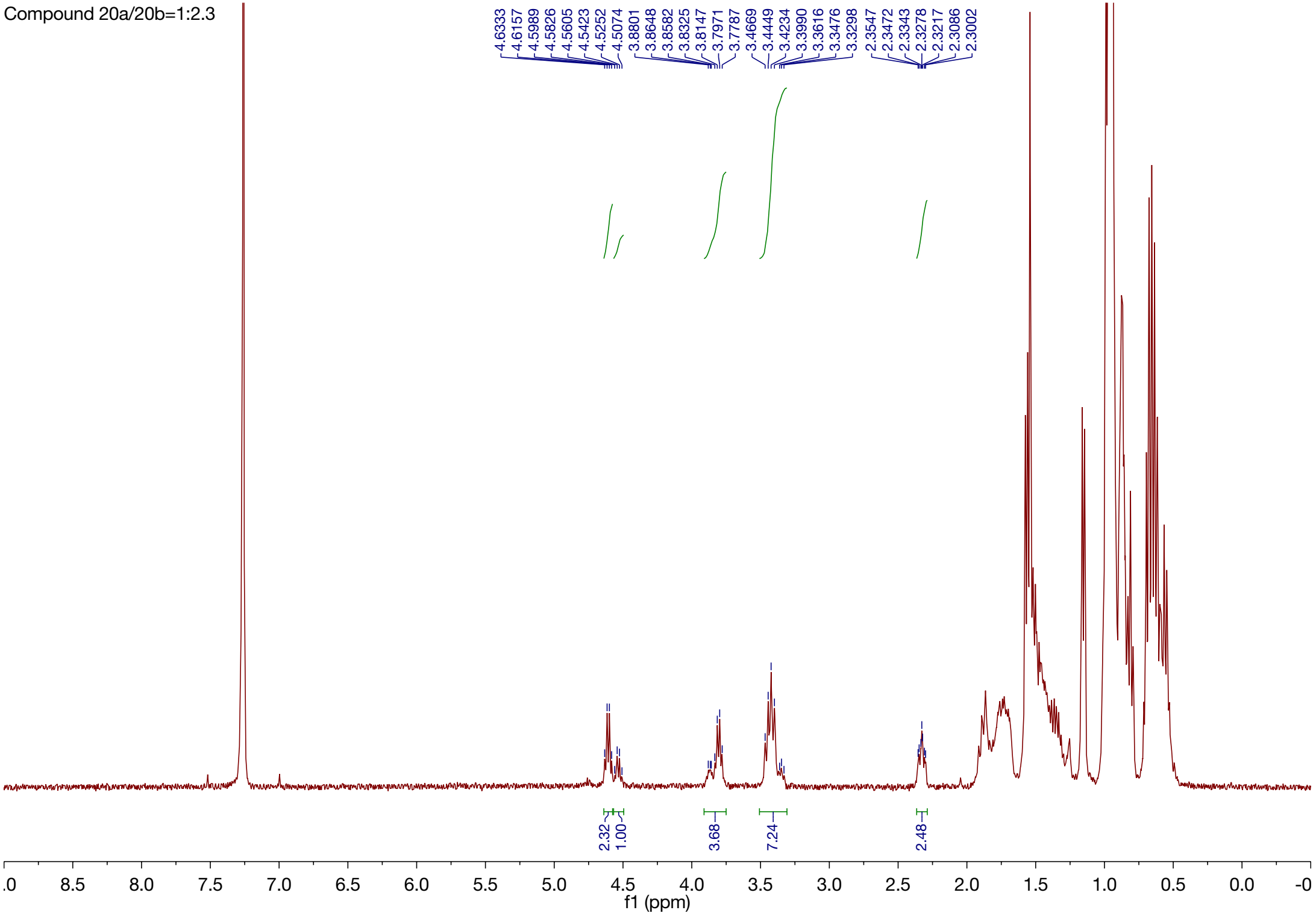
Compound 20a/20b=1:2.3
4.6333
4.6157
4.5989
4.5826
4.5605
4.5423
4.5252
4.5074
3.8801
3.8648
3.8582
3.8325
3.8147
3.7971
3.7787
3.4669
3.4449
3.4234
3.3990
3.3616
3.3476
3.3298
2.3547
2.3472
2.3343
2.3278
2.3217
2.3086
2.3002
2.32
1.00
3.68
7.24
2.48
.0
8.5
8.0
7.5
7.0
6.5
6.0
5.5
5.0
4.5
4.0
3.5
3.0
2.5
2.0
1.5
1.0
0.5
0.0
-0
f1 (ppm)

Compound 22

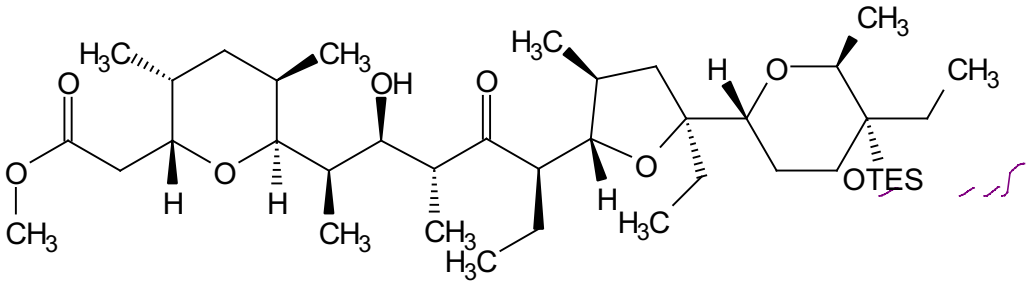
H3C
CH3
OH
O
O
O
O
O
H
H
H
H3C
CH3
CH3
CH3
H3C
H3C
H
O
CH3
CH3
OTES

3.8507
3.8424
3.8262
3.7667
3.7480
3.7305
3.5308
3.5252
3.5058
3.5002
3.4660
3.4382
3.1962
3.1815
2.8066
2.3215
2.3114
2.2885
2.2784
1.8574
1.8272
1.8000
1.7650
1.7446
1.6314
1.5997
1.5386
1.5264
1.5115
1.5053
1.4944
1.4868
1.4830
1.4717
1.4631
1.4492
1.4308
1.4204
1.4123
1.3940
1.3841
1.3008
1.2962
1.2822
1.2789
1.2621
1.1247
1.1076
0.9887
0.9782
0.9744
0.9681
0.9586
0.9483
0.9439
0.9386
0.9132
0.8955
0.8772
0.8673
0.8543
0.8492
0.8357
0.8308
0.8170
0.7677
0.7505
0.6558
0.6362
0.6220
0.6184
0.6155
0.6018
0.5942
0.5820
0.5728
0.5610
0.5388
1.00
1.00
1.12
4.02
0.99
1.01
1.00
1.00
0.99
0.97
1.03
0.98
5.28
10.35
3.15
2.85
34.21
6.06
9.96
.0
8.5
8.0
7.5
7.0
6.5
6.0
5.5
5.0
4.5
4.0
3.5
3.0
2.5
2.0
1.5
1.0
0.5
0.0
-0
f1 (ppm)

Compound 22

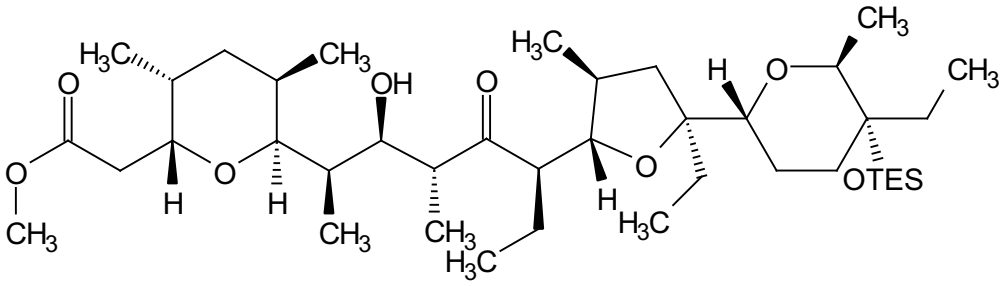

215.7639
174.6516
84.5870
83.8220
77.4775
77.1597
76.8431
76.6599
75.3654
74.9973
73.9576
71.9766
70.4209
57.7517
52.7321
47.1887
37.0274
36.3358
34.9926
32.3083
31.8014
28.9208
26.9763
17.7747
17.6466
16.1123
15.5470
13.6468
12.4959
11.7018
7.9687
7.4649
7.2460
7.0551
6.9543
6.7495

Compound 23

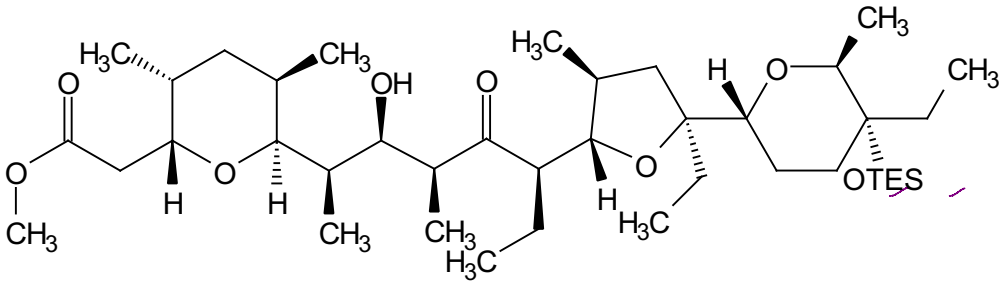

3.7006 3.6939 3.6822 3.5035 3.4794 3.4370 3.4309 3.4233 3.4176 2.2304 1.7946 1.7865 1.7741 1.7659 1.6803 1.6154 1.5889 1.5818 1.4824 1.4674 1.4471 1.4362 1.4290 1.4227 1.4185 1.4115 1.3136 1.3070 1.2960 1.2895 1.2825 1.2714 1.2648 1.2030 1.1966 1.1855 1.1790 1.1279 1.1218 1.1107 1.1045 0.9556 0.9449 0.9385 0.9247 0.9180 0.9049 0.8986 0.8844 0.8784 0.8672 0.8612 0.8483 0.8422 0.8297 0.8235 0.8172 0.8048 0.7986 0.7860 0.7806 0.7732 0.7668 0.7560 0.7498 0.7337 0.7275 0.7164 0.7100 0.6219 0.6156 0.6022 0.5961 0.5822 0.5768 0.5654 0.5596 0.5535

1.03 0.95 5.32 1.00 2.16 1.05 1.01 1.01 2.31 4.43 0.93 2.38 7.88 3.52 3.52 3.27 34.68 7.18

.0 8.5 8.0 7.5 7.0 6.5 6.0 5.5 5.0 4.5 4.0 3.5 3.0 2.5 2.0 1.5 1.0 0.5 0.0 -0

f1 (ppm)

Compound 23

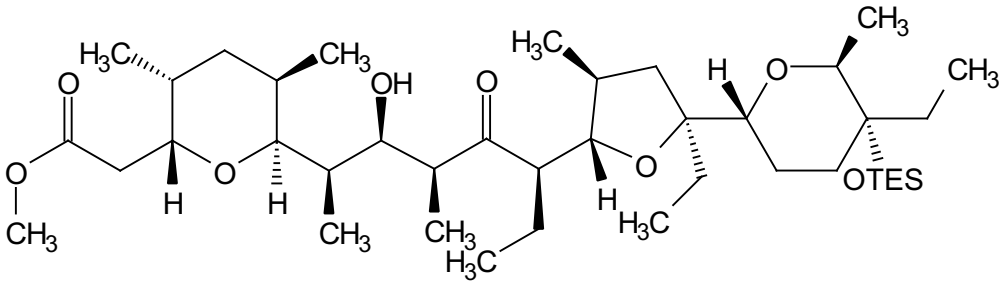

215.0843
174.4631
84.8977
83.9030
77.4793
77.1600
76.8420
76.6815
75.2290
74.9599
73.8825
71.2776
69.4293
55.7100
52.2223
48.1714
40.9319
37.8829
37.6167
35.0249
31.6105
31.5877
30.4429
28.9318
26.9562
18.8938
17.6677
16.7527
15.5302
15.4030
12.2511
11.7770
8.6186
8.0872
7.3884
6.9821

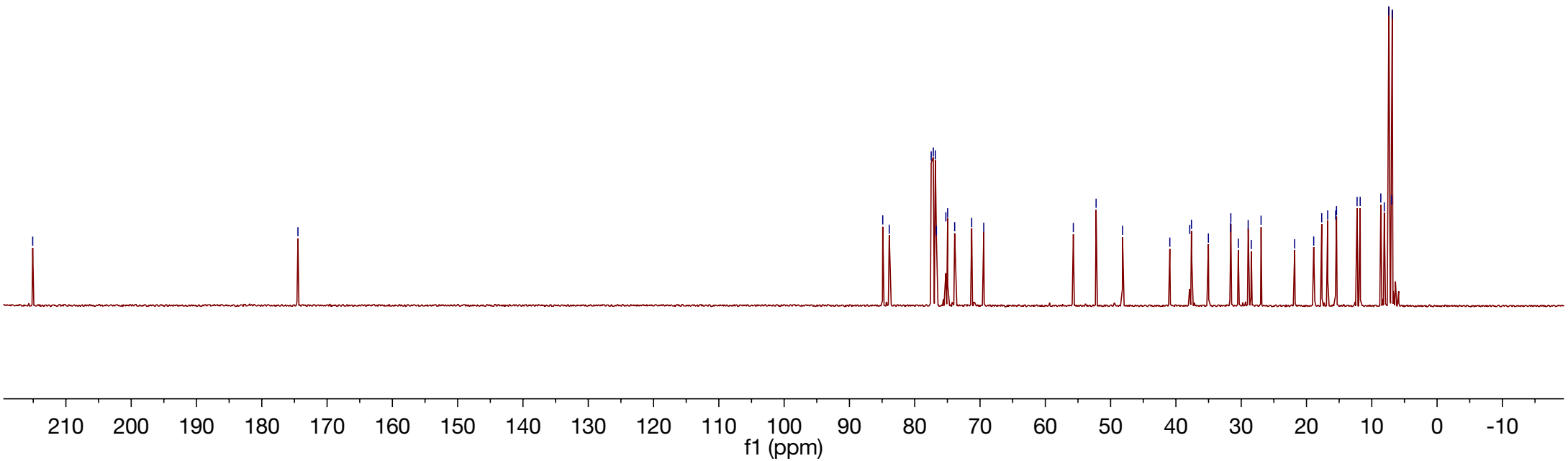

Compound 24

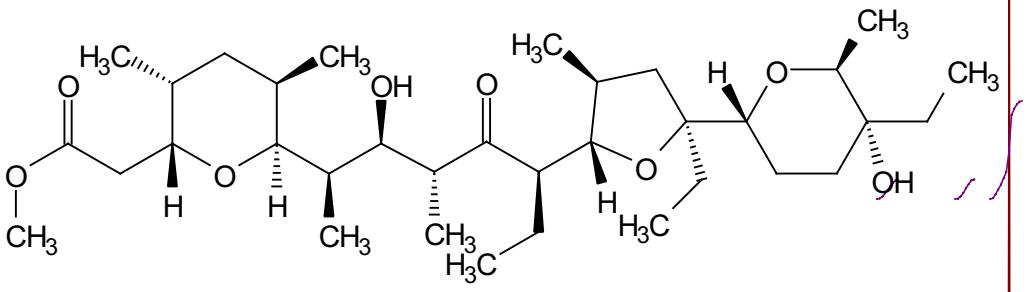

3.8259 3.8172 3.8012 3.7924 3.7749 3.7624 3.7408 3.5372 3.5314 3.5180 3.5122 3.5064 3.4910 3.2690 3.2540 2.8109 2.7793 2.6996 2.6904 2.6827 2.6750 2.6667 2.3276 2.3173 2.2944 2.2844 1.8305 1.8107 1.7995 1.7798 1.6612 1.6340 1.6303 1.6031 1.5843 1.5773 1.5652 1.5563 1.5500 1.5435 1.5384 1.5231 1.5061 1.5004 1.4966 1.4861 1.4808 1.4720 1.4625 1.4534 1.4420 1.4349 1.4239 1.4168 1.4072 1.3893 1.3527 1.3342 1.3171 1.2993 1.2477 1.1801 1.1629 0.9963 0.9804 0.9590 0.9416 0.9158 0.9115 0.8963 0.8786 0.8554 0.8371 0.8186 0.7713 0.7673 0.7539 0.7499
1.01 1.04 5.21 2.04 1.00 1.04 1.05 2.03 1.12 0.95 4.21 14.63 3.08 3.14 3.08 9.18 3.39 6.01
8.5 8.0 7.5 7.0 6.5 6.0 5.5 5.0 4.5 4.0 3.5 3.0 2.5 2.0 1.5 1.0 0.5 0.0
f1 (ppm)

Compound 24

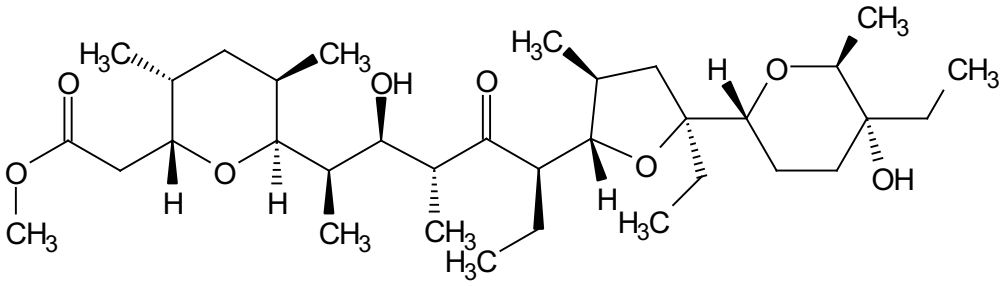

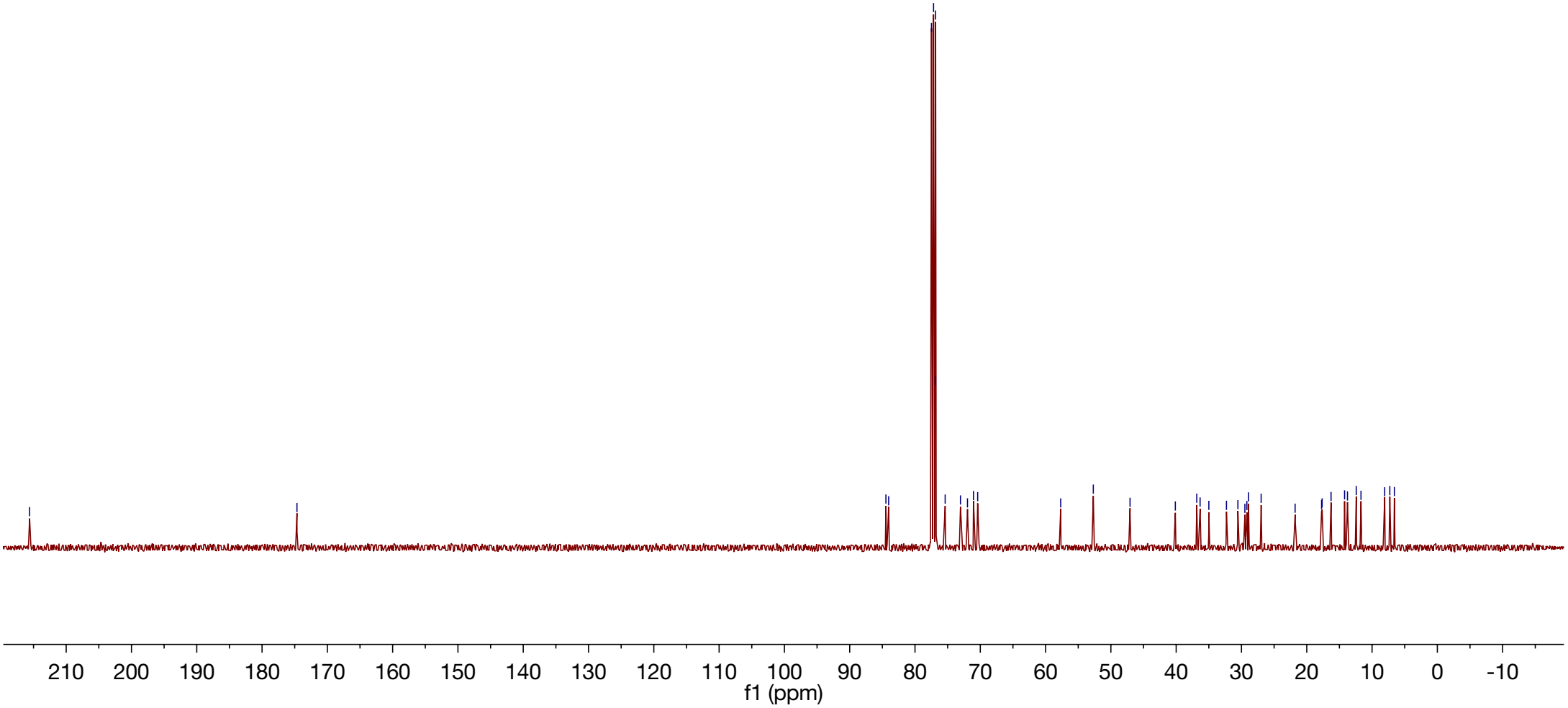
215.5996
174.6547
84.4536
84.0352
77.4778
77.1594
76.8749
76.8421
75.3796
73.0345
71.9614
71.0407
70.4010
57.6856
52.6910
47.0653
40.1268
36.8444
36.3373
34.9953
32.2980
30.5469
29.4759
29.1746
28.9182
26.9863
21.7849
17.7300
17.6447
16.2804
14.2099
13.7662
12.4217
11.6943
8.0633
7.2788
6.5831
210
200
190
180
170
160
150
140
130
120
110
100
90
80
70
60
50
40
30
20
10
0
-10
f1 (ppm)

Compound 25

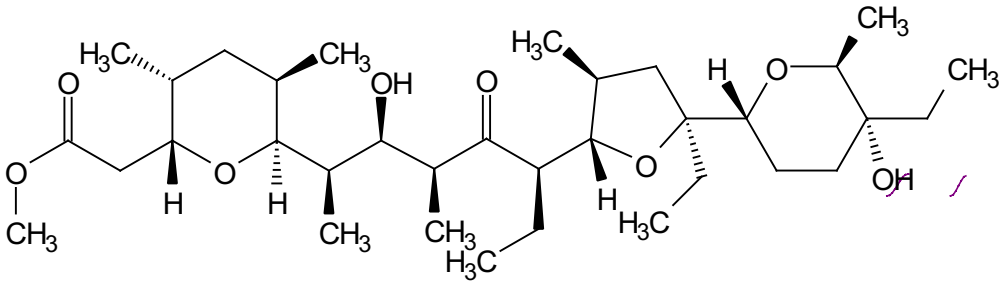

3.9916 3.9814 3.7480 3.7309 3.7106 3.6876 3.6776 3.6643 3.6541 3.5164 3.5107 3.4919 3.4862 3.4708 3.4563 3.4460 2.9160 2.9112 2.8188 2.7875 2.6020 2.5930 2.5847 2.5805 2.5704 2.2863 2.2770 2.2536 2.2442 1.9144 1.8970 1.8912 1.8813 1.8738 1.8618 1.8416 1.7978 1.7892 1.6024 1.5954 1.5788 1.5684 1.5585 1.5447 1.5398 1.5226 1.5116 1.4896 1.4835 1.4697 1.4516 1.4420 1.4324 1.4249 1.4072 1.3980 1.3422 1.3237 1.3173 1.2997 1.2815 1.2109 1.1937 1.1763 0.9616 0.9472 0.9060 0.8894 0.8736 0.8686 0.8537 0.8349 0.8160 0.7974 0.7835 0.7664 0.7445 0.7272
1.00 0.91 5.07 3.02 1.00 1.00 1.80 1.09 1.00 2.90 1.15 11.57 2.29 6.45 2.95 12.58 2.99 3.06
.0 8.5 8.0 7.5 7.0 6.5 6.0 5.5 5.0 4.5 4.0 3.5 3.0 2.5 2.0 1.5 1.0 0.5 0.0 -0
f1 (ppm)

Compound 25

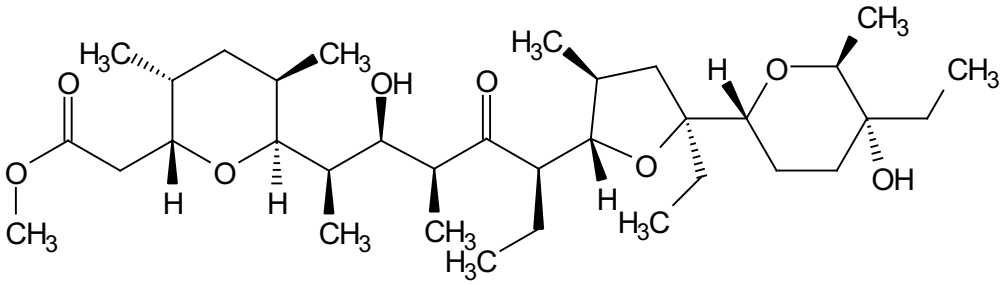

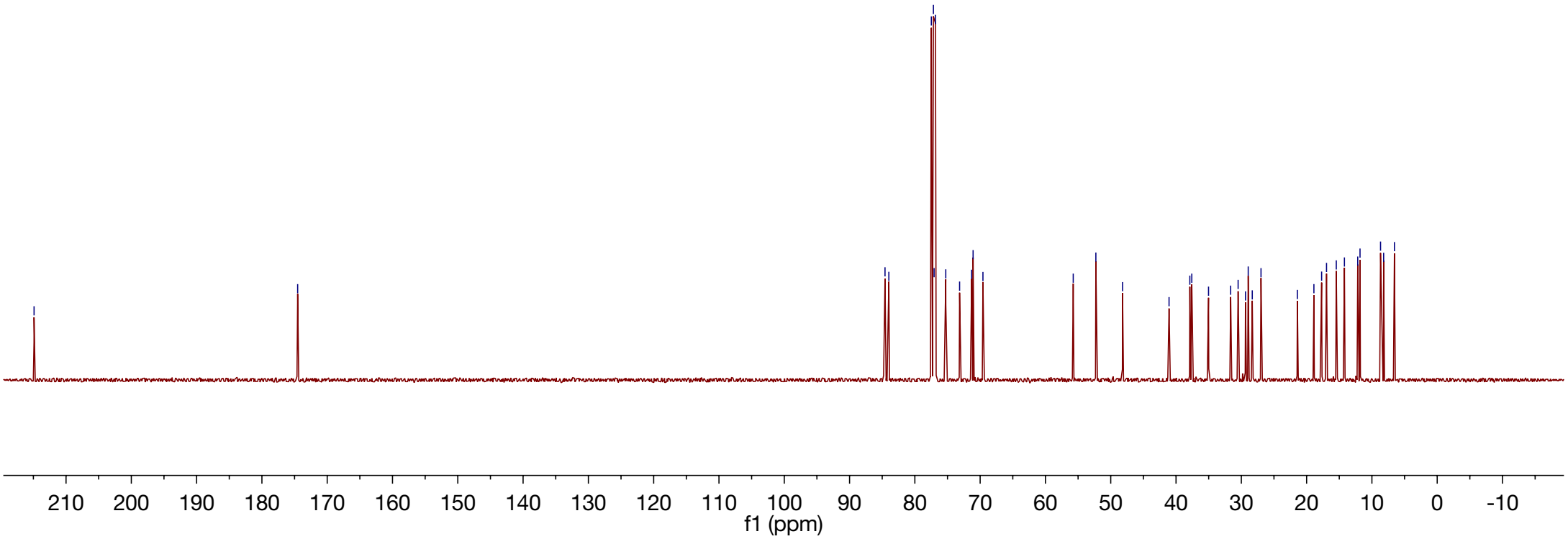
214.8954
174.5254
84.5702
83.9816
77.4766
77.1593
77.0500
76.8415
75.2650
73.1473
71.3041
71.0788
69.5720
55.7430
52.2778
48.1885
41.0696
37.8856
37.5844
35.0216
31.6326
30.4910
29.3591
28.9435
28.3239
26.9857
21.4177
18.8843
17.7013
16.9504
15.4561
14.2108
12.1700
11.8216
8.6778
8.2027
6.5515
210
200
190
180
170
160
150
140
130
120
110
100
90
80
70
60
50
40
30
20
10
0
-10
f1 (ppm)

Compound 26

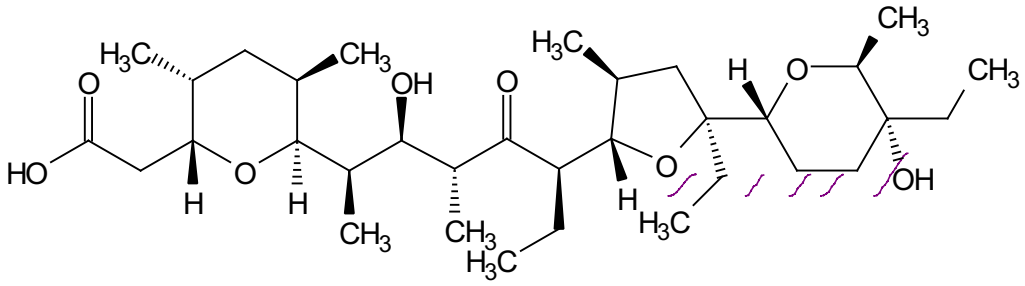

4.0448 4.0406 4.0188 4.0145 3.8900 3.8718 3.8650 3.7832 3.7658 3.6208 3.6151 3.5958 3.5900 3.3183 3.3142 3.3099 3.3056 3.3014 2.7629 2.7579 2.7350 2.7287 2.3521 1.9902 1.8993 1.8904 1.8837 1.8720 1.8676 1.8551 1.8489 1.8408 1.8076 1.7877 1.6456 1.6278 1.6215 1.6103 1.6016 1.5895 1.5753 1.5676 1.5609 1.5481 1.5429 1.5255 1.5058 1.4507 1.4324 1.4262 1.4164 1.4107 1.4025 1.3977 1.3918 1.3833 1.3398 1.3346 1.3209 1.3161 1.1970 1.1797 1.0409 1.0252 0.9841 0.9666 0.9235 0.9070 0.9010 0.8907 0.8833 0.8688 0.8637 0.8501 0.8047 0.7917 0.7874 0.7744

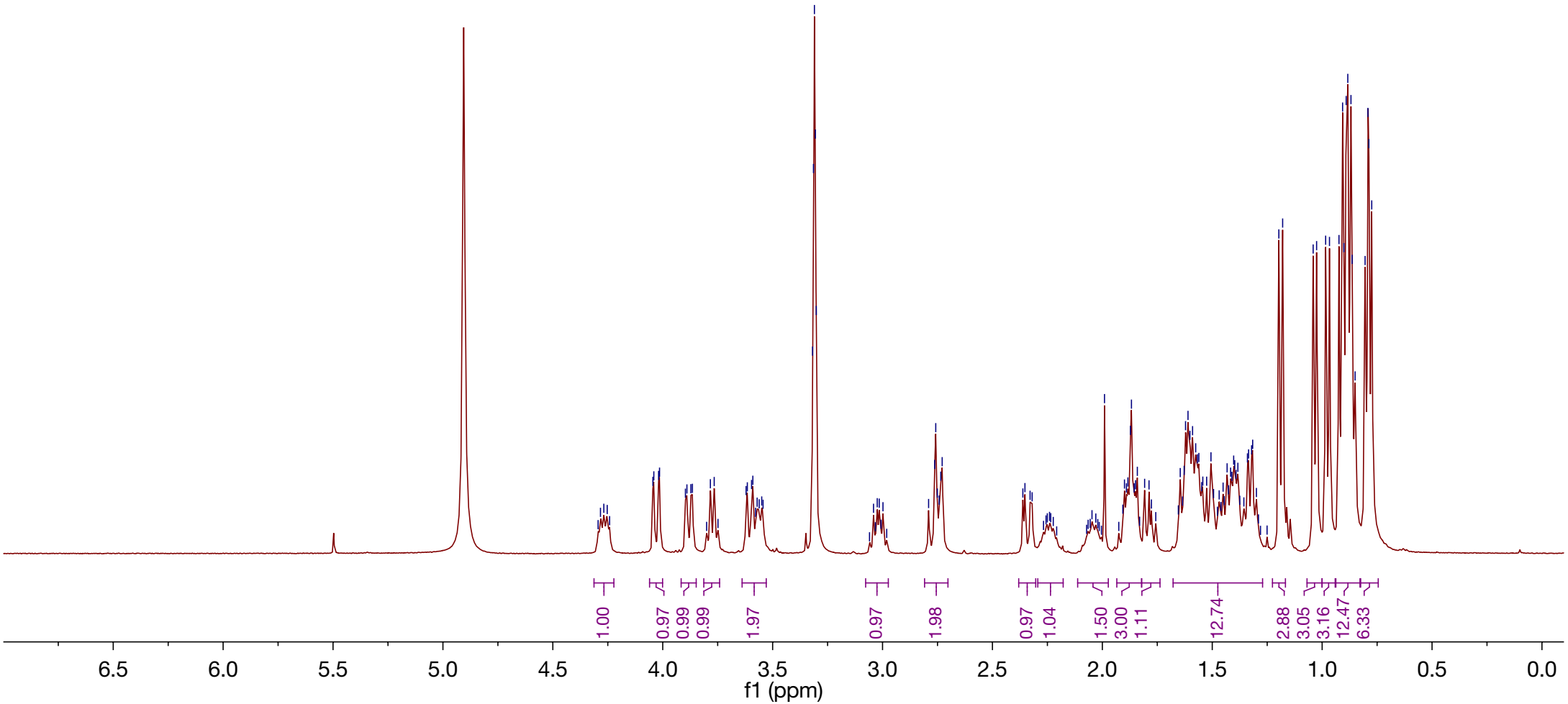

Compound 26

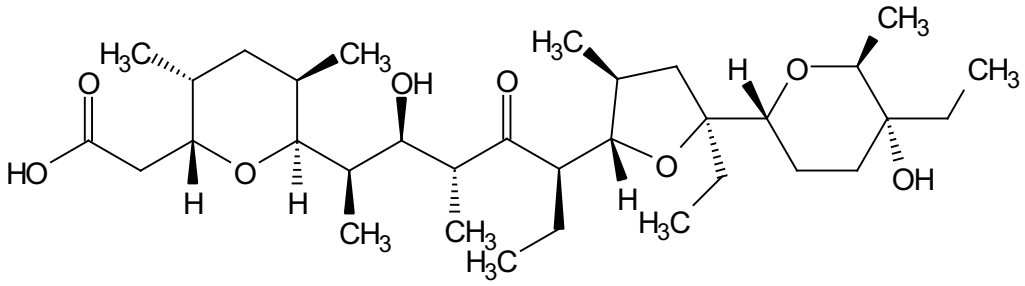

218.4693
177.6942
86.4622
85.5507
77.2372
73.9560
73.6315
72.1508
71.5366
58.8961
49.6393
49.4258
49.2129
48.9995
48.7875
48.5746
48.3608
47.9854
37.6368
37.3559
30.6898
30.6067
30.2274
28.5273
18.1886
17.8476
16.0362
14.9156
14.1421
13.1777
12.0248
8.3652
7.5821
20 210 200 190 180 170 160 150 140 130 120 110 100 90 80 70 60 50 40 30 20 10 0 -10
f1 (ppm)

Compound 27

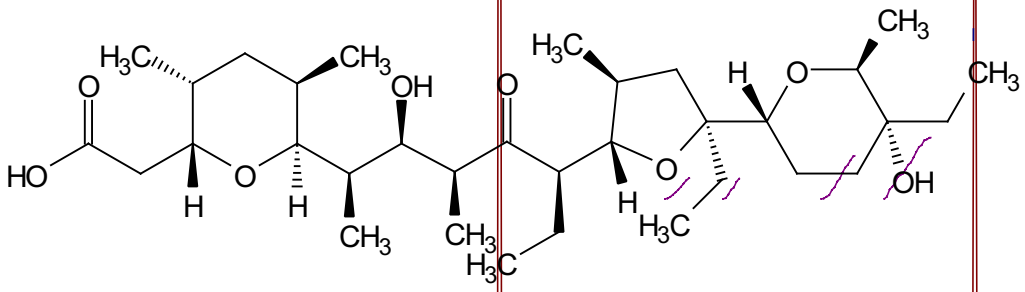

4.1156 4.0921 3.7809 3.7637 3.7472 3.7383 3.7234 3.7143 3.5954 3.5897 3.5708 3.5651 3.5363 3.5158 3.5072 3.4990 3.4815 3.3184 3.3143 3.3100 3.3057 3.3015 2.9540 2.9474 2.6965 2.6736 1.9888 1.9032 1.8850 1.8710 1.8515 1.8328 1.7387 1.7117 1.7066 1.6793 1.6503 1.6239 1.6135 1.6081 1.5989 1.5884 1.5740 1.5661 1.5547 1.5094 1.4891 1.4719 1.4531 1.4375 1.4072 1.4013 1.3424 1.3235 1.3045 1.2905 1.2145 1.2020 1.1973 1.1847 1.1799 1.1623 1.0173 1.0015 0.9363 0.9188 0.9136 0.8993 0.8953 0.8807 0.8765 0.8639 0.8469 0.8284 0.8019 0.7940 0.7847 0.7765
1.03 1.00 2.12 3.02 1.04 0.94 1.08 0.94 1.09 1.44 3.10 12.32 2.94 7.48 3.14 13.55 6.69
6.5 6.0 5.5 5.0 4.5 4.0 3.5 3.0 2.5 2.0 1.5 1.0 0.5 0.0
f1 (ppm)

Compound 27

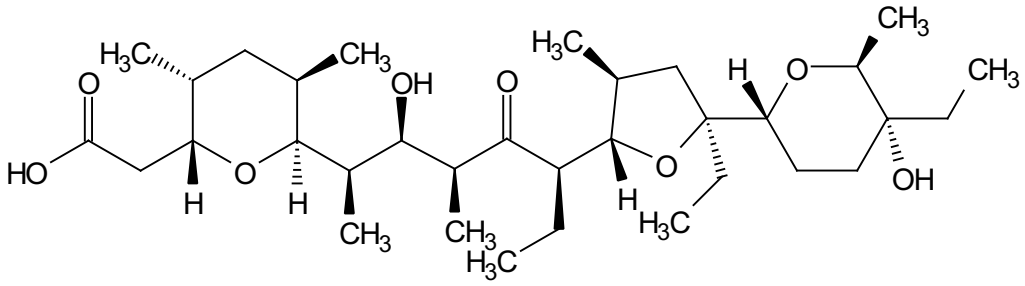

216.5420
178.0131
86.5465
84.9501
77.4492
76.8874
74.1669
72.4694
72.1510
71.0192
66.8637
64.2498
56.8100
49.6399
49.4915
49.4261
49.2132
49.0012
48.7880
48.5750
48.3615
38.9503
38.5637
32.4293
30.1638
28.4685
19.5915
17.8482
17.0896
15.9262
14.9558
12.4242
12.2969
8.9420
8.6026
20
210
200
190
180
170
160
150
140
130
120
110
100
90
80
70
60
50
40
30
20
10
0
-10
f1 (ppm)

Compound 6

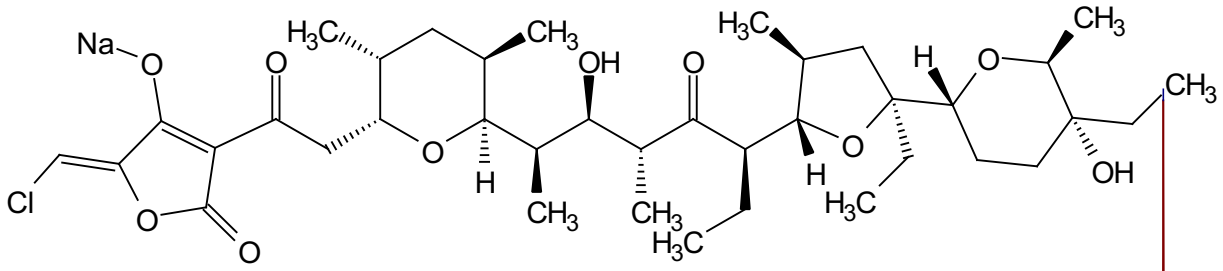
Na
O
O
Cl
O
O
H3C
CH3
OH
O
O
H
CH3
CH3
H3C
H3C
O
H
O
H3C
CH3
CH3
OH

6.043
4.466
4.454
4.151
4.142
4.133
3.908
3.789
3.775
3.769
3.755
3.749
3.663
3.649
3.505
3.486
3.415
3.393
3.369
3.360
3.342
3.331
2.861
2.848
2.841
2.828
2.629
2.611
2.471
2.463
2.445
2.049
2.041
1.923
1.916
1.752
1.729
1.716
1.699
1.584
1.565
1.563
1.538
1.475
1.443
1.422
1.409
1.394
1.350
1.325
1.297
1.256
1.232
1.207
1.194
1.190
1.179
1.173
1.160
1.076
1.063
0.955
0.943
0.868
0.854
0.841
0.826
0.811
0.802
0.796
0.788
0.782
0.774
0.768
0.750
0.737
0.668
0.655
0.49
0.90
0.91
0.94
1.89
0.93
1.01
0.97
0.78
0.90
1.01
0.80
0.96
0.98
3.91
1.97
8.04
2.11
2.98
2.97
2.93
3.14
5.91
5.94
3.00
9.5
9.0
8.5
8.0
7.5
7.0
6.5
6.0
5.5
5.0
4.5
4.0
3.5
3.0
2.5
2.0
1.5
1.0
0.5
0.0
−0.5
f1 (ppm)

Compound 6

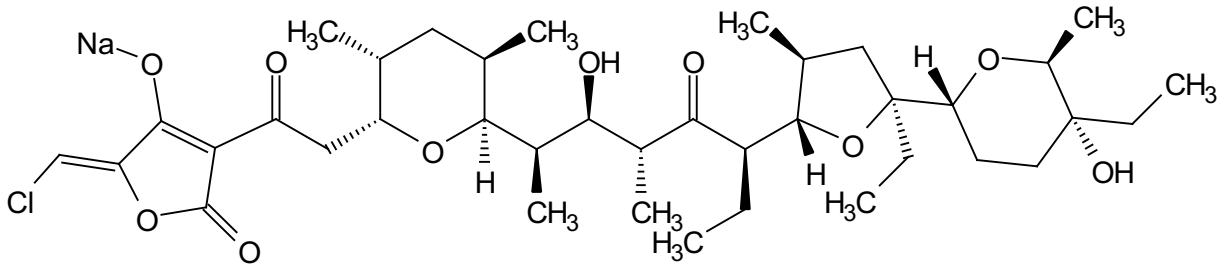

214.498
193.148
178.426
167.880
148.895
94.162
94.135
84.134
83.696
75.434
74.692
72.519
70.793
69.618
69.483
56.318
46.106
40.147
39.939
39.730
39.522
39.313
39.104
38.896
35.881
35.729
31.421
28.879
28.402
27.494
17.364
15.744
14.559
13.284
12.838
11.929
7.821
7.334

230 220 210 200 190 180 170 160 150 140 130 120 110 100 90 80 70 60 50 40 30 20 10 0 −10

f1 (ppm)

Compound 29

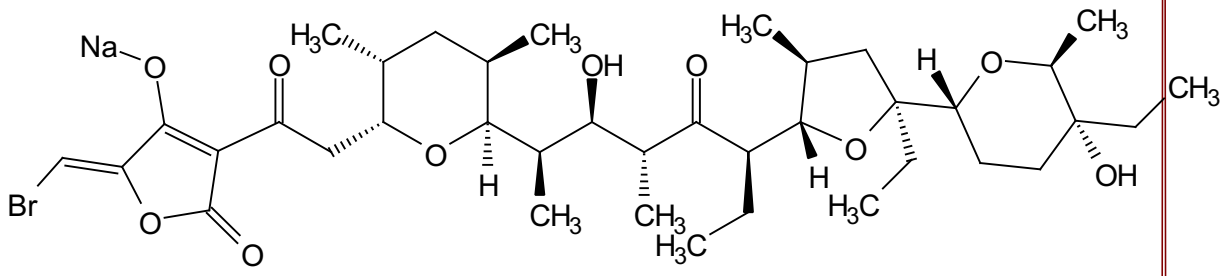

6.057 4.461 4.449 4.148 4.139 3.904 3.779 3.772 3.759 3.752 3.660 3.646 3.504 3.486 3.412 3.390 3.365 3.356 2.636 2.631 2.625 2.618 2.612 2.507 2.503 2.500 2.496 2.492 2.482 2.466 2.457 1.760 1.734 1.714 1.697 1.567 1.557 1.541 1.531 1.472 1.441 1.415 1.402 1.387 1.348 1.342 1.327 1.327 1.324 1.314 1.299 1.295 1.255 1.232 1.206 1.192 1.185 1.177 1.170 1.075 1.062 0.956 0.943 0.867 0.853 0.837 0.823 0.807 0.801 0.797 0.787 0.782 0.771 0.767 0.748 0.735 0.667 0.654

Compound 29

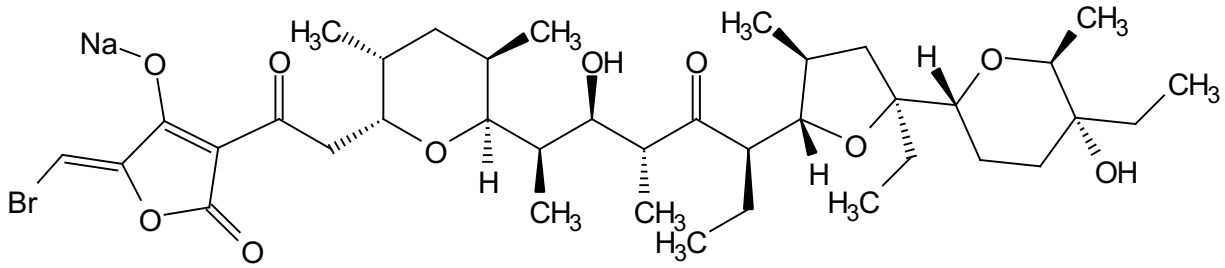

214.666
193.374
178.021
167.996
151.007
94.277
84.187
83.689
82.786
75.435
74.693
72.423
70.729
69.638
69.490
56.184
46.141
40.146
39.937
39.729
39.520
39.312
39.104
38.894
35.823
35.700
31.405
28.390
27.482
17.340
15.717
14.514
13.288
12.894
11.893
7.858
7.319

Compound 30

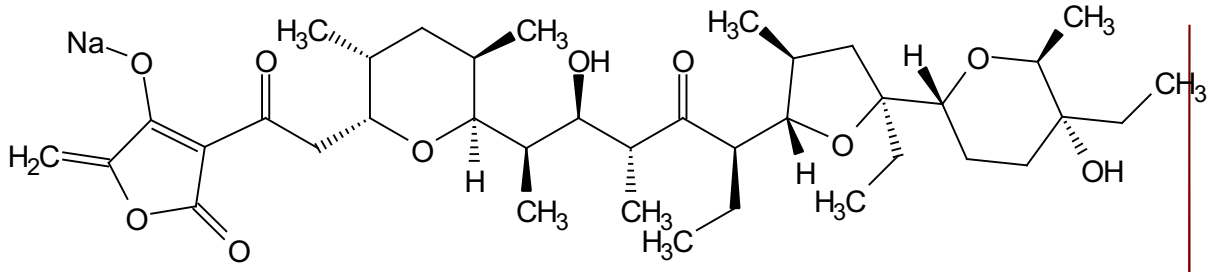

4.737 4.578 4.563 4.485 4.152 4.140 4.129 3.921 3.795 3.785 3.778 3.770 3.752 3.746 3.667 3.650 3.515 3.490 3.431 3.419 3.397 3.388 2.856 2.847 2.623 2.616 2.609 2.602 2.500 2.464 2.441 2.431 2.409 1.772 1.757 1.751 1.737 1.720 1.697 1.593 1.579 1.570 1.560 1.550 1.537 1.525 1.478 1.470 1.439 1.420 1.402 1.386 1.360 1.348 1.343 1.324 1.307 1.289 1.231 1.198 1.194 1.177 1.159 1.080 1.063 0.955 0.940 0.872 0.854 0.834 0.790 0.781 0.766 0.755 0.749 0.738 0.673 0.656

1.01 1.04 0.99 0.91 1.02 1.97 1.02 1.06 1.81 0.98 0.96 1.42 1.07 1.11 3.76 2.27 10.90 3.15 3.00 17.24 3.44

9.0 8.5 8.0 7.5 7.0 6.5 6.0 5.5 5.0 4.5 4.0 3.5 3.0 2.5 2.0 1.5 1.0 0.5 0.0

f1 (ppm)

Compound 30

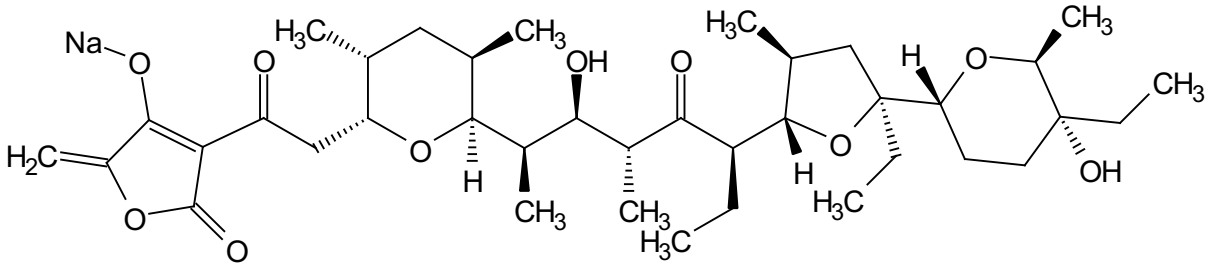

214.704
193.333
180.028
169.281
154.184
94.719
85.482
84.173
83.680
75.471
74.845
72.454
70.713
69.607
69.495
56.198
40.146
39.937
39.728
39.520
39.311
39.104
38.894
35.834
35.696
31.420
28.893
28.413
27.547
17.395
15.728
14.542
13.301
12.961
11.924
7.865
7.338
6.408

Compound 31

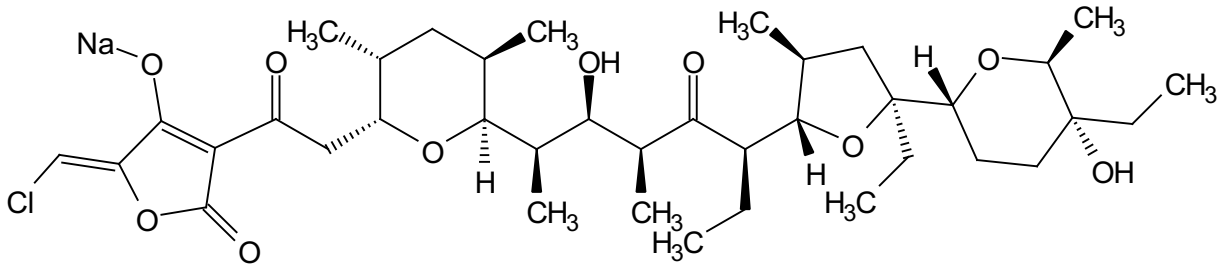

4.629 3.874 3.773 3.758 3.741 3.639 3.625 3.614 3.607 3.596 3.589 3.488 3.468 3.377 3.364 3.332 3.326 2.785 2.772 2.765 2.752 2.538 2.525 2.521 2.500 2.036 2.024 1.843 1.829 1.804 1.779 1.764 1.753 1.739 1.724 1.709 1.697 1.607 1.607 1.585 1.584 1.565 1.549 1.540 1.522 1.434 1.419 1.405 1.376 1.361 1.347 1.319 1.238 1.230 1.221 1.209 1.194 1.186 1.179 1.171 1.158 1.085 1.071 1.063 1.050 0.914 0.902 0.806 0.800 0.791 0.785 0.776 0.771 0.738 0.724 0.709 0.659 0.645

0.41 0.71 0.78 0.94 0.90 1.93 1.01 0.88 0.92 0.57 0.75 0.92 0.84 3.08 3.04 5.91 4.55 5.81 3.00 14.30 3.02

9.0 8.5 8.0 7.5 7.0 6.5 6.0 5.5 5.0 4.5 4.0 3.5 3.0 2.5 2.0 1.5 1.0 0.5 0.0 -0.5

f1 (ppm)

Compound 31

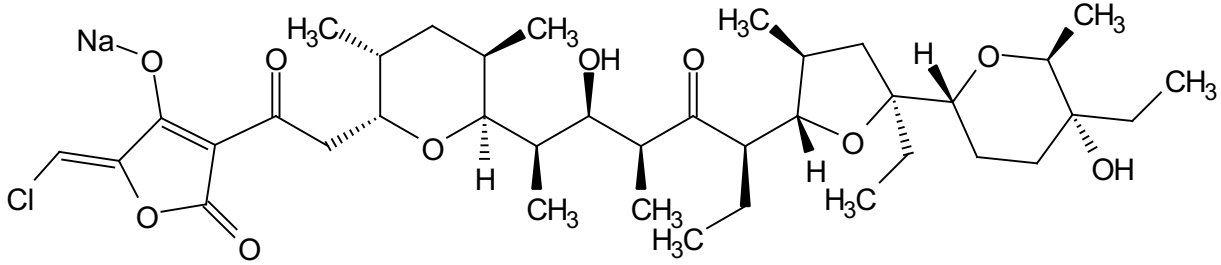

213.371

94.168
84.188
82.548
75.585
74.391
73.090
70.444
69.528
68.458
54.774
47.488
40.553
40.146
39.937
39.728
39.521
39.311
39.103
38.894
37.191
37.017
36.213
34.873
31.385
29.420
28.279
27.739
27.331
20.917
17.707
17.251
16.655
15.905
14.601
11.623
11.556
8.064
7.862
6.438

230 220 210 200 190 180 170 160 150 140 130 120 110 100 90 80 70 60 50 40 30 20 10 0 −10

f1 (ppm)

Compound 32

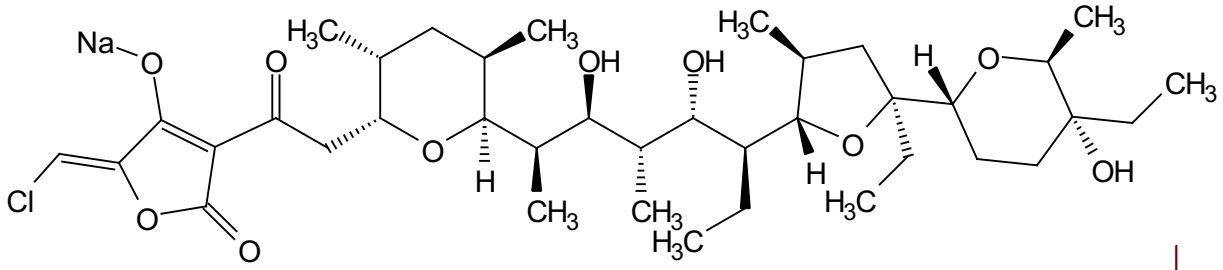

6.064 4.183 4.169 4.168 4.157 4.132 4.116 3.898 3.880 3.856 3.856 3.793 3.768 3.666 3.649 3.560 3.544 3.535 3.511 3.487 3.438 3.412 3.407 3.370 3.353 3.329 2.499 2.461 2.432 2.038 2.034 1.941 1.923 1.905 1.830 1.810 1.799 1.779 1.736 1.682 1.665 1.655 1.639 1.619 1.609 1.586 1.575 1.555 1.518 1.499 1.484 1.435 1.415 1.399 1.360 1.332 1.233 1.211 1.192 1.173 1.120 1.103 0.912 0.897 0.879 0.861 0.850 0.843 0.833 0.816 0.799 0.780 0.732 0.715 0.621 0.604 0.592 0.575

0.70 1.83 1.83 0.88 0.99 2.01 1.27 1.21 0.74 0.92 0.98 1.11 1.13 13.41 3.97 2.93 15.00 2.99 5.43

9.5 9.0 8.5 8.0 7.5 7.0 6.5 6.0 5.5 5.0 4.5 4.0 3.5 3.0 2.5 2.0 1.5 1.0 0.5 0.0 -0.5

f1 (ppm)

Compound 32

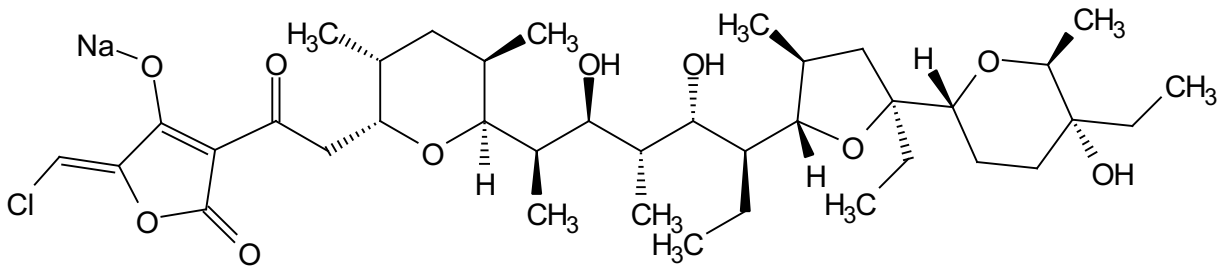

194.027
178.368
168.749
148.833

94.520
94.389
84.163
83.687
75.741
74.141
72.770
70.315
69.841
69.601
67.659
42.551
40.146
39.937
39.729
39.520
39.313
39.103
38.894
37.593
36.954
35.984
34.904
34.858
31.191
29.536
28.335
28.027
27.226
20.658
17.819
17.172
15.801
14.568
13.940
11.738
9.613
8.158
7.343
6.423

230 220 210 200 190 180 170 160 150 140 130 120 110 100 90 80 70 60 50 40 30 20 10 0 −10

f1 (ppm)